April 2019

Routing and Designing Networks for Two Transportation Problems

Liu Su
University of South Florida, liusugeneral@gmail.com

Routing and Designing Networks for Two Transportation Problems

by

Liu Su

A dissertation submitted in partial fulfillment
of the requirements for the degree of
Doctor of Philosophy
Department of Industrial and Management Systems Engineering
College of Engineering
University of South Florida

Major Professor: Changhyun Kwon, Ph.D.
Hadi Charkhgard, Ph.D.
Mingyang Li, Ph.D.
Xiaopeng Li, Ph.D.
He Zhang, Ph.D.

Date of Approval:
March 15, 2019

Keywords: Hazardous Materials Transportation, Risk Management, Spectral Risk,
Conditional Value-at-Risk, Dynamic Wireless Charging

Dedication

This dissertation is dedicated to my parents Yingan Su and Yulan Liu for their unconditional support in all my endeavors. I also dedicate this dissertation to my husband Shiyang Huang for his encouragements and inspirations.

Acknowledgements

Chapter 2 of this dissertation is derived in part from an article published in IISE Transactions, 30 September 2018, copyright Taylor & Francis, available online: https://www.tandfonline.com/doi/abs/10.1080/24725854.2018.1530488.

There are many people that I would like to express my heartfelt thanks to. More specifically, I would like to thank people without whom this dissertation would not have been possible.

First of all, I would like to thank my major advisor Dr. Changhyun Kwon. I am more than grateful that he can give me the opportunity to join in the PhD program at University of South Florida. It is his guidance and patience that makes me go through those hard times in research.

The dissertation would not be possible without my committee: Dr. Changhyun Kwon, Dr. Hadi Charkhgard, Dr. Xiaopeng Li, Dr. Mingyang Li and Dr. He Zhang. I gained a lot in the class instructed by Dr. Hadi Charkhgard and found it extremely useful in my research. Also, I would like to thank Dr. Hadi Charkhgard, Dr. Xiaopeng Li, Dr. Mingyang Li and Dr. He Zhang for their advice, guidance and support through my doctoral study.

Last but not the least, I would like to express my deepest gratitude to my family and friends. This dissertation would not have been possible without their warm love, continued patience, and endless support.

Table of Contents

List of Tables

List of Figures

Abstract

Routing and designing are essential for transportation networks. With effective routing and designing policies, transportation networks can work safely and efficiently. There are two transportation problems: hazardous materials (hazmat) transportation and warehouse logistics. This dissertation addresses the routing of networks for both problems. For hazmat transportation, the routing can be regulated via network design. Due to catastrophic consequences of potential accidents in hazmat transportation, a risk-averse approach for routing is necessary. In this dissertation, we consider spectral risk measures, for risk-averse hazmat routing. In addition, we introduce a network design problem to select a set of closed road segments for hazmat traffic with conditional value-at-risk (CVaR) to regulate hazmat routing. In warehouses, the routing of electric forklifts with sufficient battery levels is for material handling. The optimization model of dynamic wireless charging lane location is proposed under the workflow congestion in parallel-aisle warehouses. Considering the uncertainty of demands, the wireless charging lane location problem is formulated as a two-stage stochastic programming model. We confirm the efficiency of the proposed algorithms in solving these problems and the key advantages of use the proposed routing and designing policies via case studies.

1 General Introduction

With transportation networks, vehicle routing aims at finding an optimal route that achieves the minimum cost, the minimum risk of transporting commodities or other goals. The users of transportation networks respond differently to different network designs with various considerations. Therefore, routing is essential for transportation networks. With effective routing and designing policies, transportation networks can work safely and efficiently. Routing and designing the policies are of great interests for two transportation problems — hazardous materials transportation and warehouse logistics. This dissertation addresses the routing and designing of networks for both problems. In hazmat transportation, the routing of hazmat carriers focuses on minimizing the risk. Hazmat network design which is regulated by government or transportation agencies includes toll-pricing and road banning. Compared to toll-pricing for hazmat cargos, road banning is easier to be implemented and modified without additional toll-collection facilities. In this dissertation, the hazmat network design is selecting a set of road segments to be closed. For warehouse logistics, the forklift routing addresses the minimum travel time and congestion alleviation in order to achieve high operation efficiency while ensuring the safety of operation. With dynamic wireless charging technologies, we can determine the locations of wireless charging lanes to support the routing of electric forklifts.

The U.S. Occupational Safety and Health Administration (2017) defines hazardous materials (hazmat) as "chemical hazards and toxic substances which pose a wide range of health hazards such as irritation, sensitization, and carcinogenicity and physical hazards such as flammability, corrosion, and explosibility." Widely used for hazmat transportation are cargo tank trucks. Cargo tank trucks transporting with road networks can

bring potential risks for the public. According to incident statistics from Pipeline and Hazardous Materials Safety Administration (2017), there were 3,391 highway transit incidents involving hazmat, causing $32,806,352 of damages in 2017. The average cost for hazmat accident on nation's highways is about $414,000 per accident, while non-hazmat cargo accidents are averaged about $340,000 per accident (Federal Motor Carrier Safety Administration, 2001). When hazmat is released at the accident, the average cost increases to $536,000. Furthermore, if a fire or an explosion is involved, the average cost of hazmat accidents increases to $1,150,000 and $2,070,000, respectively. In order to protect the road network from severe hazmat accidents, risk and regulatory analyses have been conducted to provide effective solutions for operations and management in hazmat transportation.

In this dissertation, we consider a hazmat routing problem to determine a safe path between an origin-destination (OD) pair. As a risk-averse approach, CVaR is used in hazmat routing (Kwon, 2011; Toumazis and Kwon, 2013). CVaR is defined as the "average of the $\alpha 100\%$ worst cases in the long tail." While CVaR exhibits several desirable properties such as coherency in the sense of Artzner et al. (1999a), it has a couple of limitations. First, CVaR completely ignores what happens in the dominating $(1-\alpha)100\%$ cases, by only considering the $\alpha 100\%$ worst cases in the long tail; hence, CVaR cannot distinguish random risk variables when their CVaR values are identical. Second, CVaR places a uniform weight in the long tail for the consequences that pass the "cutoff" and, therefore, may fail to provide risk-averseness against extremely large consequences with very small probabilities. Due to these two properties, decision-making based solely on CVaR can lead to less desirable outcomes. As a way to overcome these limitations, it is natural to consider weighted average of all possible consequences, called the *spectral risk measure* (SRM) (Acerbi, 2002) of the underlying probabilistic risk distribution. The weight function is referred as the spectrum function. Any admissible spectrum function is required to be nonnegative, non-decreasing, and normalized for the spectral risk measure to be coherent. In connection with expected utility theory, some literatures (Dowd et al.,

2008; Brandtner, 2016) suggested some legitimate spectrum functions for constructing spectral risk measures. Spectral risk measures have been studied for financial portfolio optimization problems Acerbi and Tasche (2002); Acerbi (2004); Acerbi and Simonetti (2008); Dowd and Blake (2006) and some researchers (Dowd et al., 2008; Brandtner, 2016) gave guidances on the choice of spectrum functions. In hazmat routing, SRM as a more general and risk-averse approach is applied in this dissertation.

Despite that regulating policies of routing are given based on risk models, hazmat routing is ultimately performed by hazmat carriers. According to a hazmat routing survey (Battelle, 2006), hazmat carriers consider various factors such as tunnels, bridges, the population exposure, the state of regulations, and the directness of route, among others, to determine the route. This indicates that there would be factors that are unobserved by the government or a central authority. Even when multiple factors are modeled, the weights among various factors are difficult to determine. To design hazmat network which determines a set of road segments to be closed aiming at minimizing the risk level of hazmat transportation in the network, predicting the carriers' routes of transporting hazmat from origin-destination (OD) pairs is essential. With Random Utility Model (RUM), we can directly relates the probability of a route choice with the its utility and model the stochasticity of hazmat carriers. By introducing CVaR as a risk-averse measure of a hazmat network, we model both probabilistic behavior of hazmat carriers and probabilistic consequences from hazmat accidents.

Different from hazmat transportation which involves risks and uncertainties in routing, warehouse logistics can be guided by the centralized decision system. As a special type of electric vehicles (EVs), battery-based forklifts in warehouses are utilized for order-picking and item transactions. Realistic practices can be found in Utah State University and Korea Advanced Institute of Science and Technology (KAIST) where the dynamic wireless charging for their electric buses is implemented. The pioneer of wireless charging, WiTricity announced the acquisition from Qualcomm of the wireless charging plat-

form for EVs in 2019. With extensive increasing of EV applications, there is a great potential market for dynamic wireless charging technologies that enable vehicle charging while moving. Warehouse logistics focus on working efficiently when the safety of people and properties are ensured. The congestion that lead to damaged properties, injured workers (Tompkins et al., 2010) and inefficient operations (Heath et al., 2013) brings negative impacts on both efficiency and safety. Therefore, it is necessary to alleviate congestions in warehouses. With dynamic wireless charging, electric forklifts can work more efficiently without changing batteries and take advantage of unavoidable congestions as charging opportunities.

The dissertation can be summarized as follows. Chapter 2 proposes a SRM minimization model for a safe path and develop an efficient algorithm to solve the problem. Chapter 3 presents a CVaR minimization problem for hazmat network design and develops an efficient algorithm that combines line search with Benders decomposition to solve the problem. Chapter 4 introduces a two-stage stochastic programming model for optimal deployment of dynamic wireless charging lanes for electric forklifts in a congested warehouse. Chapter 5 concludes the dissertation with discussions of proposed models and directions for future research.

2 Spectral Risk Measure Minimization in Hazardous Materials Transportation

2.1 Introduction

To assess the risk of hazmat transportation, Erkut et al. (2007) identified three key steps including hazard and exposed receptor identification, frequency analysis and consequence modeling and risk calculation. Hazard and exposed receptor identification involves identifying the potentional sources, the types, and the quantities of compounds that impact the health and safety on the surrounding environment based on Oggero et al. (2006); Yang et al. (2010). In frequency analysis, the probability of an undesirable event, the level of potential receptor exposure and the severity of consequence are considered by Woodruff (2005); Marhavilas et al. (2011); Rayas and Serrato (2017). To calculate the risk, Tomasoni et al. (2010); Van Raemdonck et al. (2013); Torretta et al. (2017) proposed that all the data related to the relevant area can be collected using GIS. Various models of risk measures for hazmat transport risk are considered in the literature. Most notably, the notion of conditional value-at-risk (CVaR) has been proposed as a risk measure (Toumazis et al., 2013; Toumazis and Kwon, 2016) to provide a flexible routing tool that can incorporate the decision maker's risk preference. By varying the probability threshold value in the CVaR framework, we can provide routing solutions adequate for risk-neutral to risk-averse decision makers. In addition, Hosseini and Verma (2018) proposed an optimization model for train configuration and routing of rail hazmat shipments with conditional value-at-risk (CVaR).

For the first time, we introduce SRM as a more general and risk-averse approach in transportation problems, particularly, hazmat routing. We note that some existing hazmat

risk measures including CVaR are special cases of SRMs and demonstrate that a weighted sum of those existing hazmat risk measures can be represented as an SRM. Hence, we emphasize that the theory and algorithm developed for SRM minimization can provide a unified framework for hazmat routing in various settings. We also show that SRMs with a special class of discrete spectrum functions can be formulated as the weighted sum of CVaR measures. We devise efficient algorithms for both special and general classes of spectrum functions to find the minimal SRM paths for hazmat routing. We confirm the efficiency of the algorithms and the key advantages of SRM via case studies.

In Section 2.2 we review various risk measures for hazmat routing and illustrate limitations of the existing CVaR-based approach. After we define the SRM in Section 2.3, we study a special class of SRMs and propose an efficient algorithm to solve the SRM minimization model in Section 2.4. For general spectral risk measures, we propose an approximation scheme to simplify the problem in Section 2.5. Case studies of road networks are conducted and comparisons for different hazmat routing models are introduced in Section 2.6. Section 2.7 provides concluding remarks for this chapter.

2.2 Review of Risk Measures for Hazmat Routing

For a graph $G(\mathcal{N}, \mathcal{A})$, we denote the accident probability and the accident consequence in arc $(i,j) \in \mathcal{A}$ by p_{ij} and c_{ij}, respectively. To transport a commodity, the approximated risk distribution along path l can be written as Jin and Batta (1997):

$$\Pr[R^l = x] \approx \begin{cases} 1 - \sum\limits_{(i,j)\in\mathcal{A}^l} p_{ij} & \text{if } x = 0 \\ p_{ij} & \text{if } x = c_{ij} \text{ for some } (i,j) \in \mathcal{A}^l \end{cases} \tag{2.1}$$

Note that the approximation is from the fact that $p_{ij} \ll 1$ for hazmat accidents, and therefore, $p_{ij}p_{i'j'} \approx 0$ for any $(i,j),(i',j') \in \mathcal{A}$. Kang et al. (2014a) presented the accident

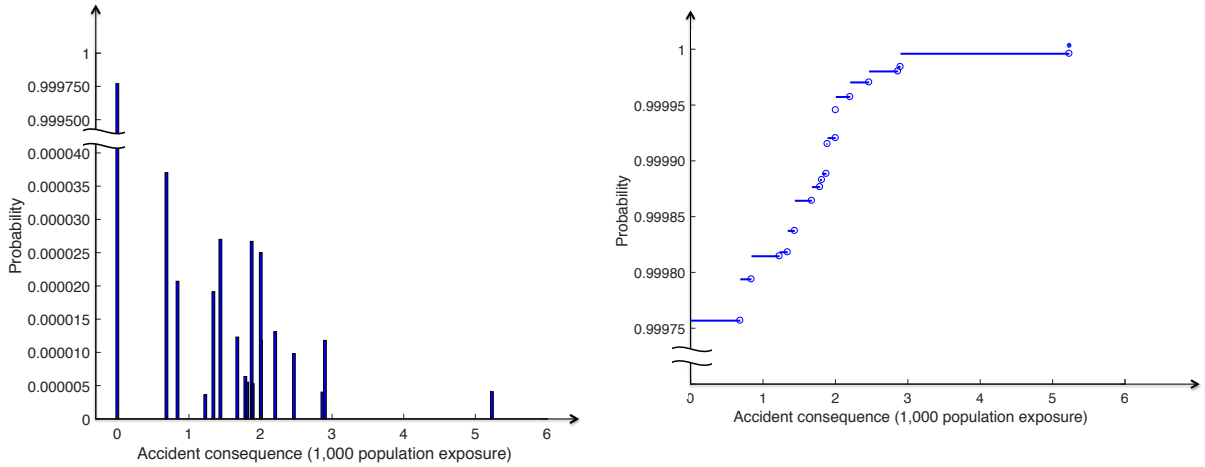

(a) pmf (b) cdf

Figure 2.1: The pmf and cdf for the accident consequence of a path

consequence (loss) in path l:

$$R^l = \begin{cases} 0, & \text{w.p. } 1 - \sum_{i=1}^{|\mathcal{A}^l|} p^l_{(i)} \\ c^l_{(1)}, & \text{w.p. } p^l_{(1)} \\ \vdots & \\ c^l_{(|\mathcal{A}^l|)}, & \text{w.p. } p^l_{(|\mathcal{A}^l|)} \end{cases} \tag{2.2}$$

where $\mathcal{A}^l$ is the set of arcs contained in path l, $c^l_{(i)}$ is the i-th smallest in the set $\{c_{ij} : (i,j) \in \mathcal{A}^l\}$, and $p^l_{(i)}$ is the probability corresponding to $c^l_{(i)}$. The probability mass function (pmf) and cumulative distribution function (cdf) for R^l of a path in the Ravenna network[1] is shown in Figure 2.1. Note that the accident probabilities are as small as 10^{-5}.

For the random risk variable R^l, several measures of risk have been proposed in the literature, as summarized in Table 2.1. Let us consider two risk measures that are popular in the literature: the traditional risk (TR) and the maximum risk (MM). The TR is the expected consequence along a path, and the MM is the maximum arc consequence in

[1]The path is 106 → 1 → 2 → 7 → 17 → 19 → 28 → 34 → 39 → 47 → 55 → 52 → 53 → 48 → 51 → 63 → 67 → 71, and the details about the Ravenna network in Bonvicini and Spadoni (2008); Erkut and Gzara (2008) are presented by Section 2.6.

Table 2.1: Measures of hazmat transport risk along path l. $\mathbb{E}[R^l]$ and $\mathbb{VAR}[R^l]$ denote the expected value and the variance of random risk R^l in path l, respectively. Note that q, k, p, and α are some model-specific scalars.

Model	Risk Measure	
Expected Risk [1]	$\mathsf{TR}^l = \mathbb{E}[R^l]$	$\approx \sum_{(i,j)\in\mathcal{A}^l} p_{ij}c_{ij}$
Population Exposure [2]	PE^l	$= \sum_{(i,j)\in\mathcal{A}^l} c_{ij}$
Incident Probability [3]	$\mathsf{IP}^l = \Pr[R^l > 0]$	$\approx \sum_{(i,j)\in\mathcal{A}^l} p_{ij}$
Perceived Risk [4]	$\mathsf{PR}^l = \mathbb{E}[(R^l)^q]$	$\approx \sum_{(i,j)\in\mathcal{A}^l} p_{ij}(c_{ij})^q$
Maximum Risk [5]	$\mathsf{MM}^l = \sup R^l$	$= \max_{(i,j)\in\mathcal{A}^l} c_{ij}$
Mean-Variance [5]	$\mathsf{MV}^l = \mathbb{E}[R^l] + k\mathbb{VAR}[R^l]$	$\approx \sum_{(i,j)\in\mathcal{A}^l} (p_{ij}c_{ij} + kp_{ij}(c_{ij})^2)$
Disutility [5]	$\mathsf{DU}^l = \mathbb{E}[\exp(kR^l)]$	$\approx \sum_{(i,j)\in\mathcal{A}^l} p_{ij}[\exp(kc_{ij}) - 1]$
Conditional Risk [6]	$\mathsf{CR}^l = \mathbb{E}[R^l \mid R^l > 0]$	$\approx \left(\sum_{(i,j)\in\mathcal{A}^l} p_{ij}c_{ij}\right) \Big/ \left(\sum_{(i,j)\in\mathcal{A}^l} p_{ij}\right)$
Value-at-Risk [7]	$\mathsf{VaR}^l_p = \inf\{x : \Pr[R^l \le x] \ge p\}$	
Conditional VaR [8]	$\mathsf{CVaR}^l_\alpha = \frac{1}{1-\alpha}\int_\alpha^1 \mathsf{VaR}^l_p \, \mathrm{d}p$	$\approx \min_r \left(r + \frac{1}{1-\alpha}\sum_{(i,j)\in\mathcal{A}^l} p_{ij}[c_{ij} - r]^+\right)$

[1] Alp (1995); [2] ReVelle et al. (1991); [3] Saccomanno and Chan (1985); [4] Abkowitz et al. (1992a); [5] Erkut and Ingolfsson (2000a); [6] Sivakumar et al. (1993); [7] Kang et al. (2014b); [8] Toumazis et al. (2013)

a path. Both measures invoke some problems in hazmat transportation. First, the TR measure considers the expected value, which is risk-neutral. In hazmat transportation, it is recommended to use risk-averse approaches to avoid catastrophic consequences. On the other hand, the MM measure, although risk-averse, often leads to a circuitous path based on Erkut and Ingolfsson (2005).

2.2.1 VaR and CVaR Defined

As a flexible alternative that covers risk attitudes between the attitudes of TR and MM, the notion of value-at-risk (VaR) and conditional value-at-risk (CVaR) have been proposed. VaR and CVaR are defined as follows:

Definition 1 (VaR Measure)**.** *The value-at-risk (VaR) along path l is defined as follows:*

$$\mathsf{VaR}_p^l = \inf\{x : \Pr[R^l \leq x] \geq p\} \tag{2.3}$$

where $p \in (0,1)$ is a threshold probability.

Definition 2 (CVaR Measure)**.** *The conditional value-at-risk (CVaR) along path l is defined as follows:*

$$\mathsf{CVaR}_\alpha^l = \frac{1}{1-\alpha}\int_\alpha^1 \mathsf{VaR}_p^l \,\mathrm{d}p \tag{2.4}$$

for a threshold probability $\alpha \in (0,1)$.

In the context of hazmat transportation, VaR and CVaR, with a threshold probability α, become identical to TR when α is sufficiently small, and identical to MM when α is sufficiently large in Toumazis et al. (2013). Therefore, VaR and CVaR in hazmat transportation provide risk measures that are more general than both the TR and MM measures.

Artzner et al. (1999a) propose the four axioms for any risk measure ξ, which maps a random loss X to a real number, to be *coherent*:

- Translation Invariance: for any real number m, $\xi(X+m) = \xi(X) + m$.
- Subadditivity: for all X_1 and X_2, $\xi(X_1 + X_2) \leq \xi(X_1) + \xi(X_2)$.
- Positive homogeneity: for all $\lambda \geq 0$, $\xi(\lambda X) = \lambda\xi(X)$.
- Monotonicity: for all X_1 and X_2 with $X_1 \leq X_2$ a.s., $\xi(X_1) \leq \xi(X_2)$.

Not all risk measures in Table 2.1 are coherent. Most notably, VaR is not a coherent risk measure, while CVaR is coherent from Rockafellar and Uryasev (2002a).

2.2.2 Limitation of CVaR: an Illustrative Example

While CVaR provides a flexible and coherent risk measure for hazmat routing to avoid high consequence events, it has a limitation. For the demonstration purpose, let us con-

sider the following three discrete random variables:

$$R^1 = \begin{cases} 0 & \text{w.p. } 0.900 \\ 5 & \text{w.p. } 0.090 \\ 10 & \text{w.p. } 0.008 \\ 50 & \text{w.p. } 0.002 \end{cases}, \quad R^2 = \begin{cases} 0 & \text{w.p. } 0.900 \\ 5 & \text{w.p. } 0.090 \\ 18 & \text{w.p. } 0.010 \end{cases}, \quad R^3 = \begin{cases} 0 & \text{w.p. } 0.900 \\ 10 & \text{w.p. } 0.090 \\ 18 & \text{w.p. } 0.010 \end{cases}. \tag{2.5}$$

CVaR measures for the above three random (loss) variables with various probability threshold values can be computed as Rockafellar and Uryasev (2002a); Pflug (2000):

$$\mathsf{CVaR}^i_\alpha = \min_r \left\{ r + \frac{1}{1-\alpha} \mathbb{E}[R^i - r]^+ \right\}$$

for each $i = 1, 2, 3$ where $[x]^+ = \max\{0, x\}$. We obtain the following values.

α	CVaR^1_α	CVaR^2_α	CVaR^3_α
0.900	6.3	6.3	10.8
0.990	18.0	18.0	18.0
0.998	50.0	18.0	18.0

From the above, it is obvious that R^2 is the most desirable, since it is a non-dominated solution for all probability thresholds. It is, however, not straightforward to make R^2 outstanding using CVaR. When R^1, R^2, and R^3 are compared at $\alpha = 0.990$, both have the identical CVaR value, and hence CVaR-based decision making is indifferent among the three random variables. We note, however, that R^1 has a significant loss of 50 with probability 0.002, which should be avoided. To distinguish R^1 from R^2, increasing α to 0.998 does not help, because it will still remain indifferent between R^2 and R^3. Although R^3 exhibits the same long-tail behavior as R^2 does, R^3 certainly has a higher CVaR value than R^2 when $\alpha = 0.900$; hence R^2 should be preferred to R^3. As a remedy, one can

consider a weighted sum as follows:

$$\mathsf{WS}^l = w_1 \mathsf{CVaR}^l_{0.900} + w_2 \mathsf{CVaR}^l_{0.990} + w_3 \mathsf{CVaR}^l_{0.998},$$

which surely confirms R^2 as the least risky choice for any positive weight parameters w_1, w_2, and w_3. For risk-aversion, it is desirable to have $w_1 < w_2 < w_3$. Note that WS^l may or may not be a coherent risk measure depending on how the weight parameters are chosen. This motivates us to consider another class of coherent risk measures that are more general than CVaR.

2.3 Defining the Spectral Risk Measure

To extend and generalize the notion of CVaR, we define the spectral risk measure—a coherent risk measure first introduced by Acerbi (2002).

Definition 3 (Spectral Risk Measure)**.** *The spectral risk measure (SRM) for hazmat routing risk along path l is defined as follows:*

$$\mathsf{SRM}^l_\phi = \int_0^1 \phi(p) \mathsf{VaR}^l_p \, \mathrm{d}p \tag{2.6}$$

where $\phi : [0,1] \to \mathbb{R}_+$ is a nonnegative and non-decreasing function such that

$$\int_0^1 \phi(p) \, \mathrm{d}p = 1. \tag{2.7}$$

Note that (2.7) is necessary for the translational invariance condition (Acerbi, 2004).

We can easily see that CVaR is a special case of spectral risk measures, by noting that

$$\phi(p) = \begin{cases} 1/(1-\alpha) & \text{if } p > \alpha \\ 0 & \text{if } p \leq \alpha \end{cases}$$

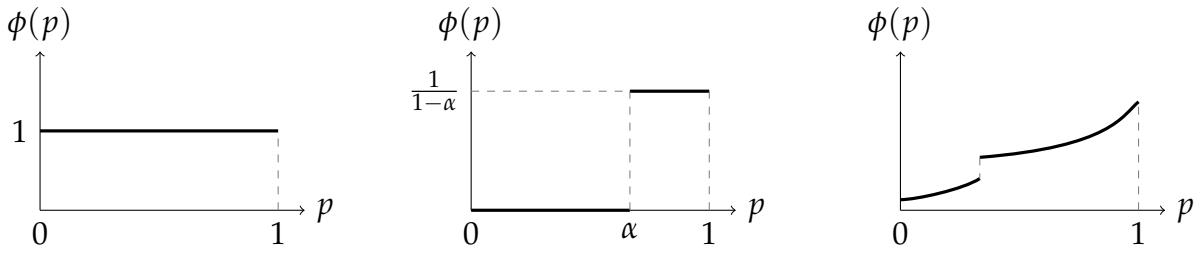

(a) $\phi(p)$ for TR (b) $\phi(p)$ for CVaR (c) A general $\phi(p)$

Figure 2.2: Example spectrum functions

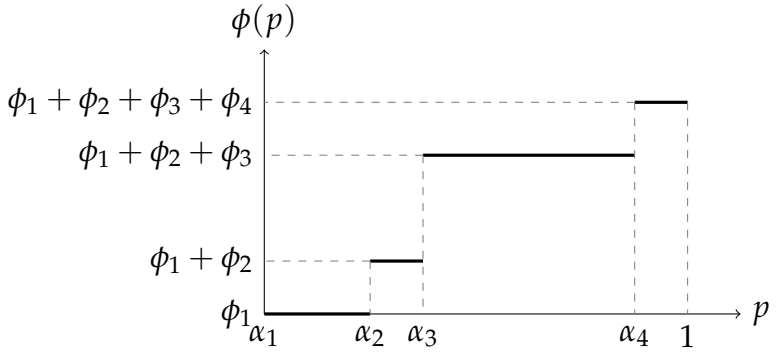

Figure 2.3: An example of the spectral risk measure (2.8) with $n = 4$

for a certain probability $\alpha \in (0, 1)$. Since TR and MM are the same as CVaR when α is very small and large, respectively (Toumazis et al., 2013; Toumazis and Kwon, 2016), TR and MM are also special cases of spectral risk measures. The comparisons can be seen in Figure 2.2. It is illustrated that TR covers full probability spectrum $[0, 1]$ uniformly, while CVaR covers only $[\alpha, 1]$ uniformly. A general spectrum function $\phi(p)$ may be defined to cover the full probability spectrum $[0, 1]$, but non-uniformly.

2.4 A Class of Spectral Risk Measures Applied in Hazmat Transportation

In this section, we consider a special class of spectrum functions; namely, nondecreasing step functions. We show that the spectral risk measure defined by such spectrum functions can be represented as a weighted sum of CVaR measures.

Let us consider a spectrum function ϕ that is a non-decreasing, step function. In particular, we consider

$$\phi(p) = \begin{cases} \phi_1, & \forall p \in (\alpha_1, \alpha_2] \\ \phi_1 + \phi_2, & \forall p \in (\alpha_2, \alpha_3] \\ \phi_1 + \phi_2 + \phi_3, & \forall p \in (\alpha_3, \alpha_4] \\ \vdots & \\ \phi_1 + \phi_2 + \ldots + \phi_n, & \forall p \in (\alpha_n, 1) \end{cases} \tag{2.8}$$

where the values of ϕ_k are nonnegative constants and $\alpha_1 \geq 0$. An example of such ϕ is provided in Figure 2.3 when $n = 4$.

Lemma 1 (Normalization)**.** *For a step function* (2.8)*, the values of ϕ_k must satisfy $\sum_{k=1}^{n} \phi_k(1 - \alpha_k) = 1$.*

When the spectrum function of the form (2.8) is used, the spectral risk measure can be simplified as a weighted sum of CVaR measures.

Theorem 1. *With* (2.8)*, the spectral risk measure for path l with spectrum function ϕ can be written as follows:*

$$\mathsf{SRM}_{\phi}^{l} = \sum_{k=1}^{n} \phi_k(1 - \alpha_k)\mathsf{CVaR}_{\alpha_k}^{l} \tag{2.9}$$

where

$$\mathsf{CVaR}_{\alpha_k}^{l} = \min_{r_k} \left[r_k + \frac{1}{1 - \alpha_k} \sum_{(i,j) \in \mathcal{A}^l} p_{ij}[c_{ij} - r_k]^+ \right] \tag{2.10}$$

for all $k = 1, \ldots, n$.

As a corollary, Theorem 2 demonstrates how to construct a weighted sum of TR, CVaR, and MM, while maintaining coherency, as a special case of SRM.

Theorem 2. *Consider a weighted sum of TR, CVaR with α, and MM for path $l \in \mathcal{P}$ as follows:*

$$\Sigma^l = w_1 \mathsf{TR}^l + w_2 \mathsf{CVaR}^l_\alpha + w_3 \mathsf{MM}^l \tag{2.11}$$

where $w_1, w_2, w_3 \geq 0$ and $\alpha \in (0,1)$. Let p^l be a constant such that $\Pr[R^l = \max_{(i,j)\in\mathcal{A}^l} c_{ij}] < p^l < 1$ and $\alpha < p^l$. If $w_1 + w_2(1-\alpha) + w_3(1-p^l) = 1$, then the weighted sum Σ^l itself is an SRM.

2.4.1 Spectral Risk Measure Minimization

The routing problem based on the spectral risk measure is to choose a path $l \in \mathcal{P}$ that minimizes the spectral risk measure from an origin to a destination; that is,

$$\min_{l\in\mathcal{P}} \mathsf{SRM}^l_\phi. \tag{2.12}$$

Note that (2.12) is a path-based formulation for hazmat transportation, which requires path enumeration. Instead of the path-based formulation, we present an arc-based formulation that can represent all feasible paths implicitly using flow conservation constraints. Let us define:

$$\Omega \equiv \left\{ x : \sum_{(i,j)\in\mathcal{A}} x_{ij} - \sum_{(j,i)\in\mathcal{A}} x_{ji} = b_i \quad \forall i \in \mathcal{N}, \text{ and } x_{ij} \in \{0,1\} \quad \forall (i,j) \in \mathcal{A} \right\}$$

where the parameter b_i has the following values.

$$b_i = \begin{cases} 1 & \text{if } i = \text{origin} \\ -1 & \text{if } i = \text{destination} \\ 0 & \text{otherwise} \end{cases}$$

We obtain the following results.

Theorem 3. *The hazmat routing problem with SRM* (2.12) *is equivalent to:*

$$\min_{l\in\mathcal{P}} \mathsf{SRM}_{\phi}^{l} = \min_{r} \left[\sum_{k=1}^{n} \phi_k(1-\alpha_k) r_k + z(r) \right] \tag{2.13}$$

where $z(r)$ is obtained by a shortest path problem

$$z(r) = \min_{x\in\Omega} \sum_{(i,j)\in\mathcal{A}} \left\{ \sum_{k=1}^{n} \phi_k p_{ij} [c_{ij} - r_k]^+ \right\} x_{ij} \tag{2.14}$$

and $r = [r_1, \ldots, r_n]^\top \in \mathbb{R}^n$.

With Theorem 3, we can solve the routing problem (2.12) by searching the space of r. With each search of r, we can obtain the path and its spectral risk measure value by solving a shortest-path problem (2.14). It is, however, inefficient to search r within $\mathbb{R}^n$ when the dimension n is large. We provide useful results to reduce the searching efforts for r.

Lemma 2 (Kang et al. 2014a)**.** *For any $\alpha \in (0,1)$, we have $\mathsf{VaR}_{\alpha}^{l} \in \{0\} \cup \{c_{ij} : (i,j) \in \mathcal{A}\}$.*

Lemma 3. *For all $0 < \alpha_1 < \alpha_2 < 1$, there exist minimizers $r^{\alpha_1} = \mathsf{VaR}_{\alpha_1}^{l}$ and $r^{\alpha_2} = \mathsf{VaR}_{\alpha_2}^{l}$ of $F_{\alpha_2}^{l}(r)$ and $F_{\alpha_2}^{l}(r)$, respectively, such that $r^{\alpha_1} \le r^{\alpha_2}$ where*

$$F_{\alpha}^{l}(r) = r + \frac{1}{1-\alpha} \sum_{(i,j)\in\mathcal{A}^l} p_{ij}[c_{ij} - r]^+$$

Therefore we only need to search for $r \in \{0\} \cup \{c_{ij} : (i,j) \in \mathcal{A}\}$ to obtain $\mathsf{CVaR}_{\alpha}^{l}$. For solving the SRM minimization problem (2.13), Lemma 2 says that it is sufficient to search the mesh determined by 0 and c_{ij} only, and the number of searches is $(|\mathcal{A}|+1)^n$. In addition, Lemma 3 indicates that there is no need to search any r such that $r_k > r_{k+1}$ for any k.

The computational method inspired by Lemmas 2 and 3 searches all valid combinations thus guaranteeing an exact optimal solution. In addition, we can also consider a

mixed integer linear programming (MILP) reformulation of (2.13) after linearization, and use an optimization solver for a solution.

2.4.2 MILP Reformulation

The SRM minimization model (2.13) can be reformulated as a mixed integer linear programming (MILP) problem. We introduce new continuous variables y_{ijk}. When x_{ij} are binary, we observe

$$y_{ijk} = [c_{ij} - r_k]^+ x_{ij} = \max\{c_{ij} - r_k, 0\} x_{ij} = \max\{c_{ij} x_{ij} - r_k, 0\}.$$

Therefore, we obtain the following equivalent formulation:

$$\min_{l \in \mathcal{P}} \mathsf{SRM}^l_\phi = \min_{r,x,y} \left[\sum_{k=1}^{n} \phi_k (1 - \alpha_k) r_k + \sum_{(i,j) \in \mathcal{A}} \sum_{k=1}^{n} \phi_k p_{ij} y_{ijk} \right] \tag{2.15}$$

subject to

$$\begin{aligned}
& x \in \Omega \\
& x_{ij} \in \{0, 1\} && \forall (i,j) \in \mathcal{A} \\
& y_{ijk} \geq c_{ij} x_{ij} - r_k && \forall (i,j) \in \mathcal{A}, k = 1, \ldots, n \\
& y_{ijk} \geq 0 && \forall (i,j) \in \mathcal{A}, k = 1, \ldots, n.
\end{aligned}$$

The computational time for both approaches—the exact search method based on Lemmas 2 and 3 and any exact algorithms for solving the MILP problem (2.15)—increases exponentially as n increases.

2.4.3 A Multi-dimensional Cyclic Coordinate Search Method with Mapping

We propose a heuristic search algorithm to find a quality solution more efficiently. The algorithm still utilizes the results from Lemmas 2 and 3 but we only need to evaluate a very limited number of combinations of $\{0\} \cup \{c_{ij} : (i,j) \in \mathcal{A}\}$ values in ascending order

of r. It is a modification of the multi-dimensional cyclic coordinate search algorithm by mapping the infeasible points to the feasible region. For each dimension, we use a line search method. The algorithm is summarized in Algorithm 1.

The definition of $z(r)$ is provided in (2.14) and the function value can be obtained by solving a shortest path problem for any given r value. To find the minimum on each dimension in Step 2, we solve the shortest path problem only when the first component of the objective $\sum_{k=1}^{n} \phi_k(1-\alpha_k)r_k^t$ is smaller than the current best minimum. Furthermore, we can utilize a line search algorithm such as golden section search on all the values in $\{0\} \cup \{c_{ij} : (i,j) \in \mathcal{A}\}$ to speed up the solution process. The above algorithm obtains the minimum value by searching each dimension sequentially, while enforcing the ascending order of r. This is realized by mapping a search point to the diagonal direction when it surpasses the diagonal line. Since this algorithm does not guarantee the global optimality, we may begin with multiple initial points to ensure the quality of the final solution.

Algorithm 1 A Multi-dimensional Cyclic Coordinate Search Method with Mapping for A Class of SRM Hazmat Routing Problems

1: Let $Z = +\infty$. Sample an initial solution r^0 uniformly from $\{0\} \cup \{c_{ij} : (i,j) \in \mathcal{A}\}$. Sort the elements of r^0 in ascending order. Let $r^c = r^0$, $r^l = r^0$.
2: Let $k = 1$ and go to Step 3.
3: Find the value $\lambda_k \in \{0\} \cup \{c_{ij} : (i,j) \in \mathcal{A}\}$ such that the objective value $z(r^t)$ is minimized where

$$r_m^t = \begin{cases} r_m^c, & \text{if } r_m^c < \lambda_k, m < k \text{ or } r_m^c > \lambda_k, m > k \\ \lambda_k, & \text{otherwise,} \end{cases} \qquad \forall m = 1, \ldots, n.$$

Let $r^c = r^t$ and go to Step 4.
4: If $k < n$, let $k = k + 1$ and go to Step 3; otherwise go to Step 5.
5: If r^c equals r^l, then let $Z = \sum_{k=1}^{n} \phi_k(1-\alpha_k)r_k^c + z(r^c)$ and terminate. Otherwise, let $r^l = r^c$ and go to Step 2.

Examples of the search process for OD pair (1,84) in the Buffalo network (Toumazis and Kwon, 2016) with two dimensions are shown in Figure 2.4. In this example, we used $n = 3$, $\alpha_2 = 0.999970, \alpha_3 = 0.999985$, and $\phi_1 = 0, \phi_2 = 22222.22, \phi_3 = 22222.22$.

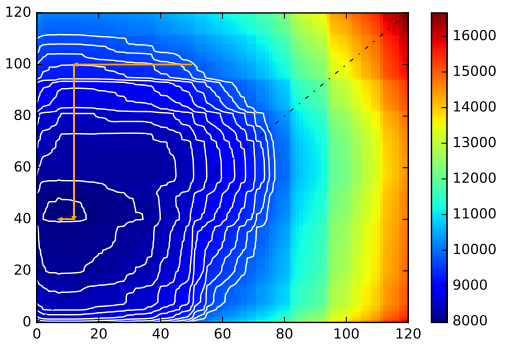

(a) without diagonal direction

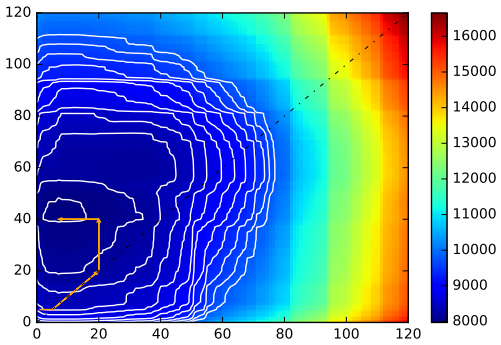

(b) with diagonal direction

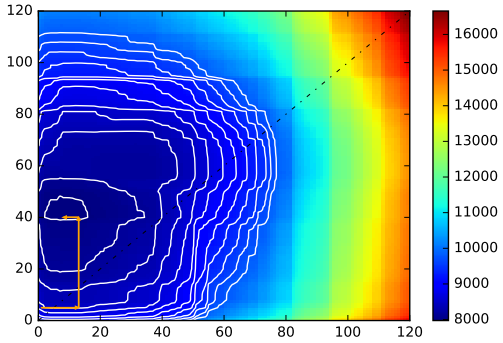

(c) without enforcing ascending order of r

Figure 2.4: Search processes

Figure 2.4a shows the algorithm process without hitting the diagonal line while Figure 2.4b demonstrates one with searching the direction on the diagonal line. For the same starting point as in Figure 2.4b, Figure 2.4c shows the search process with a traditional multi-dimensional cyclic search without enforcing the ascending order of r. By comparing Figures 2.4b and 2.4c, we can see how the points that surpass the diagonal line are mapped. While both algorithms reach the same optimal solution in this example, we also have found some examples that can obtain worse solutions in higher dimensions without enforcing an ascending order of r . In general, enforcing an ascending order of r helps finding an optimal solution.

2.5 General Spectral Risk Measures Applied in Hazmat Transportation

In this section, we consider the spectral risk measures with any general spectrum function. For any integrable, non-decreasing spectrum function $\phi(\cdot)$ that satisfies the normalization condition (2.7), we can define the general spectral risk measure of path l based on Definition 3. While the general spectrum function can be continuous, the underlying random risk variable in hazmat transportation is still discrete as shown in (2.2).

The general SRM minimization model in hazmat transportation is represented as follows:

$$\begin{aligned}\min_{l\in\mathcal{P}} \mathsf{SRM}_{\phi}^{l} &= \int_0^1 \phi(p)\mathsf{VaR}_p^l \,\mathrm{d}p \\ &= \sum_{k=0}^{|\mathcal{A}^l|} \int_{\pi_{(k)}^l}^{\pi_{(k+1)}^l} \phi(p) c_{(k)}^l \,\mathrm{d}p \\ &= \sum_{k=0}^{|\mathcal{A}^l|} \phi_{(k)}^l c_{(k)}^l \end{aligned} \tag{2.16}$$

where

$$\pi_{(k)}^l = \begin{cases} 0, & \text{if } k = 0 \\ 1 - \sum_{i=k}^{|\mathcal{A}^l|} p_{(i)} & \text{if } k = 1, 2, \ldots, |\mathcal{A}| \\ 1, & \text{if } k = |\mathcal{A}| + 1 \end{cases}$$

$$\phi_{(k)}^l = \int_{\pi_{(k)}^l}^{\pi_{(k+1)}^l} \phi(p) \,\mathrm{d}p$$

and $c_{(0)}^l = 0$. Different from the case with step spectrum functions, the general SRM minimization problem does not allow a transformation into an arc-based formulation.

2.5.1 Exponential and Power Spectral Risk Measures

We introduce possible choices for the spectrum function $\phi(\cdot)$. Inspired by popular utility functions from expected utility theory, Dowd et al. (2008) proposed the following

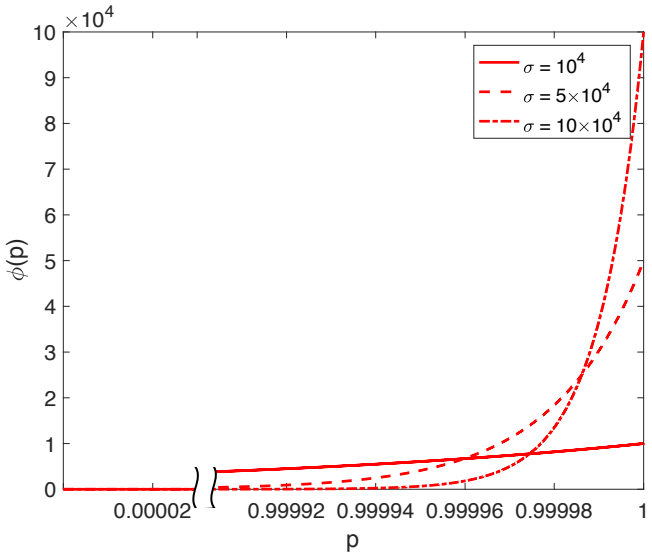

Figure 2.5: Exponential spectrum functions

spectrum functions:

$$\phi(p) = \frac{\sigma e^{-\sigma(1-p)}}{1-e^{-\sigma}}, \sigma > 0 \tag{2.17}$$

$$\phi(p) = \kappa p^{\kappa-1}, \kappa \geq 1 \tag{2.18}$$

Equation (2.17) is the exponential function while Equation (2.18) is the power function. In fact, Dowd et al. (2008) proposed another class of power functions, which creates some inconsistencies between the risk measure value and the risk-aversion level of decision makers. Hence, we only consider (2.17) and (2.18). Figures 2.5 and 2.6 show the exponential and power spectrum functions with some parameters. Power functions exhibit similar properties as exponential functions if parameters are large.

Wächter and Mazzoni (2013) concluded that the inconsistencies found in Dowd et al. (2008) arise because of an inappropriate construction of the link between utility functions and the risk spectrum. Recently, Brandtner and Kürsten (2017) proposed procedures to develop spectrum functions with which spectral risk and expected utility users can have the same decisions. The linking procedure to produce spectrum functions, however, requires knowledge of the risk distribution beforehand. In this chapter, the risk distribution

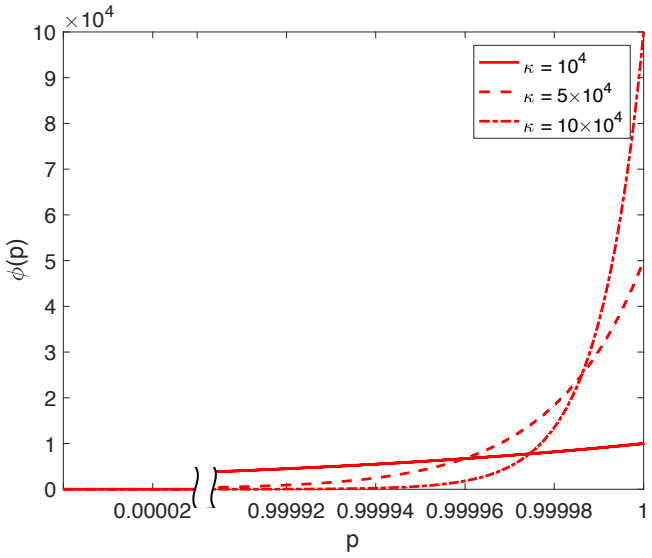

Figure 2.6: Power spectrum functions

is dependent on the path choice of hazmat transportation. Therefore, the linking approach cannot be applied to our work.

In hazmat transportation, the distribution of risk is highly skewed to the right due to extremely small probabilities for accidents. If we use small σ and κ in spectral risk measures, it addresses very limited weights for catastrophic accident consequences thus having similar results to TR. To develop appropriate spectral risk measures reflecting a risk-averse attitude towards hazmat transportation, large parameters for exponential functions and power functions are used.

2.5.2 Computational Methods for the General Cases

The general SRM minimization problem (2.16) cannot be transformed into an arc-based formulation. While we can solve the problem directly based on the path-based formulation in (2.16), the path-based formulation requires path enumeration beforehand. Once we prepare a set of feasible paths, the spectral risk measure SRM_{ϕ}^{l} in (2.16) can be computed for each path l from the set. While full path enumeration guarantees optimality of the solution obtained, it costs enormous computational effort as the number of avail-

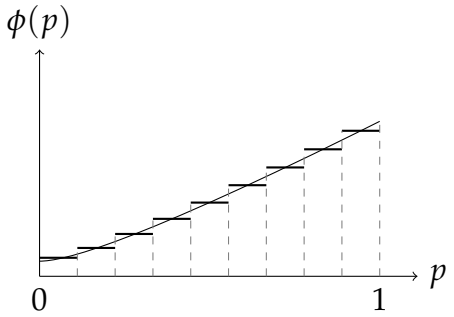

Figure 2.7: Approximating a general spectrum function by a step function

able paths between an OD pair increases exponentially. A possible method in such a case is to limit the problem to a set of geographically dissimilar paths (Akgün et al., 2000; Kang et al., 2014a) and choose a path from those dissimilar paths.

Another approach is to approximate the general spectrum function $\phi(\cdot)$ by a step function of the form in (2.8) and solve the corresponding SRM minimization problem as discussed in Section 2.4. Figure 2.7 demonstrates an example. We can use Algorithm 1 in Section 2.4.3 to solve such approximated problems. To approximate $\phi(\cdot)$ accurately, however, we require a large number of steps. Such an approximation is inefficient for large-scale problems, since the dimension of the search space increases exponentially and we need to solve many shortest-path problems.

We can also combine the two ideas. The approximation based on a step function determines probability breakpoints α_k for $k = 1, \ldots, n$ and corresponding CVaR measures $\mathsf{CVaR}^l_{\alpha_k}$ for path l. For each k, we can find the minimal CVaR path, which can be done by solving a series of shortest-path problems. For the solution procedure for finding the minimal CVaR path, see Toumazis et al. (2013); it is a single-dimensional special case of Algorithm 1. By collecting the minimal CVaR paths, we can form a set of paths for the given OD pair. The spectral risk measure (2.16) can be computed for each path in the set, thus determining the minimal SRM path. We summarize the two methods based on approximation in Algorithms 2 and 3.

Algorithm 2 A Multi-dimensional Cyclic Coordinate Search Method with Mapping for General SRM Hazmat Routing Problems

1: Approximate the given spectrum function $\phi(\cdot)$ using a step function and obtain $\alpha_1, \ldots, \alpha_n$ and $\phi_1, \ldots, \phi_n$.
2: Solve the corresponding minimization problem using Algorithm 1.

Algorithm 3 A CVaR Path Generation Method for General SRM Hazmat Routing Problems

1: Approximate the given spectrum function $\phi(\cdot)$ using a step function and obtain $\alpha_1, \ldots, \alpha_n$ and $\phi_1, \ldots, \phi_n$.
2: For each $k = 1, \ldots, n$, solve

$$\min_{l \in \mathcal{P}} \mathsf{CVaR}_{\alpha_k}$$

using the method in Toumazis et al. (2013), and call the obtained path l_k.
3: Compute $\mathsf{SRM}_{\phi}^{l_k}$ in Equation (2.16) for each $k = 1, \ldots, n$. Choose the path with the minimal value.

Although we consider a limited number of paths, Algorithm 3 is expected to produce optimal or near-optimal solutions, since minimal CVaR paths can be regarded as safe paths already and hence are good candidates for the minimal SRM path. Furthermore, the value of n in Algorithm 3 can be made much larger than in Algorithm 2. While the computational complexity in Algorithm 1 used by Algorithm 2 increases exponentially as n increases, it increases linearly in Algorithm 3.

2.5.3 Optimal Approximation by Step Functions

We propose an optimization procedure to approximate the general spectrum function by a step function. Suppose we use n number of probability breakpoints $\alpha_1, \ldots, \alpha_n$. In each interval $[\alpha_{k-1}, \alpha_k]$, we approximate $\phi(\cdot)$ by a constant h_k, as shown in Figure 2.8. To minimize the approximation error, we formulate an optimization problem as follows:

$$\min E(\alpha, h) = \sum_{k=1}^{n} \int_{\alpha_{k-1}}^{\alpha_k} (\phi(p) - h_k)^2 \, \mathrm{d}p \tag{2.19}$$

$$\text{s.t.} \sum_{k=1}^{n} h_k(\alpha_k - \alpha_{k-1}) = 1 \tag{2.20}$$

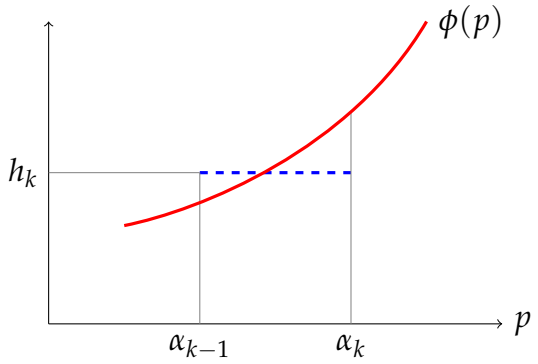

Figure 2.8: Approximating $\phi(p)$ by h_k in the interval of $[\alpha_{k-1}, \alpha_k]$.

$$\alpha_{k-1} \leq \alpha_k, k = 1, \cdots n. \tag{2.21}$$

where α_0 is set to zero. To make it consistent with the notation in Section 2.4, we can let $h_k = \sum_{s=1}^{k} \phi_s$ or $h_k - h_{k-1} = \phi_k$ with $\alpha_0 = 0$ and $\alpha_n = 1$. Problem (2.19) minimizes the sum of the squared approximation errors, while enforcing the normalization condition (2.7) in constraint (2.20). As done similarly in Maybee et al. (1979), we obtain the following results.

Theorem 4. *The optimal approximation problem* (2.19) *is equivalent to the following unconstrained optimization problem:*

$$\min J(\alpha) = -\sum_{k=1}^{n} \frac{[\Phi(\alpha_k) - \Phi(\alpha_{k-1})]^2}{\alpha_k - \alpha_{k-1}} \tag{2.22}$$

where $\Phi(\alpha_k) = \int_0^{\alpha_k} \phi(p)\, \mathrm{d}p$. *Once optimal* α_k *values are determined, we can determine*

$$h_k = \frac{\Phi(\alpha_k) - \Phi(\alpha_{k-1})}{\alpha_k - \alpha_{k-1}} \tag{2.23}$$

for all $k = 1, \ldots, n$.

To minimize $J(\alpha)$, a gradient projection algorithm is implemented. Note that $\frac{\partial \Phi(\alpha_k)}{\partial \alpha_k} = \phi(\alpha_k)$ and the derivative of $J(\alpha)$ with respect to α is

$$\frac{\partial J(\alpha)}{\partial \alpha_k} = \frac{[\Phi(\alpha_k) - \Phi(\alpha_{k-1})]^2}{(\alpha_k - \alpha_{k-1})^2} - 2\frac{\Phi(\alpha_k) - \Phi(\alpha_{k-1})}{\alpha_k - \alpha_{k-1}}\phi(\alpha_k) - \frac{[\Phi(\alpha_{k+1}) - \Phi(\alpha_k)]^2}{(\alpha_{k+1} - \alpha_k)^2} + 2\frac{\Phi(\alpha_{k+1}) - \Phi(\alpha_k)}{\alpha_{k+1} - \alpha_k}\phi(\alpha_k) \quad (2.24)$$

for all $k = 1, \ldots, n$. The algorithm is summarized in Algorithm 4.

Algorithm 4 Optimization for Approximating General Spectrum Functions

1: Initialize α with $\alpha_0 = 0$, $\alpha_n = 1$ and $\alpha_k \leq \alpha_{k+1}$ for all $k = 1, \ldots, n-1$. Set $t \leftarrow 1$.
2: Compute the gradient $\frac{\partial J(\alpha^t)}{\partial \alpha_k}$ using (2.24).
3: Let $\alpha_k^{t+1} = \alpha_k^t - \theta^t \frac{\partial J(\alpha)}{\partial \alpha_k^t}$ and $\alpha_{(k)}^{t+1}$ be the k-th smallest in set $\{\alpha_k^{t+1} : k = 1, 2, \ldots, n\}$. Set $\alpha_k^{t+1} \leftarrow \alpha_{(k)}^{t+1}$ for all k and $t \leftarrow t+1$. Repeat Step 2 until $||\alpha^t - \alpha^{t-1}|| \leq \epsilon$.

Step 3 guarantees $\alpha_{k-1} \leq \alpha_k$ by sorting $\{\alpha_k : i = 1, 2, \ldots, n\}$ in ascending order in each iteration. Note that ϵ is a small positive constant and θ^t is the step size at iteration t. We use the diminishing step size rule for θ^t. When α is obtained, h can be calculated by (2.23) and ϕ in the optimal step function will be given accordingly. Figure 2.9 shows an arbitrary step function and the optimal solution to approximate an exponential function with $\sigma = 10^4$ using 3 steps.

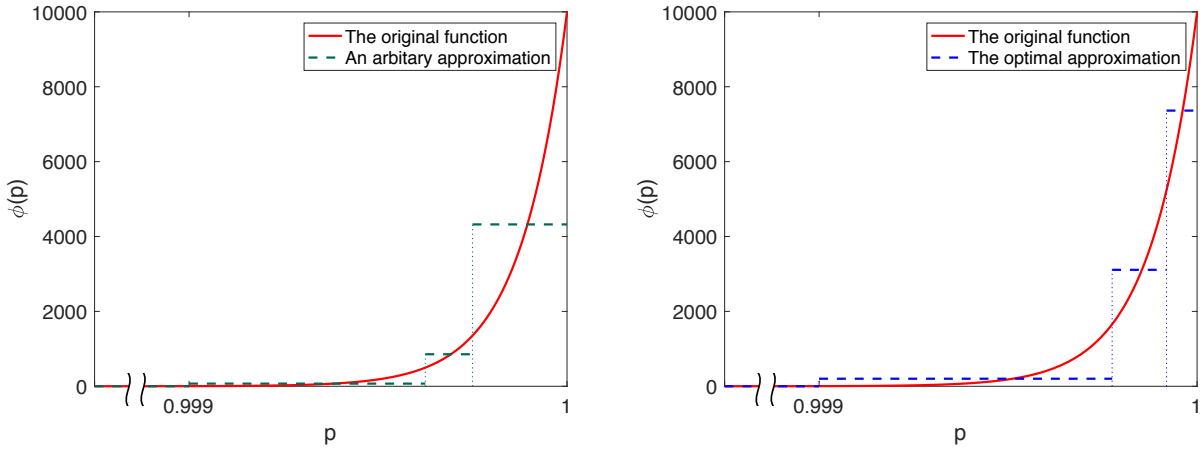

(a) An arbitrary approximation (b) The optimal approximation

Figure 2.9: Different approximations for a spectral risk function

2.6 Numerical Experiments

In this section, applications of the proposed model are shown. We conduct the numerical experiments on the Ravenna (Bonvicini and Spadoni, 2008; Erkut and Gzara, 2008), the Albany (Kang et al., 2014b), the Buffalo (Toumazis and Kwon, 2016) and the Barcelona (Transportation Networks for Research Core Team, 2018) networks. Ravenna is a small town located in Italy where large amounts of hazardous materials are processed annually. In the Ravenna network, there are 105 nodes and 134 undirected arcs. The data set includes the length, the population that hazmat would influence and the probability of accidents for each arc. The size of Albany and Buffalo networks are similar to Ravenna network. The Barcelona network is large and complicated with 1020 nodes and 2522 directed arcs. For the Barcelona network, accident probabilities and accident consequences are randomly generated.

All computational schemes introduced in this chapter are coded in Python. The Gurobi solver version 6.5.1 is used. The experiments are implemented on a 2.2 GHz Xeon processor and 32 GB of RAM.

2.6.1 Comparisons for Algorithms

To show the performances of the proposed algorithms, the computation time and optimality gap are provided in Table 2.2. MILP reformulation introduced in Section 2.4.2 is directly solved by Gurobi while k shortest path approach generates 10,000 candidates to obtain minimal SRM path. With the optimal step function obtained by Algorithm 4, we implement MILP reformulation, Algorithms 2 and 3 for finding a safe path in hazmat transportation. In Table 2.2, Algorithms 2 and 3 are always more efficient than the k shortest path approach. For small networks such as Buffalo, Ravenna and Albany, Algorithm 2 can still solve the SRM hazmat routing problem efficiently with extremely small or none optimality gaps although MILP reformulation usually performs best in such cases. Algo-

Table 2.2: Comparisons of different algorithms

Network	OD pair	σ	Computation time in seconds (optimality gap)							
			MILP reformulation		k shortest path		Algorithm 2		Algorithm 3	
Buffalo	(1,15)	10^4	0.427	(0%)	441.890	(0%)	5.049	(0%)	175.464	(0%)
		10^5	0.633	(0%)	438.998	(0%)	9.960	(0%)	166.252	(0%)
		10^6	4.609	(0%)	439.000	(0%)	22.601	(2.63%)	179.742	(0%)
Ravenna	(106,71)	10^4	21.550	(0%)	402.870	(0%)	16.161	(0%)	186.103	(0%)
		10^5	2.920	(0%)	402.789	(0%)	10.401	(0%)	184.690	(0%)
		10^6	1.135	(0%)	407.712	(0%)	10.451	(3.34%)	200.474	(0%)
Albany	(1,15)	10^4	0.431	(0%)	318.061	(0%)	5.064	(0%)	150.950	(0%)
		10^5	1.057	(0%)	318.057	(0%)	16.100	(0%)	147.464	(0%)
		10^6	0.956	(0%)	318.038	(0%)	10.380	(0%)	158.821	(0%)
Barcelona	(3,600)	10^4	107.204	(0%)	7988.353	(2.18%)	57.266	(0%)	2469.816	(0%)
		10^5	39321.988	(0%)	7985.875	(6.88%)	184.726	(0%)	2567.690	(0%)
		10^6	872.329	(0%)	7984.812	(0.98%)	237.256	(0%)	2546.374	(0%)

rithms 2 and 3 can be both effective and efficient for the Barcelona network while MILP reformulation and k shortest path are inefficient. Figure 2.10 shows the computation time for the Barcelona network with various OD pairs. For this large and complicated network, we can see that Algorithm 2 is the most efficient. Algorithm 3 also performs well in most cases.

Detailed comparisons for Algorithms 2 and 3 are conducted on the Ravenna network. The results show that exponential functions and power functions share the same optimal step function approximations when $\sigma = \kappa$ under the three alternatives. Using node 106 as an origin and node 71 as a destination, the results for the minimal SRM path in hazmat routing are shown in Figures 2.11, 2.12, and 2.13.

Two algorithms can have different performances for different spectral risk measures. In Figure 2.11, it can be seen that Algorithms 2 and 3 have the same optimal solution when $\sigma = \kappa = 10^4$. With $\sigma = \kappa = 10^5$, Algorithm 2 yields the optimal solution while Algorithm 3 does not. Algorithm 3 provides the optimal solution while Algorithm 2 does not yield the optimal solution if $\sigma = \kappa = 10^6$. A local optimal solution may be found by Algorithm 2 despite a full path set based on the arc-based formulation. On the other hand, Algorithm 3 cannot guarantee the optimal solution because the optimal is chosen from a

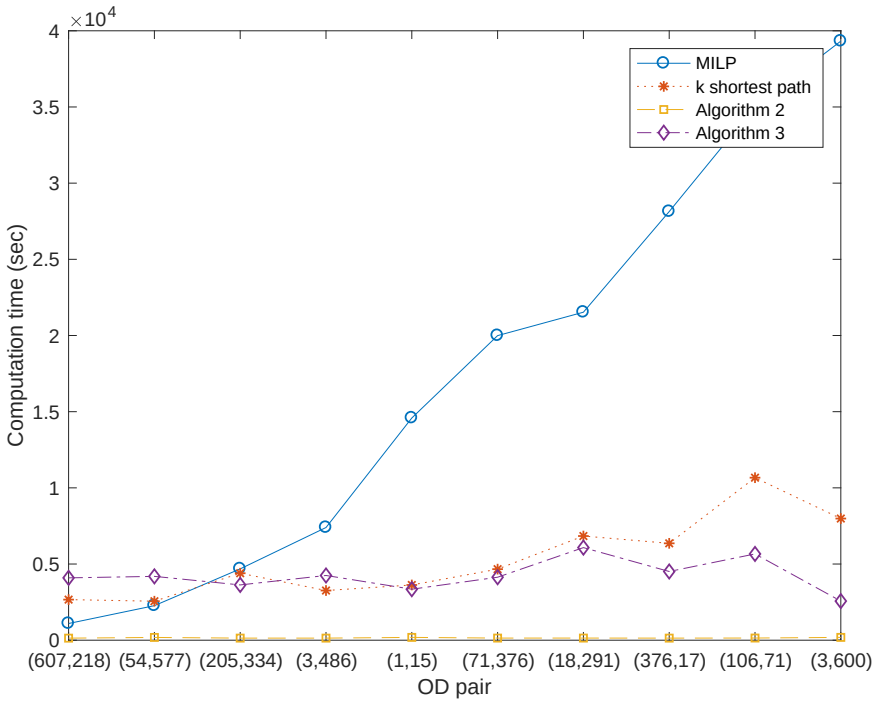

Figure 2.10: Computation time for various OD pairs with the Barcelona network when $\sigma = 10^5$

limited number of path candidates. While there exist some differences in the optimal path solutions, both algorithms obtain similar SRM values.

Both algorithms have their advantages and limitations. If the number of steps for approximation is very small, Algorithm 2 is recommended. Although losing accuracy in the objective function, the arc-based formulation in Algorithm 2 explores all feasible paths while CVaR path generation in Algorithm 3 produces only a few dissimilar paths when n is small. Algorithm 2 is inefficient if the spectrum function involves a large n. In addition, it can terminate at some local optimal solutions by Algorithm 1 given too many steps of $\phi(\cdot)$. Algorithm 3 is recommended with a large number of steps due to its linear computation complexity in n. Both algorithms can be implemented when a reasonable number of steps is chosen to approximate the general $\phi(\cdot)$.

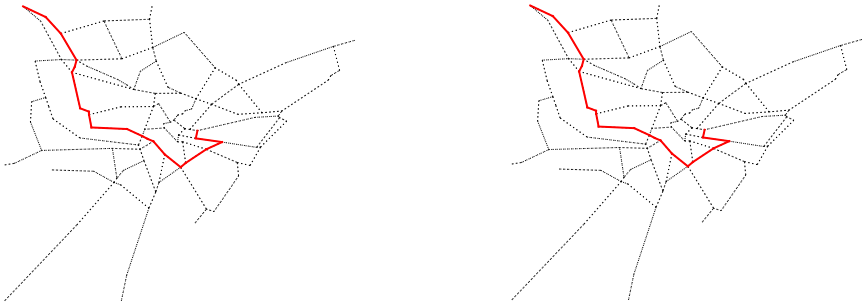

(a) $\min_{l \in \mathcal{P}} \mathsf{SRM}_{\phi}^{l} = 1791.507$ by Algorithm 2

(b) $\min_{l \in \mathcal{P}} \mathsf{SRM}_{\phi}^{l} = 1791.507$ by Algorithm 3

Figure 2.11: Comparisons for Algorithm 2 and Algorithm 3 when $\sigma = \kappa = 10^4$

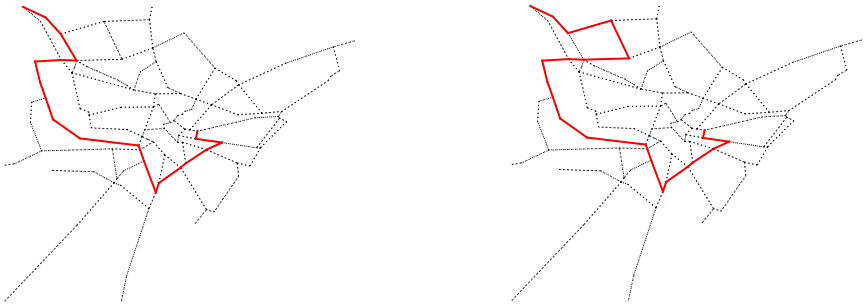

(a) $\min_{l \in \mathcal{P}} \mathsf{SRM}_{\phi}^{l} = 2555.770$ by Algorithm 2

(b) $\min_{l \in \mathcal{P}} \mathsf{SRM}_{\phi}^{l} = 2555.783$ by Algorithm 3

Figure 2.12: Comparisons for Algorithm 2 and Algorithm 3 when $\sigma = \kappa = 10^5$

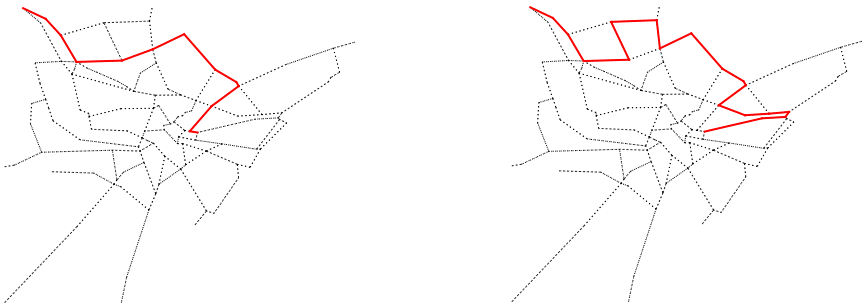

(a) $\min_{l \in \mathcal{P}} \mathsf{SRM}^l_\phi = 2688.431$ by Algorithm 2

(b) $\min_{l \in \mathcal{P}} \mathsf{SRM}^l_\phi = 2601.665$ by Algorithm 3

Figure 2.13: Comparisons for Algorithm 2 and Algorithm 3 when $\sigma = \kappa = 10^6$

Table 2.3: Comparisons of paths for different models in the Ravenna network. Optimal path names are arbitrarily given for convenient explanation.

Model			Optimal Path
TR		l_{TR}	$106 \to 1 \to 2 \to 7 \to 17 \to 19 \to 28 \to 34 \to 39 \to 47 \to 55 \to 52 \to 53 \to 48 \to 51 \to 63 \to 67 \to 71$
MM		l_{MM}	$106 \to 1 \to 2 \to 4 \to 17 \to 19 \to 23 \to 40 \to 59 \to 64 \to 61 \to 102 \to 82 \to 84 \to 103 \to 81 \to 71$
CVaR	0.9999	l_1	$106 \to 1 \to 2 \to 7 \to 5 \to 10 \to 20 \to 24 \to 26 \to 30 \to 36 \to 43 \to 46 \to 56 \to 69 \to 76 \to 75 \to 77 \to 80 \to 73 \to 71$
	0.99999	l_2	$106 \to 1 \to 2 \to 4 \to 17 \to 7 \to 5 \to 3 \to 6 \to 11 \to 14 \to 98 \to 31 \to 45 \to 54 \to 62 \to 78 \to 74 \to 76 \to 75 \to 77 \to 80 \to 73 \to 71$
	0.999999	l_3	$106 \to 1 \to 2 \to 7 \to 17 \to 4 \to 13 \to 19 \to 23 \to 40 \to 59 \to 64 \to 61 \to 102 \to 82 \to 84 \to 103 \to 81 \to 71$
SRM	10^4	l_4	$106 \to 1 \to 2 \to 7 \to 9 \to 10 \to 20 \to 24 \to 26 \to 30 \to 36 \to 43 \to 46 \to 56 \to 69 \to 76 \to 75 \to 77 \to 80 \to 73 \to 71$
	10^5	l_5	$106 \to 1 \to 2 \to 7 \to 5 \to 3 \to 6 \to 11 \to 14 \to 98 \to 31 \to 45 \to 54 \to 62 \to 78 \to 74 \to 76 \to 75 \to 77 \to 80 \to 73 \to 71$
	10^6	$l_6 = l_3$	$106 \to 1 \to 2 \to 7 \to 17 \to 4 \to 13 \to 19 \to 23 \to 40 \to 59 \to 64 \to 61 \to 102 \to 82 \to 84 \to 103 \to 81 \to 71$

2.6.2 Comparisons of Risk Measures and Limitation of CVaR

In the existing literature for hazmat transportation, there are various risk measures including TR, MM and CVaR. Table 2.3 shows a comparison of paths produced by different models in the Ravenna network. We can find that only the CVaR model with confidence level of 0.999999 and the SRM minimization model with $\sigma = 10^6$ generate the same path; i.e., $l_3 = l_6$. The CVaR model with extremely high confidence levels and the SRM model with very large parameters are equivalent because they only consider MM. Here, the MM path is different from CVaR and SRM paths with extremely large parameters due to multiple optimal solutions aiming at MM.

For the Ravenna network, Table 2.4 compares TR, MM, CVaR and SRM models with respect to various risk measures, the number of arcs and the length of the path. We can

Table 2.4: Various risk measures for different models in the Ravenna network

Model		Optimal Path l	TR^l ($\times 10^{-4}$)	MM^l	CVaR^l_α			SRM^l_σ			# of arcs	length
					0.9999	0.99999	0.999999	10^4	10^5	10^6		
TR		l_{TR}	**4.07**	5.23	2.32	3.85	5.23	1.95	3.60	5.19	17	24.33
MM		l_{MM}	6.28	**2.60**	2.22	2.60	2.60	2.05	2.56	2.60	16	39.36
CVaR	0.9999	l_1	4.30	3.47	**2.07**	3.47	3.47	1.81	3.15	3.47	20	30.15
	0.99999	l_2	5.58	2.69	2.23	**2.59**	2.69	1.92	2.56	2.69	23	45.68
	0.999999	l_3	7.62	2.60	2.27	2.60	**2.60**	2.14	2.56	2.60	18	45.58
SRM	10^4	l_4	4.10	3.47	2.07	3.47	3.47	**1.79**	3.15	3.47	20	28.64
	10^5	l_5	4.93	2.69	2.23	2.59	2.69	1.89	**2.56**	2.69	21	37.32
	10^6	$l_6 = l_3$	7.62	2.60	2.27	2.60	2.60	2.14	2.56	**2.60**	18	45.58

Table 2.5: The differences of links between l_1 and l_4

	(7,5)	(5,10)	(7,9)	(9,10)
$p_{ij}(\times 10^{-5})$	1.23	1.42	0.61	0.54
c_{ij}	1.13	1.42	1.54	0.87

re-confirm the limitation of CVaR, observed in the small example in Section 2.2.2, from the results in Table 2.4.

For the minimization problem with $\mathsf{CVaR}_{0.9999}$, path l_1 is chosen by algorithm, although l_4 also is an optimal solution for the same problem. Path l_4, however, has not only a smaller TR measure value, but also a shorter length than l_1. When SRM model with $\sigma = 10^4$ is used, l_4 is chosen. Similarly, we can also compare l_2 and l_5. While both l_2 and l_5 have the same $\mathsf{CVaR}_{0.99999}$ value, path l_5 has smaller TR measure value and shorter length.

When l_1 and l_4 are compared, the only difference is that l_1 utilizes link $7 \to 5 \to 10$, while l_4 uses link $7 \to 9 \to 10$. In these two subpaths, the accident probability and the accident consequence in each link are shown in Table 2.5. Note that in both l_1 and l_4, we have $\mathsf{VaR}_{0.9999} = 1.57$. In the evaluation fo $\mathsf{CVaR}_{0.9999}$, any link consequence that is smaller than $\mathsf{VaR}_{0.9999}$ is cut off, or ignored, as we can see from Theorem 5. Therefore, all four above links have no impact on $\mathsf{CVaR}_{0.9999}$. However, we should note that the risk in $7 \to 9 \to 10$ has the smaller expected value than in $7 \to 5 \to 10$; hence l_4 should be preferred to l_1.

Table 2.6: The differences of links between l_2 and l_5

	(2,4)	(4,17)	(17,7)
$p_{ij}(\times 10^{-5})$	3.68	3.65	3.70
c_{ij}	0.58	1.88	0.69

Table 2.7: Multiple optimal paths for $\mathsf{CVaR}_{0.999995}$ in the Barcelona network for OD pair $(3, 600)$. Optimal path names are arbitrarily given for convenient explanation.

Model	Optimal Path l	TR^l	$\mathsf{VaR}^l_{0.999995}$	$\mathsf{CVaR}^l_{0.999995}$	# of arcs
CVaR	l_1^B	0.0312	1.7473	3.4831	60
	l_2^B	0.0310	1.7473	3.4831	61
	l_3^B	0.0311	1.7473	3.4831	60
	l_4^B	0.0309	1.7473	3.4831	61
	l_5^B	0.0309	1.7473	3.4831	61
	l_6^B	0.0312	1.7473	3.4831	60
	l_7^B	0.0299	1.7473	3.4831	64
SRM	l_8^B	0.0297	1.7473	3.4831	65

Similarly, when l_2 and l_5 are compared, the only difference is that l_2 utilizes link $2 \to 4 \to 17 \to 7$, while l_5 directly moves $2 \to 7$. The probabilities and consequences respectively are shown in Table 2.6. Since $\mathsf{VaR}_{0.99999} = 2.46$ in path l_2, all above three links are cut off in computing $\mathsf{CVaR}_{0.99999}$. Hence, in the shortest-path sub-problem to compute $\mathsf{CVaR}_{0.99999}$, these three links are regarded as links with zero link costs. It is evident, however, that l_5 must be preferred to l_2.

We find multiple optimal $\mathsf{CVaR}_{0.999995}$ paths while SRM model can directly find l_8^B with a two-step spectrum function for $\alpha_2 = 0.999995$ and some $0 < \phi_1 < 1, \phi_2 = 2 \cdot 10^5(1 - \phi_1)$. Note that the SRM model is equivalent to CVaR model when $\phi_1 = 0$. Given $\phi_1 > 0$, the SRM model here considers the minimum weight average of TR and CVaR. The eight CVaR paths have significant differences in TR values among which the minimum TR path is obtained by SRM model. For large-scale networks like Barcelona, it is possible that there exsit multiple optimal CVaR paths. CVaR model, however, cannot distiguish those paths in terms of other measures of interest. With proper SRM parameters, we can

use the proposed model to find the path with both minimal CVaR value and minimal TR value.

As it is demonstrated in the above cases, SRM is obviously a better decision model than CVaR, although CVaR provides a flexible tool for risk-averse hazmat routing.

2.7 Concluding Remarks

To make risk-averse decisions, we consider spectral risk measures, which are coherent and more general than other well-known risk measures such as conditional value-at-risk. In the context of hazmat transportation, we apply spectral risk measures to the routing problem. We propose the SRM minimization model for a safe path and develop an efficient algorithm for a special class of spectral risk measures. For the general spectral risk measures, it is difficult to transform the path-based formulation to an arc-based formulation. Hence, we propose two algorithms for general spectral risk routing problems. In addition, various spectrum functions are discussed to provide some guidance for generating safe paths in hazmat transportation. The performance of algorithms are compared for various networks to show the effectiveness and efficiency of the proposed methods. The two algorithms to obtain the general minimal SRM path are also compared in different cases. In some situations, there exist differences in the optimal routing between the two algorithms, however their spectral risk measures are very close.

Through numerical examples, we have demonstrated the cases when CVaR minimization provides less desirable solutions. Often there are multiple least CVaR paths, since CVaR cuts off links whose accident consequences are smaller than VaR. In such case, CVaR minimization algorithms can find a path with greater expected risk values, which must be avoided. We demonstrated that SRM can be a solution for such cases.

Although SRM demonstrate desirable properties, there still exists a limitation. In most cases, it is unclear how the spectrum function or parameters in a spectrum function should be determined. As in Theorem 2, we can define a special SRM as a weighted av-

erage of three popular risk measures, namely, TR, CVaR, and MM. When a proper choice of the spectrum function is vague, such a weighted average can serve a practical way of determining a safe route for hazmat transportation.

3 Risk-Averse Network Design with Behavioral Conditional Value-at-Risk for Hazardous Materials Transportation

3.1 Introduction

Hazardous materials (hazmat) are defined as materials that can pose an unreasonable threat to the public and the environment (Occupational Safety and Health Administration, 2017) and about 1 million shipments of hazmat crisscross the United States every day. While the *average* nature of hazmat accidents on highways is not very different from non-hazmat cargo accidents, hazmat accidents can bring in catastrophic consequences. An extreme example is an hazmat accident in 2017 causing damages of $4,273,606 at Highway 410, Detroit, TX (Pipeline and Hazardous Materials Safety Administration, 2017). Hazmat accidents exhibit the characteristics of the low probability and high consequence events. Reducing the impact of hazmat accidents via risk-averse approaches is important for the public safety and the environment protection.

On account of the large amount of hazmat transported and high accident consequences of hazmat trucks via roads, the government and transportation agencies often consider road-ban policies to protect the public and the environment from severe accident consequences of hazmat. In a road-ban policy for hazmat transportation, the government can close certain road segments for hazmat traffic. The decision-making problem of determining which road segments to close is called a hazmat network design problem (Verter and Kara, 2008; Sun et al., 2016). In addition, the government can design toll policies to regulate hazmat transportation (Marcotte et al., 2009; Esfandeh et al., 2016). While toll pricing can provide more flexible regulatory methods, it is easier to implement and modify road-

ban policies without needs of additional toll-collection facilities. The current registry of hazmat route restriction on the U.S. highways is provided by the Federal Motor Carrier Safety Administration (2018).

For hazmat network design problems, modeling and predicting route choices of carriers is essential to determine the risk associated with transporting hazmat. Typically, hazmat network design problems for road-ban are formulated as bi-level optimization problems (Kara and Verter, 2004; Erkut and Gzara, 2008; Gzara, 2013; Fontaine and Minner, 2018; Sun et al., 2016, 2018). The upper level *selects* a set of road segments to be closed aiming at minimizing the risk level of hazmat transportation in the network. The lower level *predicts* the carriers' routes of transporting hazmat from origin-destination (OD) pairs. Most existing studies on hazmat transportation utilize the shortest path problem to model the route choices (Kara and Verter, 2004; Erkut and Gzara, 2008; Gzara, 2013; Fan et al., 2015; Esfandeh et al., 2017; Fontaine and Minner, 2018). In the lower-level shortest-path problem, the cost of carriers can be the travel time or a combination of the travel time and risk (List et al., 1991; Taslimi et al., 2017). There are, however, other factors that hazmat carriers consider for route choices. There exist factors that are *unobserved* by the government or a central authority. Even when multiple factors are modeled, the weights among various factors are difficult to determine thus bringing challenges in predicting hazmat routing.

Probabilistic approaches for modeling unobservable factors in route choice decision-making are abundant. The most popular model is arguably the Random Utility Model (RUM), which directly relates the probability of a route choice with the its utility. McFadden (1975) first proposed RUM to model general choice behaviors. In RUM, it is assumed that users' utility depends on both a fixed effect and a random observation error. Williams (1977) proposed the Multinomial Logit (MNL) model by assuming that the observation errors are from Gumbel distribution as a system evaluation criterion. To model route choices of drivers in urban road networks, Daganzo and Sheffi (1977) presented the

Table 3.1: The data for an illustrative example to show the difference between SPP and probabilistic route choice model in road banning for hazmat transportation

Arc	Travel Cost	Hazmat Risk
1	10	1.0
2	5	1.1
3	11	50.0

Multinomial Probit (MNP) model assuming that the observation errors are normally distributed. MNP model introduces a lack of tractability for researchers to perform further analysis, because it cannot provide an explicit formula which relates choice probabilities and known factors. The simple explicit form of MNL makes it incorporable with further analysis while describing users' stochastic behavior. By using MNL in transportation, the route choice probabilities can directly relate to route costs. For general freight movements, RUM and its variants have been used to model route choices using GPS tracking data (Quattrone and Vitetta, 2011; Hess et al., 2015).

Despite the popularity and effectiveness of RUM in modeling the probabilistic route choices of drivers, RUM has not been used in the hazmat transportation problems, in particular hazmat network design problems. To take account of unobservable factors in drivers' route choices, Sun et al. (2018) proposed a suboptimal decision-making model based on satisficing and robust optimization for hazmat network design problems. This chapter provides the first hazmat network design model considering probabilistic route choices.

We illustrate the importance of considering probabilistic route choices via a simple example with three arcs. We need to transport hazmat from node 1 to node 2. The data of travel cost and risk for three arcs are in Table 3.1. Assume that we can close only one arc. The results of road-ban with the shortest-path problem (SPP) and probabilistic route choice are shown in Figure 3.1. Arc 1 is the only minimum risk arc (path) and the travel cost of arc 1 is higher than arc 2. With SPP to predict the hazmat routing, the optimal solution is to close arc 2. It assumes that hazmat carriers will only follow arc 1, because it

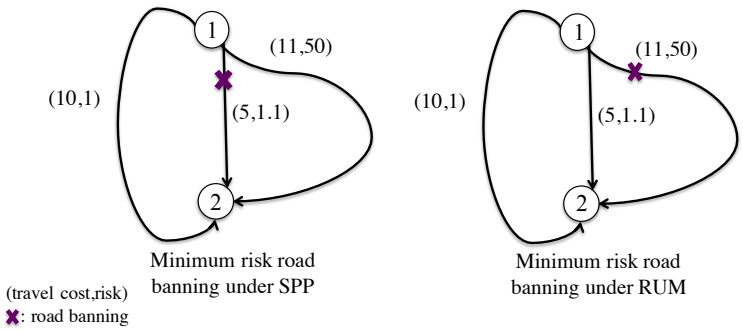

Figure 3.1: Road banning with SPP and probabilistic route choice models

provides the shortest path after closing arc 2. Note that the travel costs of arc 3 and arc 1 are very close, while arc 3 has a large risk of 50. In reality, hazmat carriers can choose arc 3 escalating the estimated risk that SPP captures. Under probabilistic route choice models, hazmat carriers are assumed to choose paths with some probabilities based on utilities, which can be represented by travel cost or other observed and unobserved factors. The optimal solution with probabilistic route choice is to close arc 3. Since the risk of arc 2 is 1.1 and the risk of arc 1 is 1, the risk for this network is still around 1 considering all available paths. Illustrated by this example, the road-ban solution with probabilistic route choice can be more preferable than SPP, which motivates this work.

The property of low probabilities but extreme accident consequences for hazmat transportation motivates researchers to consider an averse risk measure when quantifying the risk to avoid catastrophic consequences (Erkut and Ingolfsson, 2000b). Most hazmat transportation network designs consider simple risk measures such as the expectation of accident consequences. In risk management, value-at-risk (VaR), also known as α-quantile, once was commonly used to measure risk ignoring the left tail of loss distribution. Its lack of subadditivity and convexity, as discussed by Artzner et al. (1997, 1999b), however, leads researchers' attention to a coherent measure: conditional value-at-risk (CVaR). While both VaR (Duffie and Pan, 1997) and CVaR (Rockafellar and Uryasev, 2000) have been popularly used in financial portfolio optimization problems, they have

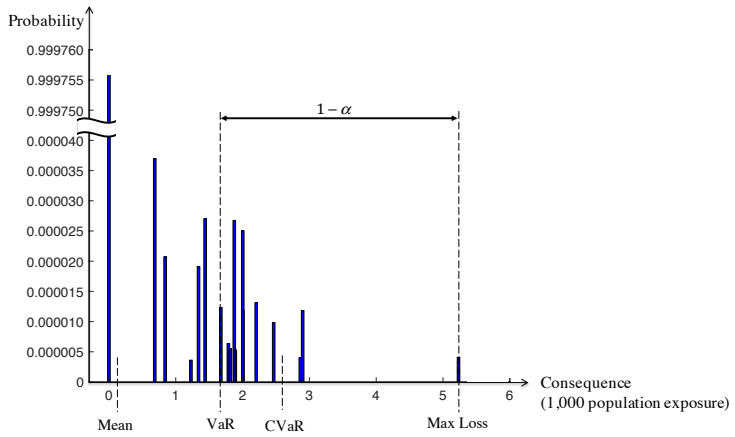

Figure 3.2: VaR and CVaR for a network only including a path (Su et al., 2017)

also been applied to hazmat routing (Kang et al., 2014b; Toumazis et al., 2013; Toumazis and Kwon, 2013, 2016; Hosseini and Verma, 2018).

Figure 3.2 shows the mean value, VaR, CVaR, and the maximum loss value for the random risk of a typical path in a hazmat transportation network. While VaR only captures a quantile, CVaR considers the expected risk (ER) beyond VaR; hence CVaR provides more risk-averse approach for mitigating tail risks. Both VaR and CVaR can be flexibly determined between the mean value and the maximum loss, depending on the probability threshold value α.

Our main contribution is that we introduce a *risk-averse* CVaR measure to both *probabilistic behavior* of hazmat carriers and *probabilistic consequences* from hazmat accidents in hazmat network design problems. To the best of our knowledge, this work is the first attempt to mitigate both factors via an averse risk measure. While RUM is used in some urban network design problems (Davis, 1994; Liu and Wang, 2015), this is the first time to incorporate RUM in hazmat transportation network design problems. CVaR is an averse risk measure that focuses on high consequences. While CVaR has been used in hazmat routing, this is the first time for the hazmat network design problem. The CVaR measure captures high consequences stemming from probabilistic route choices of hazmat carriers as well as the nature of hazmat accidents.

Table 3.2: Risk-averse approaches in hazmat transportation problems. RO represents robust optimization. The 'Data' column represents uncertainty or inaccuracy in data for hazmat accident probability and consequence in each road segment.

	Source of Uncertainty			
Paper	Route-Choice	Accident Consequence	Data	Context
Erkut and Ingolfsson (2000b)	-	Max Loss	-	Routing
Kang et al. (2014b)	-	VaR	-	Routing
Toumazis et al. (2013)	-	VaR/CVaR	-	Routing
Kwon et al. (2013)	-	-	RO	Routing
Toumazis and Kwon (2016)	-	CVaR	RO	Routing
Sun et al. (2016)	-	-	RO	Network Design
Sun et al. (2018)	RO	-	-	Network Design
This Work	CVaR	CVaR	-	Network Design

Table 3.2 further highlights our main contribution and shows the differences between our work and other available risk-averse approaches in the literature. Risk-averse approaches focus on three sources of uncertainty in the literature: route-choice, accident consequence, and data. For uncertain route choices of hazmat carriers, Sun et al. (2018) considered their worst-case behavior using the notion of bounded rationality to derive a robust network design, while the ER as a risk-neutral measure was used to evaluate the risk from hazmat accidents. To overcome the limitation in the risk-neutral ER measure of accident consequences, however, VaR and CVaR have been used for hazmat routing (Toumazis et al., 2013; Toumazis and Kwon, 2016). In this chapter, using CVaR, we consider both sources of uncertainty in route choices and accident consequences under the network design setting for the first time.

Most operations research approaches for hazmat routing assume the availability of two critical data: accident probability and accident consequence. In practice, those data are rough estimates, usually computed from the national average, if not unavailable. To manage risk from such data uncertainty, robust optimization approaches have been used (Kwon et al., 2013; Toumazis and Kwon, 2016; Sun et al., 2016). In this chapter, however, we assume that hazmat accident probabilities and consequences at each road segment are available. Considering all three sources of uncertainty will clearly be a next step.

We analyze the proposed CVaR minimization problem for hazmat network design theoretically and develop an efficient algorithm that combines line search with Benders decomposition to solve the problem. In addition, we provide case studies on realistic road networks to confirm the validity of CVaR concept incorporating probabilistic-route choices and the practicability of the proposed algorithms.

3.2 A Deterministic Model for Hazmat Network Design

In this section, we review a deterministic model for hazmat transportation network design. Later, we extend the deterministic model to consider CVaR and uncertain route choices.

Let us consider a transportation network $G = (\mathcal{N}, \mathcal{A})$ where $\mathcal{N}$ is the set of nodes and $\mathcal{A}$ is the set of arcs. In a multi-commodity transportation network, let $\mathcal{S}$ denote the set of shipments. In practice, S specifies the OD pair, and the type of hazmat. Let N^s be the demand of shipment $s \in \mathcal{S}$ that represents the number of trucks carrying hazmat. Each arc (i, j) is known with the travel cost t_{ij}, the accident probability p_{ij}, and the accident consequence c_{ij}^s for each shipment $s \in \mathcal{S}$. Accidents caused by various kinds of hazmat can have different influences on a road network making it possible that different shipments can have different accident consequences. Let $\mathcal{K}_s$ be the set of available paths for shipment $s \in \mathcal{S}$.

To transport shipment $s \in \mathcal{S}$, the approximated risk distribution for a single demand (truck) along path $k \in \mathcal{K}_s$ can be written as follows (Jin and Batta, 1997):

$$\Pr\{R^{sk} = x\} \approx \begin{cases} 1 - \sum_{(i,j)\in\mathcal{A}^k} p_{ij} & \text{if } x = 0 \\ p_{ij} & \text{if } x = c_{ij}^s \text{ for some } (i,j) \in \mathcal{A}^k \end{cases} \tag{3.1}$$

where $\mathcal{A}^k$ is the set of arcs for path k.

One of the most common approaches that regulators use to measure the risk is expected value of consequences for potential hazmat truck accidents. It is a common assumption that hazmat carriers travel along the shortest path. We also assume that hazmat carriers only follow the shortest path in the deterministic model for hazmat transportation network design. Erkut and Gzara (2008) solved a bi-level hazmat transport network design problem based on an arc-based formulation. Verter and Kara (2008) proposed a path-based approach for hazmat transport network design by simplifying the shortest path problem with the closest assignment constraints. Similarly, the deterministic path-based hazmat transportation network design is formulated as follows:

$$\min_{y,z} \sum_{s\in\mathcal{S}} \sum_{k\in\mathcal{K}_s} \sum_{(i,j)\in\mathcal{A}} N^s p_{ij} \delta_{ij}^{sk} c_{ij}^s \gamma^{sk} \tag{3.2}$$

$$\text{s.t. } z^{sk} \geq \sum_{(i,j)\in\mathcal{A}} \delta_{ij}^{sk} y_{ij} - \sum_{(i,j)\in\mathcal{A}} \delta_{ij}^{sk} + 1, \qquad \forall s \in \mathcal{S}, \forall k \in \mathcal{K}_s \tag{3.3}$$

$$z^{sk} \leq y_{ij} - \delta_{ij}^{sk} + 1, \qquad \forall s \in \mathcal{S}, \forall k \in \mathcal{K}_s, \forall (i,j) \in \mathcal{A} \tag{3.4}$$

$$\sum_{k\in\mathcal{K}_s} z^{sk} \geq 1, \qquad \forall s \in \mathcal{S} \tag{3.5}$$

$$\gamma^{sk} \leq z^{sk}, \qquad \forall s \in \mathcal{S}, k \in \mathcal{K}_s \tag{3.6}$$

$$\gamma^{sk} \geq z^{sk} - \sum_{j=1}^{k-1} z^{sj}, \qquad \forall s \in \mathcal{S}, k \in \mathcal{K}_s \tag{3.7}$$

$$\sum_{(i,j)\in\mathcal{A}} (1 - y_{ij}) \leq N \tag{3.8}$$

$$\gamma^{sk}, z^{sk} \text{ binary }, \qquad \forall s \in \mathcal{S}, \forall k \in \mathcal{K}_s \tag{3.9}$$

$$y_{ij} \text{ binary }, \qquad \forall (i,j) \in \mathcal{A} \tag{3.10}$$

where y is the design variable, z is the path availability variable and γ is the route-choice variable. If arc (i,j) is open for transportation of hazmat, $y_{ij} = 1$; otherwise, $y_{ij} = 0$. If path k is available for transportation of shipment $s \in \mathcal{S}$, $z^{sk} = 1$; otherwise, $z^{sk} = 0$. If path k is chosen for transportation of shipment $s \in \mathcal{S}$, $\gamma^{sk} = 1$; otherwise, $\gamma^{sk} = 0$. In

addition, δ_{ij}^{sk} is the parameter to define a path. If $\delta_{ij}^{sk} = 1$, arc (i, j) is on path k for shipment s; otherwise, $\delta_{ij}^{sk} = 0$.

In the single-level problem by a path-based formulation, the objective minimizes the ER as (3.2) shows. Path-based network design constraints are defined by (3.3)–(3.10). Constraints (3.3) and (3.4) define path availability for shipments. A path is available only when all arcs on the path are open. If there exist closed arcs on a path, the path is out of service. In addition, at least one path for a shipment is available to ensure transportation as (3.5) shows. Constraints (3.6) state that the chosen path for shipments must come from available paths. All paths for a shipment are sorted from 1 to k by lengths meaning that the length of path 1 for any shipment has shortest length among all possible paths. Constraints (3.7) guarantee that the available path with the smallest index is used for each shipment. Because of the sorted path data, (3.7) is equivalent to the shortest path problem in a path-based context. Due to the cost associated with closing arcs, (3.8) restricts the number of closed arcs. Constraints (3.9) and (3.10) are binaries for decision variables. The path-based hazmat transportation network design problem is a mixed-integer linear programming (MILP) problem.

3.3 Hazmat Risk Modeling with Probabilistic Route Choices

There are works that model the risk distribution for a hazmat transportation network by using shortest path problems. The route choice behavior of hazmat carriers, however, is not only resulted from known factors such as travel cost (Ben-Akiva et al., 1984) thus making it possible that the shortest path problem (SPP) and other hazmat routing optimization may fail to predict the routing decision. To consider the uncertainty of route choices, probabilistic route choice models are used. In probabilistic route choice models, hazmat carriers choose an available path with a probability. The risk distribution for a hazmat transportation network is redefined to incorporate with probabilistic route

choices. In this section, probabilistic route choice models are reviewed and utilized in risk distribution for hazmat transportation network.

3.3.1 Random Utility and Probabilistic Route Choice Models

RUM assumes that the utility of a choice that decision makers perceive comes from two sources: a deterministic (observable) component and a random (unobservable) component (Dial, 1971). In the context of route choices, the utility U^{sk} of path k for shipment $s \in \mathcal{S}$ is defined by:

$$U^{sk} = -\theta^s t^{sk} + \xi^{sk} \tag{3.11}$$

where t^{sk} is the generalized cost of observable attributes, θ^s is a positive parameter, and ξ^{sk} is a random variable for unobservable attributes. To consider both travel cost and risk in hazmat routing, the utility can also be formulated as:

$$U^{sk} = -\theta^s (t^{sk} + \beta \cdot \text{risk}^{sk}) + \xi^{sk} \tag{3.12}$$

Usually, t^{sk} is travel time. It is assumed to be additive with respect to arc costs.

$$t^{sk} = \sum_{(i,j)\in\mathcal{A}} t_{ij}\delta_{ij}^{sk} \tag{3.13}$$

where t_{ij} is the generalized travel cost associated with arc (i,j), and $\delta_{ij}^{sk} = 1$ if arc (i,j) is on path k for shipment $s \in \mathcal{S}$ and 0 otherwise. Note that risk^{sk} can be the expected risk of path k for shipment $s \in \mathcal{S}$ or any other risk measure depending on their attitudes towards risk.

Different distributions for random components ξ^{sk} result in various forms of probabilities π^{sk} of choosing path $k \in \mathcal{K}_s$ for shipment $s \in \mathcal{S}$. By assuming that the random component ξ^{sk} are independently and identically from Gumbel distribution, the MNL

model can be obtained as follows (Ben-Akiva et al., 1985):

$$\pi^{sk} = \frac{\rho^{sk}}{\sum_{l \in \mathcal{K}_s} \rho^{sl}} \tag{3.14}$$

$$\rho^{sk} = e^{-\theta^s (t^{sk} + \beta \cdot \text{risk}^{sk})} \tag{3.15}$$

for all $s \in \mathcal{S}, k \in \mathcal{K}_s$.

There exist other logit-type models with different formulations of ρ^{sk} (Cascetta et al., 1996; Ben-Akiva and Bierlaire, 1999; Ramming, 2001; Prashker and Bekhor, 2004). In C-logit model, for example, a commonality factor is introduced while a path size is defined in path-size logit model. Path size is calculated based on the length of arcs within a path and the relative lengths of paths that share an arc. Both the commonality factor and the path size are used to measure the similarity among paths. They are used to adjust the utilities of paths and address issues caused by overlapping arcs. To obtain the commonality factor and the path size, however, we need to know the path set $\mathcal{K}_s$ for shipment $s \in \mathcal{S}$ beforehand. Therefore, C-logit model and path-size model are computationally expensive to be applied in the hazmat network design problem. We use MNL of the form (3.14)–(3.15) to model the probabilistic route choices.

3.3.2 The Risk Distribution for Hazmat Transportation

In this section, the risk distribution for hazmat transportation is defined based on the probabilistic route choice model. Various shipments $s \in \mathcal{S}$ can have different accident consequences. Let $\mathcal{A}^k$ denote the set of arcs for path $k \in \mathcal{K}_s$ to transport shipment $s \in \mathcal{S}$. It is assumed that hazmat carriers operate independently. Among N^s demands of hazmat for shipment $s \in \mathcal{S}$, demand (truck) 1 and demand (truck) 2 have the same risk distribution along path $k \in \mathcal{K}_s$. Choosing path $k \in \mathcal{K}_s$ to transport shipment $s \in \mathcal{S}$, the

risk distribution for n-th truck can be approximated as follows (Jin and Batta, 1997):

$$R_n^{sk} = \begin{cases} 0 & \text{with probability } 1 - \sum\limits_{(i,j)\in\mathcal{A}^k} p_{ij} \\ c_{ij}^s & \text{with probability } p_{ij} \text{ for } (i,j) \in \mathcal{A}^k \end{cases} \tag{3.16}$$

When there are multiple paths available for each truck to transport shipment $s \in \mathcal{S}$, we assume that a path is chosen with the probability described by the probabilistic route choice model introduced in Section 3.3.1. Let R_n^s be the random risk variable for n-th truck to transport $s \in \mathcal{S}$, distributed among all available paths in $\mathcal{K}_s$. Under the consideration of available paths, the probability of taking risk x of shipment $s \in \mathcal{S}$ by n-th truck is:

$$\Pr\left[R_n^s = x\right] = \sum_{k\in\mathcal{K}_s} \Pr\left[R_n^s = x \mid \text{path } k \text{ chosen}\right] \Pr\left[\text{path } k \text{ chosen for shipment } s\right] \tag{3.17}$$

$$= \sum_{k\in\mathcal{K}_s} \Pr\left[R_n^{sk} = x\right] \pi^{sk} \tag{3.18}$$

where π^{sk} is given in (3.14). Hence, R_n^s is distributed as follows:

$$R_n^s = \begin{cases} 0 & \text{with probability } 1 - \sum\limits_{k\in\mathcal{K}_s} \sum\limits_{(i,j)\in\mathcal{A}^k} \pi^{sk} p_{ij} \\ c_{ij}^s & \text{with probability } p_{ij} \sum\limits_{k\in\mathcal{K}_s} \pi^{sk} \delta_{ij}^{sk} \text{ for } (i,j) \in \bigcup\limits_{k\in\mathcal{K}_s} \mathcal{A}^k \end{cases} \tag{3.19}$$

where δ_{ij}^{sk} is the incidence parameter for $s \in \mathcal{S}, k \in \mathcal{K}_s, (i,j) \in \mathcal{A}$. If $\delta_{ij}^{sk} = 1$, arc (i,j) is on path k for shipment s; if $\delta_{ij}^{sk} = 0$, arc (i,j) is not on path k for shipment s. The risk for a given transportation network comes from all demands among all shipments. Therefore, the risk for a transportation network is:

$$R = \sum_{s\in\mathcal{S}} \sum_{n=1}^{N^s} R_n^s \tag{3.20}$$

Since different trucks are operated separately transporting multiple units of hazmat, we can assume that the risks for multiple units of hazmat among all shipments are independently distributed. According to the North America data on hazmat transportation accident statistics, the probabilities of an accident to take place are very small ranging from 10^{-8} to 10^{-6} (Abkowitz et al., 1992b). Utilizing

$$p_{ij}p_{i'j'} \approx 0 \tag{3.21}$$

for all $(i,j),(i',j') \in \mathcal{A}$, we can obtain the probability that the risk variable becomes 0 as follows:

$$\begin{aligned}
\Pr\left[R=0\right] &= \prod_{s\in\mathcal{S}}\prod_{n=1}^{N^s}\Pr\left[R_n^s=0\right] \\
&= \prod_{s\in\mathcal{S}}\prod_{n=1}^{N^s}\left(1-\sum_{k\in\mathcal{K}_s}\sum_{(i,j)\in\mathcal{A}^k}\pi^{sk}p_{ij}\right) \\
&\approx \prod_{s\in\mathcal{S}}\left(1-N^s\sum_{k\in\mathcal{K}_s}\sum_{(i,j)\in\mathcal{A}^k}\pi^{sk}p_{ij}\right) \\
&= 1-\sum_{s\in\mathcal{S}}\sum_{k\in\mathcal{K}_s}\sum_{(i,j)\in\mathcal{A}^k}N^s\pi^{sk}p_{ij}
\end{aligned} \tag{3.22}$$

and for each $c_{ij}^s : s\in\mathcal{S},(i,j)\in\mathcal{A}$:

$$\begin{aligned}
\Pr\left[R=c_{ij}^s\right] &= \Pr\left[\sum_{s\in\mathcal{S}}\sum_{n=1}^{N^s}R_n^s=c_{ij}^s\right] \\
&\approx \sum_{n=1}^{N^s}\Pr\left[R_n^s=c_{ij}^s\right] \\
&= \sum_{n=1}^{N^s}p_{ij}\sum_{k\in\mathcal{K}_s}\pi^{sk}\delta_{ij}^{sk} \qquad (3.23) \\
&= \sum_{k\in\mathcal{K}_s}N^s\pi^{sk}p_{ij}\delta_{ij}^{sk} \qquad (3.24)
\end{aligned}$$

Therefore, the approximated risk distribution for hazmat transportation network is

$$R = \begin{cases} 0 & \text{with probability } 1 - \sum_{s\in\mathcal{S}} \sum_{k\in\mathcal{K}_s} \sum_{(i,j)\in\mathcal{A}^k} N^s \pi^{sk} p_{ij} \\ c_{ij}^s & \text{with probability } \sum_{k\in\mathcal{K}_s} N^s \pi^{sk} p_{ij} \delta_{ij}^{sk} \text{ for } (i,j) \in \mathcal{A}, s \in \mathcal{S}. \end{cases} \tag{3.25}$$

3.4 The CVaR Minimization Model for Hazmat Network Design

In this section, a CVaR minimization network design model considering drivers' probabilistic route choices is proposed. It is well-known that CVaR is a general, coherent and risk-averse measure (Rockafellar and Uryasev, 2002b). For any random loss X, the VaR and CVaR are introduced in Definitions 4 and 5, respectively. CVaR can also be redefined as an optimization problem as Theorem 5 shows.

Definition 4 (VaR Measure)**.** *The value-at-risk (VaR) is defined as follows:*

$$\mathsf{VaR}_p(X) = \inf\{x : \Pr[X \le x] \ge p\} \tag{3.26}$$

where $p \in (0,1)$ is a threshold probability.

Definition 5 (CVaR Measure)**.** *The conditional value-at-risk (CVaR) is defined as follows:*

$$\mathsf{CVaR}_\alpha(X) = \frac{1}{1-\alpha} \int_\alpha^1 \mathsf{VaR}_p(X)\, \mathrm{d}p \tag{3.27}$$

for a threshold probability $\alpha \in (0,1)$ where $\mathsf{VaR}_p(X)$ is shown in Definition 4.

Theorem 5 (Rockafellar and Uryasev, 2002b)**.** *For $r \in \mathbb{R}$, let us define*

$$\Phi_\alpha(r; X) = r + \frac{1}{1-\alpha} \mathbb{E}[X - r]^+,$$

where $[x]^+ = \max(x, 0)$. *Then the CVaR measure is equivalent to:*

$$\mathsf{CVaR}_\alpha(X) = \min_{r \in \mathbb{R}} \Phi_\alpha(r; X) \tag{3.28}$$

3.4.1 Route-Choice Probabilities Depending on Network Design

To introduce the CVaR measure for hazmat transportation, the route-choice probabilities depending on network design are clarified. Let y be the path-based network design variables and z be the path availability variables here. If arc (i, j) is open for transportation of hazmat, $y_{ij} = 1$; otherwise, $y_{ij} = 0$. If path k is available for transportation of shipment $s \in \mathcal{S}$, $z^{sk} = 1$; otherwise, $z^{sk} = 0$. The route-choice probabilities are formulated as follows:

$$z^{sk} \geq \sum_{(i,j)\in\mathcal{A}} \delta_{ij}^{sk} y_{ij} - \sum_{(i,j)\in\mathcal{A}} \delta_{ij}^{sk} + 1, \qquad \forall s \in \mathcal{S}, \forall k \in \mathcal{K}_s \tag{3.29}$$

$$z^{sk} \leq y_{ij} - \delta_{ij}^{sk} + 1, \qquad \forall s \in \mathcal{S}, \forall k \in \mathcal{K}_s, \forall (i,j) \in \mathcal{A} \tag{3.30}$$

$$\sum_{k\in\mathcal{K}_s} z^{sk} \geq 1, \qquad \forall s \in \mathcal{S} \tag{3.31}$$

$$\sum_{(i,j)\in\mathcal{A}} (1 - y_{ij}) \leq N \tag{3.32}$$

$$\pi^{sk} = \frac{\rho^{sk} z^{sk}}{\sum_{l\in\mathcal{K}_s} \rho^{sl} z^{sl}}, \qquad \forall s \in \mathcal{S}, \forall k \in \mathcal{K}_s \tag{3.33}$$

$$z^{sk} \text{ binary }, \qquad \forall s \in \mathcal{S}, \forall k \in \mathcal{K}_s \tag{3.34}$$

$$y_{ij} \text{ binary }, \qquad \forall (i,j) \in \mathcal{A} \tag{3.35}$$

Equations (3.29) and (3.30) determine the path availabilities, similarly as in Section 4.4. Equation (3.31) constrains that there exists at least one path for shipment $s \in \mathcal{S}$. Equation (3.32) states that at most N arcs can be closed in the network.

Hazmat carriers, however, do not necessarily choose the shortest path or follow the optimal path of multi-objectives which are still within SPP in all cases. To model the

uncertainty of driver behaviors, probabilistic route choice model is introduced. In the proposed model, we assume that carriers choose paths among all available paths by estimating their utilities. Then, we use RUM to model carriers' probabilistic behavior and MNL to further simplify the stochastic route-choice. Equation (3.33) shows the route-choice probabilities among all available paths. If path $k \in \mathcal{K}_s$ is unavailable for shipment $s \in \mathcal{S}$, namely $z^{sk} = 0$, its route-choice probability is 0; otherwise, the route-choice probability can be given by (3.14) and (3.15).

3.4.2 The CVaR Minimization Model

This section shows the CVaR minimization model for hazmat network design. The distribution of risk introduced in Section 3.3.2 and the route-choice probabilities in Section 3.4.1 can model the CVaR minimization network design problem. Let

$$\Phi_\alpha(r;\pi) = r + \frac{1}{1-\alpha}\mathbb{E}\left[R-r\right]^+ \tag{3.36}$$

$$\approx r + \frac{1}{1-\alpha}\Bigg\{\left(1 - \sum_{s\in\mathcal{S}}\sum_{k\in\mathcal{K}_s}\sum_{(i,j)\in\mathcal{A}^k} N^s\pi^{sk}p_{ij}\right)\left[0-r\right]^+ + \sum_{(i,j)\in\mathcal{A}}\sum_{s\in\mathcal{S}}\sum_{k\in\mathcal{K}_s} N^s\pi^{sk}p_{ij}\delta_{ij}^{sk}\left[c_{ij}^s - r\right]^+\Bigg\} \tag{3.37}$$

$$\approx r + \frac{1}{1-\alpha}\sum_{(i,j)\in\mathcal{A}}\sum_{s\in\mathcal{S}}\sum_{k\in\mathcal{K}_s} N^s\pi^{sk}p_{ij}\delta_{ij}^{sk}\left[c_{ij}^s - r\right]^+ \tag{3.38}$$

We use the optimization of CVaR in Theorem 5 to define the CVaR measure in hazmat transportation network,

$$\mathsf{CVaR}_\alpha = \min_{r\in\mathbb{R}^+}\Phi_\alpha(r;\pi) \approx \min_{r\in\mathbb{R}^+}\left[r + \frac{1}{1-\alpha}\sum_{(i,j)\in\mathcal{A}}\sum_{s\in\mathcal{S}}\sum_{k\in\mathcal{K}_s} N^s\pi^{sk}p_{ij}\delta_{ij}^{sk}\left[c_{ij}^s - r\right]^+\right]. \tag{3.39}$$

Therefore, the CVaR minimization model is,

$$\min_{\pi\in\Omega}\mathsf{CVaR}_\alpha = \min_{\pi\in\Omega, r\in\mathbb{R}^+}\Phi_\alpha(r;\pi) \tag{3.40}$$

$$\approx \min_{\pi\in\Omega, r\in\mathbb{R}^+} \left[r + \frac{1}{1-\alpha} \sum_{(i,j)\in\mathcal{A}} \sum_{s\in\mathcal{S}} \sum_{k\in\mathcal{K}_s} N^s \pi^{sk} p_{ij} \delta_{ij}^{sk} \left[c_{ij}^s - r \right]^+ \right] \tag{3.41}$$

where Ω can be defined by

$$\Omega = \{\pi : \exists y, z \text{ such that (3.29)–(3.35) hold}\}. \tag{3.42}$$

3.4.3 The Model Analysis

The CVaR minimization model for hazmat transportation network design (3.41) is a mixed integer nonlinear programming problem. If a network is complicated with a large demand of shipments, it becomes very difficult to solve the problem. In the proposed model, variable r only has an impact on the objective function and does not exist in constraints. Because the objective function is linear with r within each interval between two consecutive c_{ij}^s values, the optimal r value lies in $\Theta = \{0\} \cup \{c_{ij}^s : \forall (i,j) \in \mathcal{A}, s \in \mathcal{S}\}$ (Toumazis et al., 2013). The CVaR minimization model (3.41) is reformulated as:

$$\min_{r\in\Theta} f_\alpha(r) \tag{3.43}$$

where

$$f_\alpha(r) = \min_{\pi\in\Omega} \Phi_\alpha(r;\pi).$$

Given a large network with various kinds of hazmat, set Θ becomes large. To obtain the optimal solution of the proposed model, we should solve a large number of $f_\alpha(r)$. If some r values can be eliminated without solving optimization problems, the computation can be more efficient. Analysis is conducted to explore which r values can be eliminated from being optimal solutions for the proposed model. Let

$$0 = r_0 \le r_1 \le r_2 \le ... \le r_{q-1} \le r_q \le r_{q+1} \le ... \le r_{M_\mathcal{A}} \tag{3.44}$$

where r_q is the q-th smallest value in $\{c_{ij}^s : \forall (i,j) \in \mathcal{A}, s \in \mathcal{S}\}$ and $M_{\mathcal{A}}$ is the number of unique values in $\{c_{ij}^s : \forall (i,j) \in \mathcal{A}, s \in \mathcal{S}\}$. For each $q = 0, 1, \cdots, M_{\mathcal{A}} - 1$, we have

$$\begin{aligned}
\Phi_\alpha(r_{q+1};\pi) - \Phi_\alpha(r_q;\pi) &= r_{q+1} + \frac{1}{1-\alpha} \sum_{(i,j)\in\mathcal{A}} \sum_{s\in\mathcal{S}} \sum_{k\in\mathcal{K}_s} N^s \pi^{sk} p_{ij} \delta_{ij}^{sk} \left[c_{ij}^s - r_{q+1}\right]^+ \\
&\quad - r_q - \frac{1}{1-\alpha} \sum_{(i,j)\in\mathcal{A}} \sum_{s\in\mathcal{S}} \sum_{k\in\mathcal{K}_s} N^s \pi^{sk} p_{ij} \delta_{ij}^{sk} \left[c_{ij}^s - r_q\right]^+ \\
&= r_{q+1} - r_q \\
&\quad - \frac{1}{1-\alpha} \sum_{(i,j)\in\mathcal{A}} \sum_{s\in\mathcal{S}} \sum_{\substack{k\in\mathcal{K}_s \\ c_{ij}^s \geq r_{q+1}}} N^s \pi^{sk} p_{ij} \delta_{ij}^{sk} (r_{q+1} - r_q) \\
&= (r_{q+1} - r_q) \left(1 - \frac{1}{1-\alpha} \sum_{(i,j)\in\mathcal{A}} \sum_{s\in\mathcal{S}} \sum_{\substack{k\in\mathcal{K}_s \\ c_{ij}^s \geq r_{q+1}}} N^s \pi^{sk} p_{ij} \delta_{ij}^{sk}\right). \quad (3.45)
\end{aligned}$$

Theorem 6. *Consider an index $q \in \{0, 1, \ldots, M_{\mathcal{A}}\}$ such that the following condition holds:*

$$\frac{1}{1-\alpha} \sum_{(i,j)\in\mathcal{A}} \sum_{s\in\mathcal{S}} \sum_{\substack{k\in\mathcal{K}_s \\ c_{ij}^s \geq r_{q+1}}} N^s p_{ij} \delta_{ij}^{sk} \leq 1 \quad (3.46)$$

Then we can show that

$$\Phi_\alpha(r_q;\pi) \leq \Phi_\alpha(r_{q+1};\pi) \quad (3.47)$$

for all $\pi \in \Omega$. Further

$$f_\alpha(r_q) \leq f_\alpha(r_{q+1}) \leq \cdots \leq f_\alpha(r_{M_{\mathcal{A}}}) \quad (3.48)$$

Proof of Theorem 6. Given condition (3.46), we have

$$\frac{1}{1-\alpha} \sum_{(i,j)\in\mathcal{A}} \sum_{s\in\mathcal{S}} \sum_{\substack{k\in\mathcal{K}_s \\ c_{ij}^s \geq r_{q+1}}} N^s \pi^{sk} p_{ij} \delta_{ij}^{sk} \leq 1$$

for any π, since $\pi^{sk} \in [0,1]$ is the probability associated with path $k \in \mathcal{K}_s$ for shipment $s \in \mathcal{S}$. Based on (3.45), for any route-choice probabilities $\pi \in \Omega$

$$\Phi_\alpha(r_q;\pi) \le \Phi_\alpha(r_{q+1};\pi). \tag{3.49}$$

Note that

$$\begin{aligned}\frac{1}{1-\alpha}\sum_{(i,j)\in\mathcal{A}}\sum_{s\in\mathcal{S}}\sum_{\substack{k\in\mathcal{K}_s\\ c_{ij}^s\ge r_{M_\mathcal{A}}}} N^s\pi^{sk}p_{ij}\delta_{ij}^{sk} \le \cdots \le \frac{1}{1-\alpha}\sum_{(i,j)\in\mathcal{A}}\sum_{s\in\mathcal{S}}\sum_{\substack{k\in\mathcal{K}_s\\ c_{ij}^s\ge r_{q+2}}} N^s\pi^{sk}p_{ij}\delta_{ij}^{sk}\\ \le \frac{1}{1-\alpha}\sum_{(i,j)\in\mathcal{A}}\sum_{s\in\mathcal{S}}\sum_{\substack{k\in\mathcal{K}_s\\ c_{ij}^s\ge r_{q+1}}} N^s p_{ij}\delta_{ij}^{sk} \le 1.\end{aligned} \tag{3.50}$$

Consequently, we obtain

$$\Phi_\alpha(r_q;\pi) \le \Phi_\alpha(r_{q+1};\pi) \le \cdots \le \Phi_\alpha(r_{M_\mathcal{A}};\pi). \tag{3.51}$$

Let π_q be an optimal solution for $f_\alpha(r_q) = \min_{\pi\in\Omega}\Phi_\alpha(r_q;\pi)$; that is $f_\alpha(r_q) = \Phi_\alpha(r_q;\pi_q)$. Then, we have

$$f_\alpha(r_q) = \Phi_\alpha(r_q;\pi_q) \le \Phi_\alpha(r_q;\pi_{q+1}) \le \Phi_\alpha(r_{q+1};\pi_{q+1}) = f_\alpha(r_{q+1}). \tag{3.52}$$

Similarly,

$$f_\alpha(r_q) \le f_\alpha(r_{q+1}) \le \cdots \le f_\alpha(r_{M_\mathcal{A}}). \tag{3.53}$$

This completes the proof. □

Instead of considering all r values in Θ, we can narrow the searching range for r if there exist r values satisfying (3.46). Let $\hat{q}$ be the smallest index to satisfy (3.46). By Theorem 6, it is proved that $f_\alpha(r_{\hat{q}}) \le f_\alpha(r_{\hat{q}+1}) \le \cdots \le f_\alpha(r_{M_\mathcal{A}})$; thus excluding $r \in \{\hat{q}+1, \cdots, r_{M_\mathcal{A}}\}$

to search the minimal $f_\alpha(r)$. The CVaR minimization model (3.43) can be rewritten as:

$$\min_{r\in\{r_0,r_1,\cdots,r_{\hat{q}}\}} f_\alpha(r) \tag{3.54}$$

If (3.46) is not satisfied for any q, every $r \in \Theta$ should be considered.

3.5 A Computational Scheme for the CVaR Minimization Model

In this section, an efficient computational scheme to solve the CVaR minimization model for hazmat transportation network design is proposed. The proposed CVaR minimization model for network design is a nonlinear optimization model. Based on (3.43), the proposed network design model can be decomposed into two stages. At the first stage, we search r within a finite set. At the second stage, $f_\alpha(r)$ is solved to yield the network design solution.

$$f_\alpha(r) = \left\{ \min_{\pi,y,z} \left[r + \frac{1}{1-\alpha} \sum_{(i,j)\in\mathcal{A}} \sum_{s\in\mathcal{S}} \sum_{k\in\mathcal{K}_s} N^s \pi^{sk} p_{ij} \delta_{ij}^{sk} \left[c_{ij}^s - r \right]^+ \right] \text{ subject to (3.29)–(3.35).} \right\} \tag{3.55}$$

Because of the nonlinearity to link the route-choice probabilities and path availabilities in (3.33), we linearize as follows:

$$\sum_{l\in\mathcal{K}_s} \rho^{sl} \phi^{skl} = \rho^{sk} z^{sk}, \qquad \forall s \in \mathcal{S}, \forall k \in \mathcal{K}_s \tag{3.56}$$

$$\phi^{skl} \le z^{sl}, \qquad \forall s \in \mathcal{S}, \forall k \in \mathcal{K}_s, \forall l \in \mathcal{K}_s \tag{3.57}$$

$$\phi^{skl} \ge -(1 - z^{sl}) + \pi^{sk}, \qquad \forall s \in \mathcal{S}, \forall k \in \mathcal{K}_s, \forall l \in \mathcal{K}_s \tag{3.58}$$

$$0 \le \phi^{skl} \le \pi^{sk}, \qquad \forall s \in \mathcal{S}, \forall k \in \mathcal{K}_s, \forall l \in \mathcal{K}_s. \tag{3.59}$$

The parameter ρ can be computed with (3.15). Then, $f_\alpha(r)$ is reformulated as a MILP problem.

Despite the fact that we may use Theorem 6 to reduce the searching set for r variable, it is still time-consuming to compute $f_\alpha(r)$ given all potential r values if the scale of a network is large. Finding the optimal r can be accelerated by developing an efficient search scheme which depends on $f_\alpha(r)$. Besides, solving $f_\alpha(r)$ is very difficult when many path alternatives are considered for a complicated network. Sometimes, it is even impractical to obtain a good feasible solution for $f_\alpha(r)$.

We propose a line search with mapping to obtain optimal r as shown in Section 3.5.1 and show that Benders decomposition can generate upper and lower bounds of MILPs for given r values thus solving the $f_\alpha(r)$ problem in Section 3.5.2. Generating useful lower bounds by Benders decomposition, however, costs large computation efforts while good upper bounds can be obtained after a certain number of iterations. In this case, we terminate the algorithm by some criteria and gain the best feasible solutions from upper bounds.

3.5.1 A Line Search with Mapping

To search the optimal r value for the proposed network design model, we only consider a narrowed range of values checked by Theorem 6. Initially, we can think of obtaining an optimal solution for network design problem by visiting every value in Θ. If Θ involves a large number of values, the computation for the problem can be time-consuming because we need to solve a large number of MILPs. A searching mechanism for r based on line search methods are proposed in order to solve the problem efficiently. We use the Golden Section method. When it is applied to a strictly quasiconvex function, the Golden Section method can find a global minimal solution. The essence of the Golden Section method is to reuse one searching point in previous iteration and compare with an updated point derived by the golden ratio to reduce computations. Note that the golden ratio is 0.618.

We use the same idea to develop a discrete version of the Golden Section method, which only evaluates a limited number of r values in Θ. Usually, a line section method minimizes a nonlinear optimization problem over the interval $[a_0, b_0]$. The optimal r value lies in Θ, so $a_0 = 0$ and b_0 would be the smallest r value satisfying (3.46) by Theorem 6.

A line search algorithm usually copes with a continuous variable from a certain interval. In the proposed model, optimal r value is from a finite set. We map the updated point in iterations to value in the finite set using a simple mechanism. The simple mechanism can guarantee the correctness of searching interval. The procedures for searching optimal r for the proposed model are shown in Algorithm 5.

3.5.2 Benders Decomposition for $f_\alpha(r)$

The line search for r highly depends on obtaining optimal objective values for MILPs. As the size of the network increases, the computation time for solving $f_\alpha(r)$ given r goes up exponentially. When we solved $f_\alpha(r)$ given r with CPLEX solver of version 12.6 for the Ravenna network (Bonvicini and Spadoni, 2008; Erkut and Gzara, 2008), which has 105 nodes, 134 undirected arcs, 31 OD pairs, and 50 available paths for each OD pair, the optimality gap is 99.9% after 24 hours. This motivates us to develop an efficient algorithm solving $f_\alpha(r)$ given r. We can benefit from generating upper and lower bounds for $f_\alpha(r)$ and solving the problem iteratively rather than directly solves a large MILP with CPLEX. Seen from the structure of the MILPs, it is found that $f_\alpha(r)$ can be decomposed into: (1) optimizing network design (2) analyzing probabilities assigned for paths.

Benders decomposition is a popular algorithm framework to deal with complicating variables and large-scale optimization problems in which variables and constraints are decomposed into a master problem and subproblems. The algorithm employs cutting-planes procedures for the master problem based on subproblems until it converges. There are two categories of cuts in Benders composition. When a subproblem reaches an optimal solution but its optimal objective value is not consistent with the master problem's,

Algorithm 5 A line search with mapping

1: ***Initialization:*** Check the largest q (q^*) which satisfies (3.46). Let $k \leftarrow 0$ and $a_k \leftarrow 0$, $b_k \leftarrow r_{q^*}$. $\lambda_k = a_k + (1-\varphi)(b_k - a_k)$ and $\mu_k = a_k + \varphi(b_k - a_k)$. Find the left-closest value to λ_k (λ_{left}) and the right-closest value to μ_k (μ_{right}) among Θ. Let $\lambda_k = \lambda_{\text{left}}$, $\mu_k = \mu_{\text{right}}$ and

$$f_\alpha(\lambda_k) = \min_{\pi\in\Omega} \Phi_\alpha(\lambda_k; \pi)$$
$$f_\alpha(\mu_k) = \min_{\pi\in\Omega} \Phi_\alpha(\mu_k; \pi)$$

2: ***Convergence check:*** If $a_k = r_q$ and $b_k = r_q$ or r_{q+1} for any $q = 0, 1, \cdots, (q^* - 1)$, go to Step 6; otherwise, continue estimating $f_\alpha(\lambda_k)$ and $f_\alpha(\mu_k)$. If $f_\alpha(\lambda_k) > f_\alpha(\mu_k)$, go to Step 3; if $f_\alpha(\lambda_k) \leq f_\alpha(\mu_k)$, go to Step 4.

3: ***Reuse*** μ_k***:*** Find the right-closest value to λ_k in Θ (λ_{right}) and let $a_{k+1} = \lambda_{\text{right}}$ and $b_{k+1} = b_k$.
If $\mu_k - a_{k+1} \leq b_{k+1} - \mu_k$, let

$$\lambda_{k+1} = \mu_k, f_\alpha(\lambda_{k+1}) = f_\alpha(\mu_k)$$
$$\mu_{k+1} = \tfrac{\mu_k + b_{k+1}}{2}.$$

Find the right-closest value to μ_{k+1} in Θ (μ_{right}) and let $\mu_{k+1} = \mu_{\text{right}}$. Evaluate $f_\alpha(\mu_{k+1})$.
If $\mu_k - a_{k+1} > b_{k+1} - \mu_k$, let

$$\mu_{k+1} = \mu_k, f_\alpha(\mu_{k+1}) = f_\alpha(\mu_k)$$
$$\lambda_{k+1} = \tfrac{a_{k+1} + \mu_k}{2}.$$

Find the left-closest value to λ_{k+1} in Θ (λ_{left}) and let $\lambda_{k+1} = \lambda_{\text{left}}$. Evaluate $f_\alpha(\lambda_{k+1})$ and go to Step 5.

4: ***Reuse*** λ_k***:*** Find the left-closest value to μ_k in Θ (μ_{left}) and let $a_{k+1} = a_k$ and $b_{k+1} = \mu_{\text{left}}$.
If $\lambda_k - a_{k+1} \leq b_{k+1} - \lambda_k$, let

$$\lambda_{k+1} = \lambda_k, f_\alpha(\lambda_{k+1}) = f_\alpha(\lambda_k)$$
$$\mu_{k+1} = \tfrac{\lambda_k + b_{k+1}}{2}.$$

Find the right-closest value to μ_{k+1} in Θ (μ_{right}) and let $\mu_{k+1} = \mu_{\text{right}}$. Evaluate $f_\alpha(\mu_{k+1})$.
If $\lambda_k - a_{k+1} > b_{k+1} - \lambda_k$, let

$$\mu_{k+1} = \lambda_k, f_\alpha(\mu_{k+1}) = f_\alpha(\lambda_k)$$
$$\lambda_{k+1} = \tfrac{a_{k+1} + \lambda_k}{2}.$$

Find the left-closest value to λ_{k+1} in Θ (λ_{left}) and let $\lambda_{k+1} = \lambda_{\text{left}}$. Evaluate $f_\alpha(\lambda_{k+1})$. Go to Step 5.

5: ***Iteration update:*** $k \leftarrow k + 1$ and go to Step 2.

6: ***Determine optimal solution:*** Evaluate for $f_\alpha(a_k)$ and $f_\alpha(b_k)$. If $f_\alpha(a_k) \leq f_\alpha(b_k)$, $r^* = a_k$; otherwise, $r^* = b_k$. Stop.

an optimality cut based on dual of a subproblem is generated. On the other hand, a feasibility cut can be generated if a subproblem is infeasible. Taking advantage of the extreme ray for the dual of a infeasible subproblem can help to generate a feasibility cut. Theories and applications for Benders decomposition are developed widely. Geoffrion (1972) generalized Benders' approach to a broader class of programs in which subproblems are not restricted to linear programs. Stochastic programming problems, which is well known as its stage structure can be solved efficiently by Benders decomposition (Santoso et al., 2005).

We implement Benders decomposition to solve MILPs and obtain $f_\alpha(r)$. The network design y and path availability z are master problem variables while the probabilities related variables including π and ϕ are in subproblems.

With Benders decomposition, we present the master problem as follows:

$$\text{(master)} \min_{g,y,z} \sum_{s\in S}\sum_{k\in\mathcal{K}_s} g^{sk} \tag{3.60}$$

$$\text{s.t. (3.29)–(3.32), (3.34)–(3.35)}$$

$$g^{s_tk_t} \geq \rho^{s_tk_t} z^{s_tk_t}\lambda_t + \sum_{l\in\mathcal{K}_{s_t}} z^{s_tl}\mu_t^l + \sum_{l\in\mathcal{K}_{s_t}} (-1+z^{s_tl})v_t^l, \qquad \forall t = 1,2,\cdots \tag{3.61}$$

where t denotes the number of cuts generated by the t-th iteration of Benders decomposition. Constraints (3.61) are further explained by subproblem duals later.

The subproblems which analyze the route-choice probabilities (3.33) are decomposed by $s \in \mathcal{S}, k \in \mathcal{K}_s$ with dual variables $(\lambda, \mu^l, v^l, \omega^l)$ as follows:

$$\min_{\pi^{sk}} \sum_{(i,j)\in\mathcal{A}} N^s \pi^{sk} p_{ij} \delta_{ij}^{sk} \left[c_{ij}^s - r\right]^+ \tag{3.62}$$

$$\text{s.t.} \sum_{l\in\mathcal{K}_s} \rho^{sl}\phi^{skl} = \rho^{sk} z^{sk} \qquad (\lambda) \tag{3.63}$$

$$\phi^{skl} \leq z^{sl}, \qquad \forall l \in \mathcal{K}_s \qquad (\mu^l \leq 0) \tag{3.64}$$

$$\phi^{skl} \geq -(1-z^{sl}) + \pi^{sk}, \qquad \forall l \in \mathcal{K}_s \qquad (v^l \geq 0) \tag{3.65}$$

$$\phi^{skl} \leq \pi^{sk}, \qquad \forall l \in \mathcal{K}_s \qquad (\omega^l \leq 0) \tag{3.66}$$

$$\pi^{sk} \text{ free}, \tag{3.67}$$

$$\phi^{skl} \geq 0, \qquad \forall l \in \mathcal{K}_s \tag{3.68}$$

Feed with master problem variables, route-choice probabilities can be estimated from subproblems. Therefore, subproblems are feasible making it only necessary to generate optimality cuts from subproblem duals. The subproblem dual is defined as follows:

$$(\mathsf{SD}^{sk})\ \hat{g}^{sk} = \max_{\lambda,\mu,v,\omega} \rho^{sk} z^{sk} \lambda + \sum_{l \in \mathcal{K}_s} z^{sl} \mu^l + \sum_{l \in \mathcal{K}_s} (-1 + z^{sl}) v^l \tag{3.69}$$

$$\text{s.t. } - \sum_{l \in \mathcal{K}_s} \mu^l - \sum_{l \in \mathcal{K}_s} v^l = \sum_{(i,j) \in \mathcal{A}} N^s p_{ij} \delta_{ij}^{sk} \left[c_{ij}^s - r \right]^+ \tag{3.70}$$

$$\rho^{sl} \lambda + \mu^l + v^l + \omega^l \leq 0, \forall l \in \mathcal{K}_s. \tag{3.71}$$

In subproblem duals, we can obtain a (s_t, k_t) with the objective value $\hat{g}^{s_t k_t}$ and the solution $(\lambda_t, \mu_t^l, v_t^l, \omega_t^l)$ accordingly. Let $\tilde{g}^{s_t k_t}$ be an optimal solution for the master problem. If $\hat{g}^{s_t k_t}$ is greater than $\tilde{g}^{s_t k_t}$, an optimality cut can be generated as (3.61) using (3.69). The algorithm is summarized in Algorithm 6. In Algorithm 6, ϵ is a small positive parameter.

Algorithm 6 Benders decomposition for $f_\alpha(r)$

1: ***Initialization:*** Set $t = 0$, upper bound $\mathsf{UB} = \infty$ and lower bound $\mathsf{LB} = 0$. Go to Step 2.
2: ***Solve master problem:*** Solve the master problem and obtain the optimal solution $(\tilde{g}, \tilde{y}, \tilde{z})$. Let $\mathsf{LB} = \sum_{s \in S} \sum_{k \in \mathcal{K}_s} \tilde{g}^{sk}$ and $I = 0$. Go to Step 3.
3: ***Solve subproblem:*** For (s, k), solve SD^{sk} problem based on $\tilde{z}$ and obtain optimal solution $(\hat{\lambda}, \hat{\mu^l}, \hat{v^l}, \hat{\omega^l})$. The optimal objective value for the subproblem is $\hat{g}^{sk}$. If all (s, k) are visited, go to Step 5; otherwise, go to Step 4.
4: ***Generate an optimality cut:*** If $I = 1$ go to Step 2; otherwise, compare $\tilde{g}^{sk}$ and $\hat{g}^{sk}$. If $\hat{g}^{sk} - \tilde{g}^{sk} \geq \epsilon$, update $I \leftarrow 1, t \leftarrow t + 1, s_t \leftarrow s, k_t \leftarrow k, \lambda_t \leftarrow \tilde{\lambda}, \mu_t \leftarrow \tilde{\mu}, v_t \leftarrow \tilde{v}$ and an optimality cut is generated; otherwise, update (s, k) and go to Step 3.
5: ***Convergence check:*** If $\mathsf{UB} > \sum_{s \in S} \sum_{k \in \mathcal{K}_s} \hat{g}^{sk}$, set $\mathsf{UB} = \sum_{s \in S} \sum_{k \in \mathcal{K}_s} \hat{g}^{sk}$. If $\mathsf{UB} - \mathsf{LB} \leq \epsilon$, terminate; otherwise go to Step 1.

Besides, I is used to indicate whether an optimality cut is generated. Based on an optimal

solution for the master problem, we can generate multiple optimality cuts from different subproblems. The master problem becomes very difficult to solve if too many cuts are added at a time, which makes hard to obtain an upper bound. In order to produce upper bounds effectively, we only add one optimality cut after solving the master problem until the algorithm terminates.

We implement Benders decomposition on the Ravenna network in (Bonvicini and Spadoni, 2008; Erkut and Gzara, 2008) with 105 nodes and 134 undirected arcs. Four kinds of hazardous materials are considered including methanol, chlorine, gasoline and LPG. There are 31 shipments and each shipment defines a certain demand of a hazmat transported from an OD pair. For each shipment, we generate 50 paths using k-shortest path approach to test the performance of the proposed framework. The computation process for solving $f_{0.95}(0.454)$ is shown in Figure 3.3. We terminate the algorithm when the optimality gap is less than 5%. In this example, we can see that a good feasible solution is achieved within a small number of iterations. The improvement of lower bound, however, is very slow. Besides, it becomes more difficult to solve the master problem as iteration proceeds. It indicates that the time spent on the iteration close to the optimal solution can be far more than early iterations. An optimal solution is obtained when the upper bound and the lower bound are close.

Since we can obtain feasible solutions and useful upper bounds before reaching the convergence of Benders decomposition, a close optimal solution generated by a set of feasible solutions is used. When the upper bound does not improve, we terminate the algorithm. Different stopping criteria such as the total time limit of algorithm, the total number of iterations and the number of iterations that upper bound does not improve can be set. The local optimality can be guaranteed for the best feasible solution thus providing a practical approach. Besides, the effectiveness to terminate at a good feasible solution for $f_\alpha(r)$ accelerates the solving process.

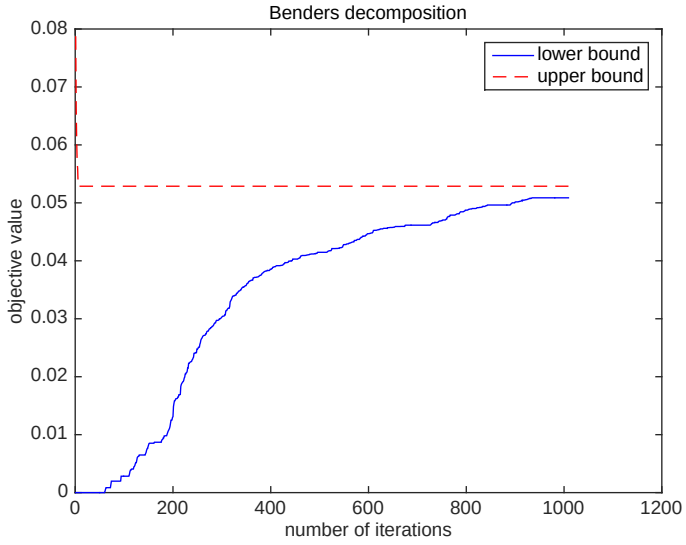

Figure 3.3: Lower bounds and upper bounds for a MILP given $r = 0.454$ and $\alpha = 0.95$ by Benders decomposition for the Ravenna network.

3.5.3 Performance of Algorithm 5 Depending on Algorithm 6

This section discusses the performance of Algorithm 5 depending on Algorithm 6. The Ravenna network with 20 paths for each shipment are used for experiments in this section. Let $\alpha = 0.95$ and the maximum number of closed arcs $N = 10$. To solve the proposed CVaR minimization model for hazmat network design, we incorporate the searching scheme for r in Section 3.5.1 with evaluations of $f_\alpha(r)$ using Algorithm 6. We can either use the optimal or the best feasible solution obtained from Algorithm 6 to proceed the searching of r in Algorithm 5. The searching process of r is shown in Figure 3.4.

It can be seen that an optimal network design is achieved when solving MILP with $r = 0.687$ and the minimum risk equals to 0.732. In Figure 3.4, it is found that the optimal r value is 0.699 and the approximated minimum risk is 0.742 by the best feasible solution of $f_\alpha(r)$. Accordingly, the network design results are shown in Figure 3.5. The number of closed arcs in both cases is 10 with 8 of which are the same. It indicates that both network designs are similar. Given the best feasible design, the CVaR is the minimum value for $\Phi(r;\pi)$ through all r values. Hence, the risk for best feasible network design is less than or

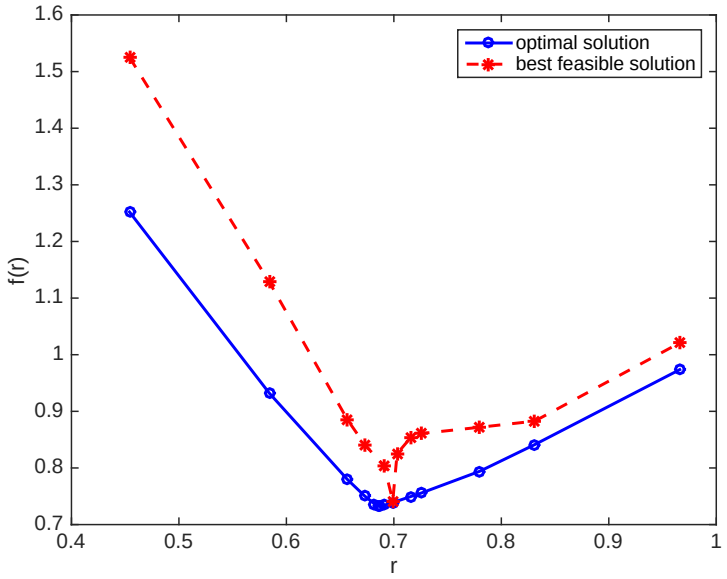

Figure 3.4: Searching of r based on the optimal and the best feasible solution by Algorithm 6

equal to 0.742. The best feasible solution by Algorithm 6 yields a network design with the objective function value no greater than 1.35% of the optimal solution. This shows that the line search for r with a best feasible solution for $f_\alpha(r)$ is close to the optimal solution. In addition, it costs 3 hours to compute an optimal hazmat network design depending on the exact value of $f_\alpha(r)$, while the best feasible design is obtained in 1 hour and 33 minutes. To improve the computation efficiency while ensuring the solution quality, we incorporate the line search for r with a best feasible solution for $f_\alpha(r)$ in Section 3.6.

3.6 Numerical Experiments

In this section, applications of the proposed model are shown. All numerical experiments in this section are conducted using the Ravenna (Bonvicini and Spadoni, 2008; Erkut and Gzara, 2008) network. Four kinds of hazardous materials are considered: methanol, chlorine, gasoline and LPG. There are 31 shipments transported through the networks. The data set includes the length of each arc, the population that each kind of

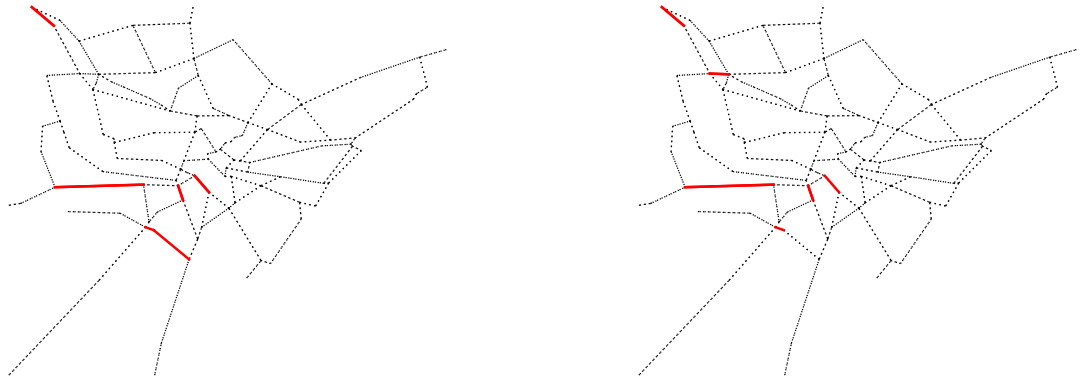

(a) An optimal solution (b) The best feasible solution

Figure 3.5: Network designs based on the optimal and the best feasible solution by Algorithm 6

hazmat can influence on each arc, the OD pairs for each kind of hazmat and the demand of hazmat accordingly.

3.6.1 Data Analysis

For a transportation network, we can obtain the network structure and related data including arc length l_{ij} and the population density τ_{ij}. For each arc (i, j), the accident probability p_{ij} and the accident consequence c_{ij}^s to transport hazmat s should also be provided. To specify the accident probability p_{ij}, we can use

$$p_{ij} = 3.19922 \times 10^{-7} \times l_{ij} \tag{3.72}$$

where 3.19922×10^{-7} is the hazmat accident rate per mile/vehicle (Federal Motor Carrier Safety Administration, 2001). The accident consequence for an arc is quantified by the population exposure impacted if that accident happens. We use the following formula to

estimate c_{ij}^{s} (Toumazis and Kwon, 2016)

$$c_{ij}^{s} = 3.14159 \times d_{s}^{2} \times \tau_{ij} \tag{3.73}$$

where 3.14159 is the ratio of a circle's circumference to its diameter. For different kinds of hazmat, the impacted radius of an accident is different. The impacted radius d_s is selected based on the recommendations of the Emergency Response Guidebook (2012) for the length of the evacuation radius in the case of an accident involving hazmat, which ranges between 0.5 and 1 mile depending on the type of the hazmat of shipment s. τ_{ij} is the population density along arc (i, j).

Our proposed model is a path-based hazmat network design model which requires specified path alternatives by hazmat carriers. The k shortest path algorithm of Yen (1971) is used to generate path sets. Despite the modifications or improvements of k shortest path algorithm, this approach rarely emphasizes on accident consequences of arcs. If the set of path alternatives obtained by k shortest path algorithm is very small, for example, only five paths for each shipment, some important arcs with high chosen probabilities and high risks can be left out. On the other hand, it is nearly impossible to solve our proposed model enumerating all paths for all shipments due to the tremendous model size. For example, there are more than 30,000 variables and 100,000 constraints for a network with 100 arcs, 3 shipments and 100 paths available for each shipment. Hazmat carriers can be restricted to some roads due to massive weights, large heights and long lengths for trucks. Usually, hazmat carriers select a route within a limited number of path alternatives. We use k shortest path algorithm to enumerate a list of paths that includes the shortest 50 paths for each shipment.

3.6.2 Computation Performance

The computational scheme in Section 3.5 is coded in the Julia Language with the JuMP.jl package (Dunning et al., 2017) and CPLEX solver of version 12.6 is used. The experiments are implemented on a computer with 8GB of RAM and a 2.7GHz processor.

Table 3.3 shows the computation time and objective values using Algorithm 2 and Algorithm 3. To accelerate the computation, Algorithm 3 is terminated when the solution is not improved within the next fifty iterations. With the proposed algorithms, the average computation time to solve CVaR minimization problem of Ravenna network is 3 hours for different probability threshold values. The exact algorithm that uses CPLEX solver of version 12.6 to solve $f_\alpha(r)$ for every r is inadequate to solve the problem, because the optimality gap solving $f_\alpha(r)$ with CPLEX is 99.9% after 24 hours.

For the Ravenna network, the road-ban decisions with different probability threshold values can be seen in Figure 3.6. For example, when $\alpha = 0.900$ and $\alpha = 0.950$, the optimal network designs are the same. Regulators for hazmat transportation have different attitudes towards risks but may end up with the same optimal network design. Theoretically, the higher the probability threshold α is, the more we focus on severe accidence consequences. With the increasing of the probability threshold value, the optimal network design for the proposed model can vary a lot. The optimal network design of $\alpha = 0.990$ only has two common closed arc – arc $(78, 74)$ and $(106, 105)$ with $\alpha = 0.900$ and $\alpha = 0.950$. For example, closing arc $(3, 6)$ plays a significant role in reducing risk with $\alpha = 0.990$ but not in $\alpha = 0.900$ and $\alpha = 0.950$ cases. If we close arc $(3, 6)$, the large accident consequences by hazmat within 1% chance to happen can be avoided while it may not be effective to reduce the risk brought by 10% potential hazmat truck accidents.

3.6.3 Comparisons for Algorithms

To solve the CVaR minimization network design model, Algorithms 2 and 3 are proposed. Algorithm 2 and the CPLEX solver can also be used to solve the problem. Al-

Table 3.3: Numerical results for different probability threshold value α in the Ravenna network

α	Computation time	Closed arcs
0.900	2hr 53min	(17, 19), (22, 38), (9, 10), (78, 74), (105, 106), (20, 10), (38, 22), (74, 78), (10, 5), (106, 105)
0.910	3hr 20min	(17, 19), (22, 38), (9, 10), (78, 74), (105, 106), (20, 10), (38, 22), (74, 78), (10, 5), (106, 105)
0.920	3hr 22min	(17, 19), (22, 38), (9, 10), (78, 74), (105, 106), (20, 10), (38, 22), (74, 78), (10, 5), (106, 105)
0.930	3hr 26min	(17, 19), (22, 38), (9, 10), (78, 74), (105, 106), (20, 10), (38, 22), (74, 78), (10, 5), (106, 105)
0.940	3hr 17min	(17, 19), (22, 38), (9, 10), (78, 74), (105, 106), (20, 10), (38, 22), (74, 78), (10, 5), (106, 105)
0.950	3hr 22min	(17, 19), (22, 38), (9, 10), (78, 74), (105, 106), (20, 10), (38, 22), (74, 78), (10, 5), (106, 105)
0.960	3hr 26min	(17, 19), (22, 38), (9, 10), (78, 74), (105, 106), (20, 10), (38, 22), (74, 78), (10, 5), (106, 105)
0.970	3hr 52min	(2, 7), (4, 17), (22, 38), (62, 54), (74, 69), (74, 76), (105, 106), (38, 22), (74, 78), (106, 105)
0.980	3hr 46min	(3, 6), (6, 11), (62, 54), (83, 66), (60, 58), (78, 74), (5, 10), (54, 62), (8, 11), (76, 74)
0.990	2hr 44min	(15, 22), (74, 76), (75, 76), (6, 3), (54, 62), (66, 83), (76, 75), (74, 78), (10, 5), (106, 105)
0.991	2hr 37min	(15, 22), (74, 76), (75, 76), (6, 3), (54, 62), (66, 83), (76, 75), (74, 78), (10, 5), (106, 105)
0.992	2hr 38min	(15, 22), (74, 76), (75, 76), (6, 3), (54, 62), (66, 83), (76, 75), (74, 78), (10, 5), (106, 105)
0.993	2hr 38min	(15, 22), (74, 76), (75, 76), (6, 3), (54, 62), (66, 83), (76, 75), (74, 78), (10, 5), (106, 105)
0.994	3hr 2min	(15, 22), (74, 76), (75, 76), (6, 3), (54, 62), (66, 83), (76, 75), (74, 78), (10, 5), (106, 105)
0.995	3hr 1min	(15, 22), (74, 76), (75, 76), (6, 3), (54, 62), (66, 83), (76, 75), (74, 78), (10, 5), (106, 105)
0.996	3hr 2min	(15, 22), (74, 76), (75, 76), (6, 3), (54, 62), (66, 83), (76, 75), (74, 78), (10, 5), (106, 105)
0.997	2hr 4min	(8, 15), (69, 56), (83, 66), (78, 74), (105, 106), (66, 83), (8, 11), (74, 78), (38, 54), (106, 105)
0.998	2hr 35min	(8, 15), (69, 56), (83, 66), (78, 74), (105, 106), (66, 83), (8, 11), (74, 78), (38, 54), (106, 105)
0.999	2hr 4min	(8, 15), (69, 56), (83, 66), (78, 74), (105, 106), (66, 83), (8, 11), (74, 78), (38, 54), (106, 105)

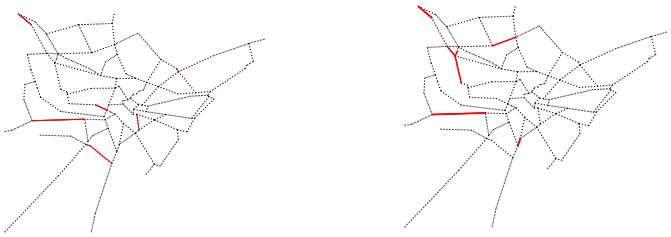

(a) Determin. (b) $\alpha = 0.900$

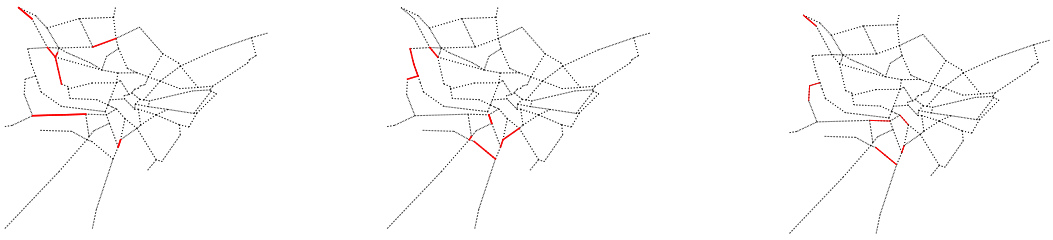

(c) $\alpha = 0.950$ (d) $\alpha = 0.990$ (e) $\alpha = 0.999$

Figure 3.6: Ravenna road-ban with different probability threshold value α

gorithm 3 and the CPLEX solver are compared for the values of $f_\alpha(r)$ obtained. CPLEX may not return an optimal solution for $f_\alpha(r)$ within limited time. We have restricted 30 minutes as time limit for both Algorithm 3 and CPLEX. Seen from (3.55), $f_\alpha(r)$ can be estimated by solving an MILP which only relates to r. Let $f_\alpha(r) = r + \frac{1}{1-\alpha}h(r)$ and $h(r)$ denote the objective value of the MILP. Given r values, Table 3.4 shows the obtained $h(r)$ by using Algorithm 3 and CPLEX solver.

It can be seen that Algorithm 3 performs better than CPLEX in solving the MILPs and obtaining $f_\alpha(r)$. Algorithm 3 can provide acceptable solutions for $f_\alpha(r)$ thus proceeding Algorithm 2.

3.6.4 Comparisons of Models

To show the value of our model, we compare SPP and RUM route-choice models with various CVaR measures in Table 3.5. Note that when $\alpha = 0$, the CVaR_α measure is equiv-

Table 3.4: Comparisons of algorithms to obtain $f_\alpha(r)$ for the Ravenna network. $f_\alpha(r) = r + \frac{1}{1-\alpha}h(r)$ and $h(r)$ is a MILP.

r value ($\times 10^3$ population exposure)	$h(r)$		$\frac{h(r)_{\text{CPLEX}} - h(r)_{\text{Algorithm 3}}}{h(r)_{\text{Algorithm 3}}}$
	Algorithm 3	CPLEX	
0.454	0.046	0.079	72.8 %
0.265	0.091	0.152	67.7 %
0.427	0.053	0.086	64.2 %
0.130	0.167	0.255	52.9 %
0.352	0.068	0.110	62.7 %
0.199	0.120	0.191	59.3 %
0.165	0.133	0.213	60.7 %
0.231	0.109	0.171	57.8 %
0.183	0.124	0.201	61.4 %
0.174	0.130	0.207	59.3 %
0.191	0.121	0.196	62.1 %
0.197	0.122	0.192	57.7 %
0.186	0.123	0.199	61.1 %
0.193	0.123	0.194	58.1 %
0.189	0.123	0.197	59.8 %
0.188	0.123	0.198	60.7 %

alent to the ER measure. When using the SPP model with $\alpha = 0$, it is equivalent to the deterministic model described in in Section 4.4. As the probability threshold value α increases, it is preferred to close short arcs in SPP-CVaR$_\alpha$ while there is no pattern for our proposed model. In addition, our proposed RUM-CVaR$_\alpha$ model tends to close higher risk (population density) arc than SPP-CVaR$_\alpha$ model does with the same probability threshold value α.

To show the value of our proposed model using RUM and CVaR, we first define various measures that are similar to the values of stochastic solutions (VSS) used to compare the performance of stochastic solutions with the performance of the deterministic solutions in stochastic environments (Birge, 1982). We define the Value of the RUM Solutions (VRS) over SPP solutions. When ER is used as the risk measure, we define VRS as follows

$$\text{VRS} = \frac{\text{(RUM-ER measure of the SPP-ER solution)} - \text{(Optimal RUM-ER)}}{\text{(Optimal RUM-ER)}} \tag{3.74}$$

Table 3.5: Comparisons of SPP-CVaR and RUM-CVaR models for the Ravenna network

Model	Probability threshold α	Risk Measure Values				Closed Arcs (in average)	
		SPP ER	RUM ER	SPP CVaR$_\alpha$	RUM CVaR$_\alpha$	Length (mile)	Population density (/mile^2)
SPP CVaR$_\alpha$	0	358.1	419.7	358.1	419.7	8.10	207.1
	0.9	364.8	396.8	698.1	783.4	6.17	215.2
	0.91	364.8	396.8	700.3	794.3	6.17	215.2
	0.92	364.8	389.9	702.4	769.3	6.42	295.6
	0.93	364.8	389.9	704.6	781.1	6.42	295.6
	0.94	364.8	389.9	707.5	796.7	6.42	295.6
	0.95	364.8	389.9	711.6	818.7	6.42	295.6
	0.96	364.8	389.9	717.8	851.6	6.42	295.6
	0.97	364.8	389.9	728.0	906.5	6.42	295.6
	0.98	364.8	389.9	748.5	1016.2	6.42	295.6
	0.99	374.2	424.9	808.5	1456.9	6.11	215.2
	0.991	374.2	424.9	820.2	1494.6	6.11	215.2
	0.992	397.5	474.8	832.4	1660.2	4.62	244.6
	0.993	397.5	474.8	839.9	1711.0	4.62	244.6
	0.994	397.5	474.8	849.8	1778.9	4.62	244.6
	0.995	397.5	474.8	863.8	1849.6	4.62	244.6
	0.996	397.4	459.8	884.2	1935.7	4.17	229.3
	0.997	397.4	459.8	911.7	2032.4	4.17	229.3
	0.998	398.1	423.4	965.9	2113.0	3.55	184.5
	0.999	398.1	423.4	1113.8	2434.2	3.55	184.5
RUM CVaR$_\alpha$	0	363.5	376.4	363.5	376.4	6.78	324.8
	0.9	372.1	405.4	718.7	762.4	7.83	345.9
	0.91	372.1	405.4	723.0	767.1	7.83	345.9
	0.92	372.1	405.4	727.5	768.1	7.83	345.9
	0.93	372.1	405.4	733.3	769.5	7.83	345.9
	0.94	372.1	405.4	741.0	812.7	7.83	345.9
	0.95	372.1	405.4	751.8	837.9	7.83	345.9
	0.96	372.1	405.4	768.0	875.6	7.83	345.9
	0.97	385.1	408.2	771.3	890.1	8.88	376.4
	0.98	402.4	423.4	846.4	970.0	4.59	181.5
	0.99	402.2	444.3	833.7	1165.4	5.08	298.9
	0.991	402.2	444.3	839.7	1205.8	5.08	298.9
	0.992	402.2	444.3	847.1	1255.0	5.08	298.9
	0.993	402.2	444.3	856.7	1315.1	5.08	298.9
	0.994	402.2	444.3	869.5	1388.1	5.08	298.9
	0.995	402.2	444.3	887.4	1442.6	5.08	298.9
	0.996	402.2	444.3	913.2	1450.3	5.08	298.9
	0.997	389.2	435.7	1239.2	1459.6	5.80	247.4
	0.998	389.2	435.7	1272.9	1463.4	5.80	247.4
	0.999	389.2	435.7	1373.7	1487.0	5.80	247.4

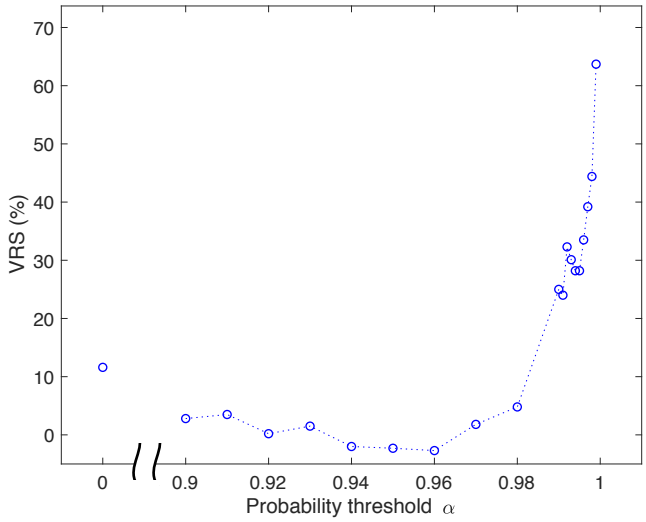

Figure 3.7: The value of RUM solutions over SPP solutions

and when CVaR_α is used as the risk measure,

$$\text{VRS} = \frac{(\text{RUM-CVaR}_\alpha \text{ of the SPP-CVaR}_\alpha \text{ solution}) - (\text{Optimal RUM-CVaR}_\alpha)}{(\text{Optimal RUM-CVaR}_\alpha)} \tag{3.75}$$

VRS measures how much we gain by considering RUM compared to SPP. Figure 3.7 presents VRS with various α values. We observe that as α increases VRS tends to increase. This shows that the value of probabilistic modeling becomes significant, when we are interested in low-probability high-consequence outcomes and more risk averse. On the other hand, for mid-range α values, VRS is not significant. Note that for some α values, VRS value becomes negative, which happens since our algorithm finds a suboptimal solution in general.

Similarly, we define the Value of the CVaR_α Solutions (VCS_α) over ER solutions. When SPP is used for route-choice modeling, we define VCS_α as follows:

$$\text{VCS}_\alpha = \frac{(\text{SPP-CVaR}_\alpha \text{ of the SPP-ER solution}) - (\text{Optimal SPP-CVaR}_\alpha)}{(\text{Optimal SPP-CVaR}_\alpha)} \tag{3.76}$$

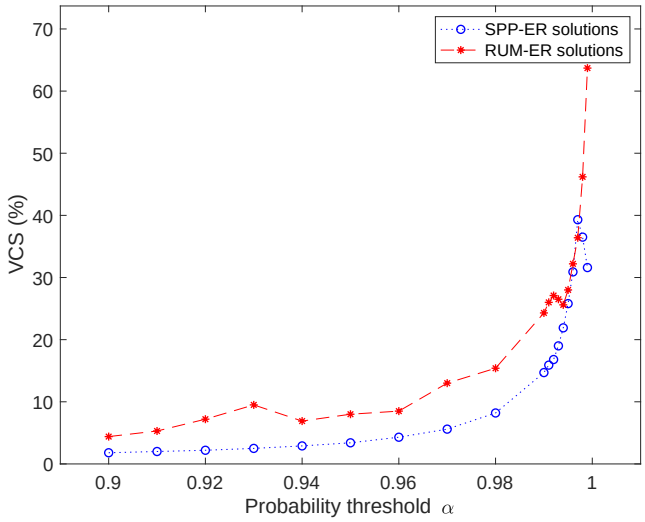

Figure 3.8: The value of CVaR_α solutions over ER solutions with SPP and RUM for route-choice modeling

When RUM is used for route-choice modeling,

$$\text{VCS}_\alpha = \frac{(\text{RUM-CVaR}_\alpha \text{ of the RUM-ER solution}) - (\text{Optimal RUM-CVaR}_\alpha)}{(\text{Optimal RUM-CVaR}_\alpha)} \tag{3.77}$$

VCS measures how much we gain by considering CVaR_α compared to ER. Figure 3.8 shows VCS with various α values for both cases with SPP and RUM for route-choice modeling. We observe that VCS increases significantly as α increases. In all α values, the value of CVaR solutions becomes more apparent when RUM is used for route-choice modeling.

Finally, we also define the Value of the RUM-CVaR_α Solutions (VRCS_α), over SPP-ER solutions:

$$\text{VRCS}_\alpha = \frac{(\text{RUM-CVaR}_\alpha \text{ of the SPP-ER solution}) - (\text{Optimal RUM-CVaR}_\alpha)}{(\text{Optimal RUM-CVaR}_\alpha)} \tag{3.78}$$

Figure 3.9 shows VRCS with various α values. For lower α values, while the overall value of RUM-CVaR_α solution is marginal in the range of 4.9% to 8.6%, it clearly gives advantages if compared with VCS in Figure 3.7. For higher α values, however, we find VRCS in the range of 16.7% to 64.1%. By using both RUM and CVaR_α in decision-making, we con-

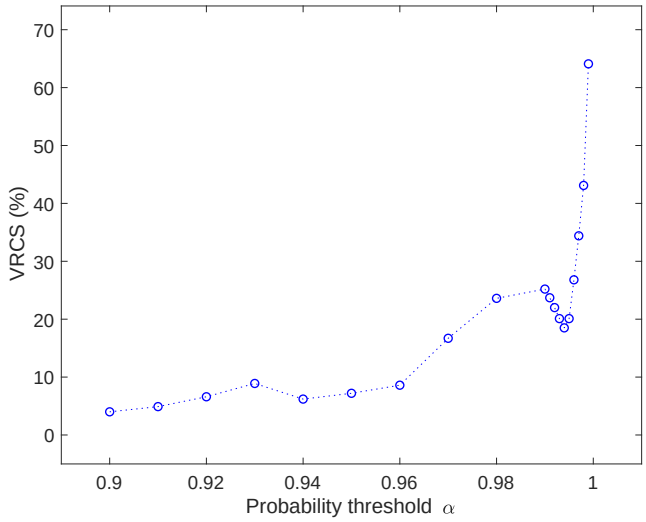

Figure 3.9: The value of RUM-CVaR$_\alpha$ solutions over SPP-ER solutions

clude that risk-averse hazmat network designers can obtain clear merits for all probability threshold values, especially for higher values.

In the Ravenna network, the optimal network designs by the proposed model and the deterministic model yield different available paths for shipments with which lead to different risks. The comparisons of available paths for transporting methanol from node 110 to node 105 by both models are shown in Table 3.6. For each path, the length, the ER to transport methanol and the probability to be chosen by hazmat carriers are given. It is found that two of the available paths are the same while the rest of them are different either in length or ER for both models. The lowest ER path in both models is Path 1. It can be seen that Path 1 has 24.6% chance to be traveled in SPP-ER model while it has the probability of 34.5% to be traveled in the proposed model. The proposed model assigns larger probabilities for low risk paths than SPP-ER model does.

3.7 Concluding Remarks

In this chapter, we formulate a road-ban problem in hazardous hazmat transportation considering the uncertainty of routing behavior and a risk-averse measure for hazmat ac-

Table 3.6: Comparisons of available paths for transporting methanol from node 110 to node 105 between RUM-CVaR and the deterministic (SPP-ER) model for the Ravenna network

Model		Path	Length	ER	Prob
RUM-CVaR$_{0.99}$	1:	$110 \to 104 \to 83 \to 78 \to 62 \to 54 \to 45 \to 31 \to 98 \to 14 \to 11 \to 6 \to 3 \to 5 \to 105$	18.24	0.0149	0.345
	14 :	$110 \to 104 \to 83 \to 78 \to 62 \to 54 \to 45 \to 43 \to 36 \to 30 \to 26 \to 24 \to 20 \to 10 \to 5 \to 105$	26.04	0.0169	0.158
	19 :	$110 \to 104 \to 83 \to 78 \to 62 \to 54 \to 56 \to 46 \to 43 \to 36 \to 30 \to 26 \to 24 \to 20 \to 10 \to 5 \to 105$	26.87	0.0168	0.146
	26 :	$110 \to 104 \to 83 \to 78 \to 62 \to 54 \to 45 \to 43 \to 36 \to 30 \to 26 \to 24 \to 20 \to 10 \to 9 \to 7 \to 5 \to 105$	28.17	0.0172	0.128
	34 :	$110 \to 104 \to 83 \to 78 \to 62 \to 54 \to 56 \to 46 \to 43 \to 36 \to 30 \to 26 \to 24 \to 20 \to 10 \to 9 \to 7 \to 5 \to 105$	29.00	0.0172	0.118
	44 :	$110 \to 104 \to 83 \to 78 \to 62 \to 54 \to 56 \to 46 \to 43 \to 45 \to 31 \to 98 \to 14 \to 11 \to 6 \to 3 \to 5 \to 105$	30.18	0.0171	0.105
SPP-ER	1 :	$110 \to 104 \to 83 \to 78 \to 62 \to 54 \to 45 \to 31 \to 98 \to 14 \to 11 \to 6 \to 3 \to 5 \to 105$	18.24	0.0149	0.246
	3 :	$110 \to 104 \to 83 \to 78 \to 62 \to 57 \to 58 \to 38 \to 54 \to 45 \to 31 \to 98 \to 14 \to 11 \to 6 \to 3 \to 5 \to 105$	19.93	0.0169	0.207
	5 :	$110 \to 104 \to 83 \to 78 \to 74 \to 76 \to 69 \to 56 \to 54 \to 45 \to 31 \to 98 \to 14 \to 11 \to 6 \to 3 \to 5 \to 105$	23.26	0.0157	0.149
	8 :	$110 \to 104 \to 83 \to 78 \to 74 \to 69 \to 56 \to 54 \to 45 \to 31 \to 98 \to 14 \to 11 \to 6 \to 3 \to 5 \to 105$	24.77	0.0160	0.128
	18 :	$110 \to 104 \to 83 \to 78 \to 74 \to 76 \to 69 \to 56 \to 46 \to 43 \to 45 \to 31 \to 98 \to 14 \to 11 \to 6 \to 3 \to 5 \to 105$	26.69	0.0164	0.106
	27 :	$110 \to 104 \to 83 \to 78 \to 74 \to 69 \to 56 \to 46 \to 43 \to 45 \to 31 \to 98 \to 14 \to 11 \to 6 \to 3 \to 5 \to 105$	28.20	0.0167	0.091
	44 :	$110 \to 104 \to 83 \to 78 \to 62 \to 54 \to 56 \to 46 \to 43 \to 45 \to 31 \to 98 \to 14 \to 11 \to 6 \to 3 \to 5 \to 105$	30.18	0.0171	0.073

cident consequences. With the probabilistic route choice, the risk distribution for hazmat transportation incorporates with not only the road accident probability but also the carriers routing behavior. Following Toumazis et al. (2013), we introduce conditional value-at-risk (CVaR) as a general, coherent, and risk-averse approach. We present a CVaR minimization model for hazmat network design problems. The proposed model is a mixed-integer nonlinear program, which can be decomposed into two stages: (1) searching the optimal solution for a nonnegative variable; (2) solving MILPs given the nonnegative variable. We develop a line search with mapping based on Benders decomposition for solving MILP sub-problems and obtain quality network design solutions.

We present case studies in the real road network of Ravenna. The comparisons of algorithms show that the proposed methods can solve the CVaR minimization network design problem efficiently and generate quality network design solutions. To highlight the value of our model, comparisons of the deterministic model and the proposed model are conducted. When the confidence level of CVaR is small, it indicates that decision makers and regulators for the transportation network pay limited attention on sever accidents.

With the proposed algorithms, the average computation time to solve CVaR minimization problem of a 105-node and 268-arc network was 3 hours for different probability threshold α values. The exact algorithm that uses CPLEX solver of version 12.6 was not inadequate to solve even a linear subproblem, because the optimality gap solving $f_\alpha(r)$ with CPLEX was 99.9% after 24 hours.

While the proposed algorithm was shown to be effective, for large-scale urban networks, we will need a faster algorithm. Since the proposed algorithm relies on solutions of multiple MILP problems, it is not suitable for large-scale networks. Developing a fast heuristic algorithm is a potential future research direction.

4 Optimal Deployment of Dynamic Wireless Charging Lanes for Electric Forklifts in Congested Warehouses

4.1 Introduction

Dynamic wireless charging infrastructures are in the early stage of commercialization. As the growing number of EVs, there is a great potential market for dynamic wireless charging technologies that allow charging when vehicles are moving. As a special type of EVs, battery-based forklifts are used for order picking and item transaction in warehouses. In such applications, dynamic wireless charging systems can be considered as a suitable option because it can improve the operation efficiency of forklifts, enhance the safety of charging batteries and prolong the lifetime of batteries with power tracks.

With some wireless charging lanes, forklifts perform routing which considers the dynamic battery level under unavoidable congestions to pick up orders. The wireless charging lane location optimization provides the optimal wireless infrastructure layout addressing order pick-ups and wireless charging needs. In the presence of wireless charging lanes and dynamic routing for orders, the traffic patterns within the warehouse change significantly. To address such changes, a congestion model for variable travel time is needed. In addition, the orders from a warehouse are pre-batched for a single trip to generate a reasonable case. A typical number of orders in a warehouse can range between 500 and 2000 per hour (Ruben and Jacobs, 1999; II, 2000; Gong and De Koster, 2008). Multiple forklifts pick up these orders with multiple trips. This chapter considers a small number of orders that a single trip can pick up with multiple forklifts. Prorated the wireless charging lane costs into short-term basis, it can be seen as a short-term operation optimization

of a warehouse. To consider the uncertainty of orders for short-term operation, different scenarios of order demand and location are sampled to formulate a two-stage stochastic programming problem.

The contributions of this chapter can be summarized as follows. To the best of our knowledge, this is the first chapter that develops a dynamic wireless charging lane location optimization model for warehouses. In addition, the chapter considers the congestions of electric forklifts in narrow aisles. Instead of simply avoiding congestions, forklifts can take advantage of congestions to charge batteries. To consider the uncertainty of orders, a two-stage stochastic programming model for optimal deployment of dynamic wireless charging lanes for electric forklifts in a congested warehouse is formulated. We introduce symmetry breaking constraints and devise a scenario decomposition algorithm to solve the stochastic programming model efficiently. We confirm the efficiency of the algorithms and the key advantages of dynamic wireless charging lanes via case studies.

4.2 Literature Review

4.2.1 Warehouse Congestion Management and Forklift Routing

Congestions in warehouses can lead to problems such as damaged properties, injured workers (Tompkins et al., 2010) and inefficient operations (Heath et al., 2013) attracting attentions over the decades. Queuing models are addressed by researchers to give some hints of facility designs with warehouse congestions. Srinivasan and Bozer (1992) presented a simulation model that identified the queuing congestion in a job shop with machines and the material handling system. In the work by Smith and Li (2001), the warehouse congestion is modeled with a $M/G/C/C$ queue to incorporate with the department assignments minimizing the expected number of customers. The work-in-process (WIP) can demonstrate the warehouse congestion in many job shops. Since it has been questioned for years that how the warehouse layout affects the congestions, Benjaafar (2002) developed a quadratic assignment model to explore the optimal facility layout

which can achieve the minimum expected WIP. This chapter also employed queuing theory to analyze the expected WIPs.

Not only designing the facility layouts and material handling systems but also proper utilization of the equipments can contribute to congestion alleviation. Typically, the material handling system that represents the movements of items within warehouses are studied. The dispatching rules and routing for those vehicles are addressed in decades for efficient warehouse operations. Egbelu and Tanchoco (1984) presented five vehicle assignment rules for AGVs in work center initiated task assignment and seven rules in vehicle initiated task assignment to show how vehicle dispatching rule can influence a job shop. Broadbent et al. (1985) solved the conflict-free shortest time vehicle routing in the context of job shop with a branch and bound algorithm. Considering multiple objectives and constraints in vehicle routing within a facility, Rajotia et al. (1998) proposed a dynamic routing which allows the trade-offs between short and safe routes to resolve the conflicts and congestions. Maza and Castagna (2005) focused on the dynamic routing for AGV system to find the shortest routes while avoiding conflicts and deadlocks. Different from analytical approaches for vehicle routing in the facilities, reinforced learning can help to estimate the travel time and other route performance factors without explaining the mechanisms. Driven by the reinforced learning, Lim et al. (2002) constructed routes that have the minimal expected total travel time. The work above emphasizes on avoiding conflicts in vehicle routing. Neither of them studied congestion alleviations by design the facility and vehicle routing.

In addition to using queuing theories and vehicle conflicts to reflect congestions, the congestion measures have been established in many papers. Maxwell and Muckstadt (1982) used vehicle blocking time to quantify congestions. Vosniakos and Davies (1989) defined a vehicle inference activity in the simulation model and used the segment utilization which is the percentage of the simulation time that an AGV has been occupying and the blockage time to demonstrate congestions. Lee et al. (1990) evaluated several factors

including total wait time, wait time at the intersections, and the utilization of AGVs to design an efficient AGV system. Among those factors, the wait time at the intersections can clearly demonstrate the vehicle congestions. Kim and Tanchoco (1993) minimized the total travel cost of vehicles considering vehicle operations such as lane restrictions to consider the workflow inferences. The works reviewed are either not analytically based due to their implementations of simulation or not clearly defined for the congestion effects. Unlike warehouse congestions, traffic congestions have been well studied with the explicit relationship between system travel time and traffic volume.

4.2.2 Wireless Charging Optimization

The recent progress in wireless charging techniques and development of commercial products have enabled safe and convenient transfer of energy. This section reviews the wireless charging techniques and their recent advances in applications for the potential use of warehouse operations. For discussion of forklift applications, the near-field wireless charging which requires close distance between chargers and devices can be used. Besides, the dynamic wireless charging for forklifts can provide power transfer while vehicles are moving. The near-field dynamic charging applications can be realized with inductive coupling and magnetic resonance coupling (Kurs et al., 2007). The major applications of near-field dynamic wireless charging include robot manipulation (Gao, 2007; Kawamura et al., 1996), people-mover systems (Jufer, 2008), high speed trains (Kim et al., 2015) and energization for the battery of electric vehicles (Severns et al., 1996; Kisacikoglu et al., 2015).

For warehouse operations, wireless charging can be applied to vehicles with batteries. The near-field charging enables charging vehicles both statically and dynamically (Lukic and Pantic, 2013). Despite that there are limited wireless charging studies for warehouse vehicles, many papers can be found discussing the installation of charging stations for EVs. Flow-capturing location model (Hodgson, 1990) is widely used to determine the

service locations such as convenience stores, gasoline stations and banking machines. The EV charging location problems can be formulated as flow-capturing models which considers the charging availability and charging access. Frade et al. (2011) proposed an optimization model to achieve the maximum demand coverage differentiating daytime and nighttime demands. The model presented by Chen et al. (2013) minimized the EV users' station access costs while penalizing unmet demand. Riemann et al. (2015) proposed a facility location model for EV stations to capture the maximum traffic flow on a network. The stochastic user equilibrium is used to analyze EV drivers' routing choice behavior and describe the interaction between traffic flow patterns and the location of the charging facilities. The works above do not consider the battery consumption of EVs in charging due to lack of data. In warehouse operations, the battery levels of vehicles can be obtained. Therefore, the charging strategy can also be considered with regard to battery lifetime, time-in-use prices and other factors. Cao et al. (2012) determined the battery charging time and charging levels by minimizing the energy cost. Jeong et al. (2015) economically allocated the power tracks and determined the battery size with the constraints of battery levels. These literatures can provide a solid foundation for the wireless charging optimization in warehouses to develop a safe, efficient and economic production system.

4.3 Problem Statement

In this section, we introduce the problem of deployment of dynamic wireless charging lanes for electric forklifts in a congested warehouse. The installation of wireless charging infrastructure in warehouses supports the order-picking by electric forklifts via necessary charging. Electric forklifts are routing to pick up the assigned order batches with sufficient battery levels.

The warehouse settings are similar to II (2000), Gong and De Koster (2008) and Hong et al. (2012). A typical warehouse layout is shown in Figure 4.1. In such warehouses,

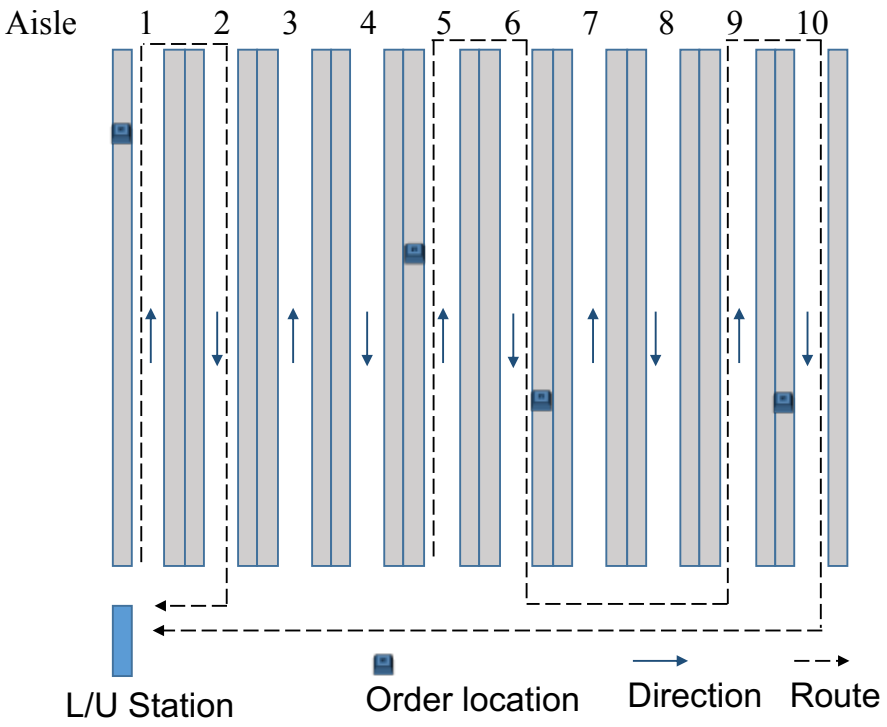

Figure 4.1: The order-picking in warehouses with electric forklifts

forklifts pick orders which are stored in bins along narrow aisles. Usually, the time spent in these narrow aisles is far more than the travel time in open space of a warehouse due to necessary loading/unloading and potential congestions in aisles. Hence, it is assumed that the travel time in open space of the warehouse is ignored. To prevent forklifts from being blocked in an aisle by pickers approaching from the opposite direction and reduce the chance of collisions of forklifts, a common approach is labeling aisles with single directions. Although large warehouses can have some bidirectional aisles, a bidirectional aisle can be considered as two separate aisles with opposite directions. These parallel aisles in warehouses can provide a simple network structure. Instead of using the node-arc representation for a network, we can simply use aisles to demonstrate the network of a warehouse. Namely, a route in a warehouse is represented by the sequence of aisles that forklifts can traverse. Due to the limited number of aisles with directions, all routes

in a warehouse can be enumerated. The properties of warehouse networks motivate us modeling the routing of electric forklifts with a route-based approach.

Different from the congestion of urban transportation, warehouse congestion involves a small number of vehicles. Congestion often happens because of the conflicts of forklift movements. For example, forklift 1 needs to pick up an order in an aisle while forklift 2 is loading an item and blocking the way for forklift 1. Forklift 1 should decelerate, stop and wait until forklift 2 completes the pick-up. Such events can be referred as interruptions along aisles. The more interruptions for forklifts on an aisle, the more likely to have long travel time. Interruption in warehouse is a common phenomenon which motivates the modeling of congestion dependent travel time in this chapter.

There can be thousands of orders that need to be processed in a warehouse every day. A warehouse can operate ranging from 8 hours to 24 hours in which multiple forklifts finish multiple trips to pick up all orders. Although existing literatures (Hong et al., 2012; Clarke and Wright, 1964; De Koster et al., 1999) considered batching for hundreds of orders in parallel-aisle warehouses, an order-batching problem can be directly formulated as MILPs. In addition to order-batching for forklifts, this work models the warehouse congestion and involves the battery level constraints which lead to great challenges in computations. Meanwhile, the modeling of warehouse congestions and battery level tracking introduces a large number of constraints with big-M parameter showed in Section 4.4. Therefore, the deployment of dynamic wireless charging problem for electric forklifts does not consider a large number of orders. This chapter considers a small number of orders that a single trip can pick up with multiple forklifts. It can be seen as a short-term operation problem of warehouse. A deterministic model for short-term deployment of dynamic wireless charging lanes for electric forklifts in a congested warehouse is developed. To consider the uncertainty of orders for short-term operation, different scenarios of order demand and location are sampled to formulate a two-stage stochastic program-

ming problem. To prepare for the model formulation, Section 4.3.1 and 4.3.2 are presented first.

4.3.1 Congestion Dependent Travel Time

It is assumed that congestions only happen in narrow aisles. Forklifts slow down when there are congestions thus increasing the travel time. There are various types of models for analyzing the congestions. Here, we use the interruption model of vehicles to link congestions and travel time. Zhang et al. (2009) proposed an optimization model of flow routing to alleviate the congestions by incorporating interruption events as Poisson process. The analytical approach in this work provides a framework for further study in warehouse management. We model the number of interruptions as space Poisson process in aisle $a \in \mathcal{A}$ and calculate the travel time with the following formula

$$t_a = \sum_{n=0}^{\infty} P_n(r_a) T_{na} \tag{4.1}$$

where $P_n(r_a)$ is the probability that n interruptions occur with interruption rate r_a and T_{na} is the travel time with n interruptions. $P_n(r_a)$ is expressed as

$$P_n(r_a) = (r_a d_a)^n \frac{e^{-r_a d_a}}{n!} \tag{4.2}$$

where d_a is the length for aisle $a \in \mathcal{A}$. To calculate the travel time with n interruptions T_{na}, we assume that the interruptions are uniformly distributed along aisle a. Given the locations of interruptions, the detailed steps of computing T_{na} can be referred (Zhang et al., 2008). The model for effect of traffic flow on congestion used in this chapter is as follows (Zhang et al., 2009).

$$r_a = 0.61 d_a^{-0.8722} e^{0.000918 f_a}. \tag{4.3}$$

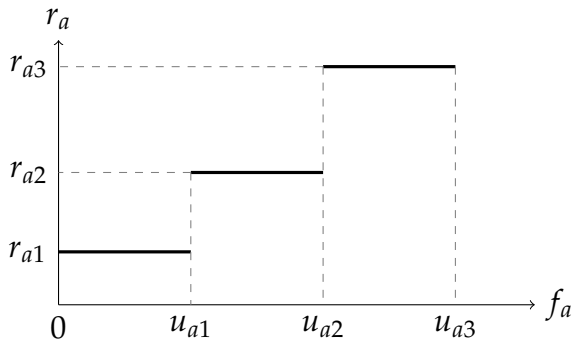

Figure 4.2: Piecewise step linearization for interruption rate of aisle $a \in \mathcal{A}$ with $|\mathcal{L}| = 3$

f_a is the number of vehicles traveling through the aisle accordingly.

Let $\mathcal{L}$ be the set of congestion level and $|\mathcal{L}|$ be the number of pieces of the step function for linearization of interruption rate. An example of linearization for a interruption model is shown in Figure 4.2. Given the value of traffic flow u_{al} at congestion level $l \in \mathcal{L}$ for aisle $a \in \mathcal{A}$, Equation (4.1) and (4.2) can be used to estimate the travel time t_{al}. In the following sections, the congestion effect for optimal deployment of dynamic wireless charging lanes for forklifts is modeled with congestion level, the traffic flow at each congestion level and the travel time accordingly. Note that the concrete model formulation of interruption rate does not matter in further model development with discrete congestion levels.

4.3.2 Routes of Order Pick-Up in Parallel-Aisle Warehouses

As the increase of aisles, the number of routes increases exponentially. Given a warehouse with single directional aisles, the number of routes are 1, 4, 12, 33, 88 and 231 when the number of aisles are 2, 4, 6, 8, 10 and 12. Due to the difficulty of capture routing for order pick-up in a large warehouse, the optimal deployment of dynamic wireless charging lanes can be even harder. With multiple orders, order-batching and routing for forklifts are considered simultaneously. If we have 10 orders stored in the same aisle and the capacity of each forklift is 5 orders, we can aggregate these 10 small orders into 2 orders with larger demand size. The aggregated order set can help to reduce the problem size of order-batching and routing for forklifts thus providing benefits for further computa-

tions. In addition, some aisles are less preferred for order-picking. For example, if there is only one order stored in aisle 10 shown by Figure 4.1. A forklift tends to travel along the shortest route to pick up this order rather than pass the route that contains all aisles. Therefore, we can focus on the preferred routes and construct route set. There are two steps to generate the route set: (1) generating an elementary route set to cover each order (2) expanding the elementary route set to a combined route set with order-batching. Clarke and Wright (1964); De Koster et al. (1999) proposed the Clark and Wright II algorithm to generate reasonable route set with order-batching. A modified Clark and Wright II algorithm (Hong et al., 2012) is used to generate the combined route set.

The procedures to construct route set is summarized in Algorithm 7. The composite level is the maximum number of elementary routes covered by a combined route. With large value of composite level, the combine route set is likely to become large. A large route set can result in accurate analysis for order-batching and routing while a small route set can benefit the computation. Therefore, there is a trade-off in setting the composite level. It is recommended to set a high composite level if the warehouse is large with a large number of aisles.

4.4 The Deterministic Model

In this section, a deterministic model for optimal deployment of dynamic wireless charging lanes for electric forklifts in a congested warehouse is introduced. Later, we extend this deterministic model to a two-stage stochastic programming model.

The notation for the deterministic model is shown in Table 4.1. Here, we consider the investment cost for dynamic wireless charging lanes and the operation costs for order-picking in the objective function. Since the installation for dynamic wireless charging lanes targets at a long-term planning, its cost is prorated on a hour-basis using the net

Algorithm 7 Route Set Construction for Order Pick-Up in Parallel-Aisle Warehouses

1: Initialize order set $\tilde{\mathcal{O}} = \mathcal{O}$, elementary route set $\mathcal{R}_e = \emptyset$ and combined route set $\mathcal{R}_c = \emptyset$.

2: Aggregate order set $\mathcal{O}$.

For order $o \in O$, do

Check if there exists order $o' \in \tilde{\mathcal{O}} \cap \{1, 2, \cdots, o-1\}$ such that it is stored in the same aisles as order o.

If yes, let $o' = \max\{i : i \in \tilde{\mathcal{O}}, i \in (1, 2, \cdots, o-1), \theta_{ia} = \theta_{oa}, \forall a \in \mathcal{A}\}$.

If aggregated demand $q_{o'} + q_o \leq C$, let $q_{o'} = q_{o'} + q_o$ and $\tilde{\mathcal{O}} = \tilde{\mathcal{O}} \backslash \{o\}$.

Update $\mathcal{O} = \tilde{\mathcal{O}}$.

3: Construct elementary route set $\mathcal{R}_e$.

For order $o \in O$, do

If $\mathcal{R}_e$ does not contain a route that passes order o, generate the shortest distance route r, then let $\mathcal{R}_e = \mathcal{R}_e \cup r$.

4: Construct elementary route set $\mathcal{R}_c$.

Set the composite level for combined route construction.

For $r_i, r_j \in \mathcal{R}_e \cup \mathcal{R}_c$,

Calculate the difference s_{ij} between the distance of combined route for r_i, r_j and distance of r_i, r_j.

Sort the difference of distance s_{ij} where $r_i, r_j \in \mathcal{R}_e \cup \mathcal{R}_c$ in decreasing order.

Select the route pair such that the combined route of r_i, r_j is less than the composite level with the maximum distance difference. Update $\mathcal{R}_c$ by adding the combined route of r_i, r_j.

Repeat above until $r \in \mathcal{R}_e$ are included in $\mathcal{R}_c$.

Table 4.1: The notation for the deterministic model of deployment of dynamic wireless charging lanes problem

Set	
$\mathcal{O}$	the set of orders.
$\mathcal{A}$	the set of aisles in warehouse network.
$\mathcal{K}$	the set of vehicles.
$\mathcal{R}$	the set of routes.
Ω^r	the set of consecutive aisle pair for route $r \in \mathcal{R}$.
$\mathcal{L}$	the set of congestion level.
Parameters	
c_a	wireless charging lane cost for aisle $a \in \mathcal{A}$.
d_a	distance for aisle $a \in \mathcal{A}$.
γ	wireless charging device lifetime in years.
δ	annual interest rate.
ρ	coefficient to convert travel time to cost per minute.
u_{al}	flow amount threshold on aisle a for l-th level congestion.
$E^{\max}$	maximum battery size.
$E^{\min}$	minimum battery size.
q_o	demand for order o.
C	capacity for a forklift.
ξ_{ra}	if $\omega_{ra} = 1$, route r passes aisle a; 0 otherwise.
θ_{oa}	if $\theta_{oa} = 1$, order o is in aisle a; 0 otherwise.
ϕ	number of hours in an annual year.
p^{dis}	the discharging rate of a forklift per minute.
p^{ch}	the charging rate of a forklift per minute.
Variables	
z_a	if $z_a = 1$, a power track is installed on aisle a; 0 otherwise.
x_{kr}	if $x_{kr} = 1$, aisle r is traveled by forklift k; 0 otherwise.
y_{ok}	if $y_{ok} = 1$, order o is picked by forklift k; 0 otherwise.
η_k	if $\eta_k = 1$, forklift k is used; 0 otherwise.
v_{al}	if $v_{al} = 1$, flow on aisle a at congestion level l; 0 otherwise.
e_{ka}	battery level for forklift k at aisle a.

present value. The prorated coefficients are defined as follows:

$$W = \frac{\delta \cdot (1+\delta)^{\gamma}}{(1+\delta)^{\gamma} - 1} \cdot \frac{1}{\phi}. \tag{4.4}$$

The operation cost for order-picking is calculated by the travel time of picking all orders that arrive for a single trip and the labor cost ρ. If forklifts cannot pick up all orders arriving in one hour with a single trip, orders are pre-batched according to arriving sequence to ensure that the order set $\mathcal{O}$ in the model does not exceed the maximum workloads for a single trip. For example if all available forklifts can only finish picking orders arrived within 20 minutes with a single trip, ρ needs to be prorated to three times of labor cost per hour. Note that the prorate horizon for the cost of dynamic wireless charging lanes is consistent with the arriving time of maximum orders that forklifts can pick with a single trip. The model is formulated as follows.

$$\min_{\mathbf{z}} \quad W \sum_{a \in \mathcal{A}} c_a z_a + \rho Q(\mathbf{z}) \tag{4.5}$$

$$\text{s.t. } z_a \in \{0,1\}, \forall a \in \mathcal{A} \tag{4.6}$$

The objective (4.5) of wireless charging location problem is to minimize the investment cost of wireless charging lanes and operation cost. Equations (4.6) are binaries to determine whether to install wireless charging lanes. Given the installation of wireless charging lanes, $Q(\mathbf{z})$ is the travel time given demand q_o and location data θ_{oa} for order $o \in \mathcal{O}$. The order batching and vehicle routing constraints in a warehouse can be referred (Hong et al., 2012).

The order batching and vehicle routing model minimizes the travel costs considering battery level and congestion constraints. $Q(z)$ is defined as follows.

$$Q(\mathbf{z}) = \min_{\mathbf{x},\mathbf{y},\boldsymbol{\eta},\mathbf{v},\mathbf{e}} \sum_{k \in \mathcal{K}} \sum_{r \in \mathcal{R}} \sum_{a \in \mathcal{A}} \xi_{ra} t_a x_{kr} \tag{4.7}$$

$$\text{s.t.} \sum_{k\in\mathcal{K}} y_{ok} = 1, \qquad \forall o \in \mathcal{O} \tag{4.8}$$

$$y_{ok} \le \eta_k, \qquad \forall k \in \mathcal{K}, o \in \mathcal{O} \tag{4.9}$$

$$\sum_{r\in\mathcal{R}} x_{kr} = \eta_k, \qquad \forall k \in \mathcal{K} \tag{4.10}$$

$$\sum_{o\in\mathcal{O}} q_o y_{ok} \le C, \qquad \forall k \in \mathcal{K} \tag{4.11}$$

$$\theta_{oa} y_{ok} \le \sum_{r\in\mathcal{R}} \xi_{ra} x_{kr}, \qquad \forall o \in \mathcal{O}, k \in \mathcal{K}, a \in \mathcal{A} \tag{4.12}$$

$$\begin{aligned} e_{ra'} \le\ & e_{ra} - p^{\text{dis}} t_a + p^{\text{ch}} t_a \\ & + M(1 - z_a) + M(1 - x_{kr}), \qquad \forall k \in \mathcal{K}, r \in \mathcal{R}, (a, a') \in \Omega^r \end{aligned} \tag{4.13}$$

$$e_{ra'} \le e_{ra} - p^{\text{dis}} t_a + M z_a + M(1 - x_{kr}), \quad \forall k \in \mathcal{K}, r \in \mathcal{R}, (a, a') \in \Omega^r \tag{4.14}$$

$$E^{\min} \le e_{ra} \le E^{\max}, \qquad \forall r \in \mathcal{R}, \forall a \in \mathcal{A} \tag{4.15}$$

$$\sum_{k\in\mathcal{K}} \sum_{r\in\mathcal{R}} x_{kr} \xi_{ra} = \sum_{l\in\mathcal{L}} f_{al}, \qquad \forall a \in \mathcal{A} \tag{4.16}$$

$$f_{al} \le u_{al} v_{al}, \qquad \forall a \in \mathcal{A}, l \in \mathcal{L} \tag{4.17}$$

$$\sum_{l\in\mathcal{L}} v_{al} = 1, \qquad \forall a \in \mathcal{A} \tag{4.18}$$

$$t_a = \sum_{l\in\mathcal{L}} t_{al} v_{al}, \qquad \forall a \in \mathcal{A} \tag{4.19}$$

$$\eta_k, x_{kr}, y_{ok}, v_{al} \in \{0, 1\}, \qquad \forall k \in \mathcal{K}, r \in \mathcal{R}, o \in \mathcal{O}, a \in \mathcal{A}, l \in \mathcal{L} \tag{4.20}$$

$$t_a, f_{al}, e_{ka} \ge 0, \qquad \forall k \in \mathcal{K}, a \in \mathcal{A}, l \in \mathcal{L} \tag{4.21}$$

Equation (4.7) minimizes the total travel time to pick up all orders. Since the model considers variable travel time due to congestions, the objective function involves nonlinearity. Let $\tau_{kra} = t_a x_{kr}$. Linearization can be performed with objective function (4.22)

$$\min_{\mathbf{x},\mathbf{y},\boldsymbol{\eta},\mathbf{v},\mathbf{e},\boldsymbol{\tau}} \sum_{k\in\mathcal{K}} \sum_{r\in\mathcal{R}} \sum_{a\in\mathcal{A}} \xi_{ra} \tau_{kra} \tag{4.22}$$

where $\boldsymbol{\tau}$ are constrained by Equation (4.23).

$$\tau_{kra} \leq t_a, \forall k \in \mathcal{K}, r \in \mathcal{R}, a \in \mathcal{A} \tag{4.23a}$$

$$\tau_{kra} \leq M x_{kr}, \forall k \in \mathcal{K}, r \in \mathcal{R}, a \in \mathcal{A} \tag{4.23b}$$

$$\tau_{kra} \geq -M(1 - x_{kr}) + t_a, \forall k \in \mathcal{K}, r \in \mathcal{R}, a \in \mathcal{A} \tag{4.23c}$$

Equations (4.8) enforce the pick-up of any orders by forklifts. Equations (4.11) constrain that the forklifts do not exceed the capacity while picking up orders. With Equations (4.9), it is ensured that a forklift is used if any order is picked by this forklift. When a forklift is used, a route must be selected with Equations (4.10). Equations (4.12) state that if order $o \in \mathcal{O}$ is assigned to forklift $k \in \mathcal{K}$, forklift k must travel a route containing the aisle of order o. Equations (4.13) and (4.14) are battery tracking constraints for forklifts $k \in \mathcal{K}$ with and without wireless charging lane in aisles. Equations (4.15) are battery level limit constraints. Equations (4.17) – (4.19) are congestion constraints which are further explained in Section 4.3.1. Equations (4.20) are binaries while Equations (4.21) are nonnegativities for variables.

4.4.1 Symmetry Breaking Constraints

Since all forklifts are assumed to be the same, all parameters in the optimization model related to forklifts are the same. Therefore, there can exist multiple optimal solutions for order assignments to vehicles by switching order batching for any pair of vehicles in an optimal solution. This symmetry for mixed integer programming (MIP) problems are common in production planing problems (Jans, 2009), operation room scheduling (Denton et al., 2010) and routing problems (Sherali et al., 2013; Coelho and Laporte, 2013) where the resources such as machines and vehicles are identical. It is discussed that the symmetry in MIPs can slow down branch-and-bound method by exploring symmetric solutions (Sherali and Smith, 2001; Margot, 2003; Ostrowski et al., 2011). Given an op-

timal order batching solution, there can be $|\mathcal{K}|!$ optimal forklift assignment solutions to these batches where $|\mathcal{K}|$ is the number of forklifts. Despite finding an optimal solution, branch-and-bound method can keep a large number of nodes which generate the symmetry solutions until solving them and proving them no better than the optimal.

To improve the efficiency of computation, we can introduce symmetry breaking constraints (SBC). The model first determines whether to use a forklift to pick up a batch of orders. To eliminate the symmetry of using forklifts, Equation (4.24) is introduced (Sherali and Smith, 2001) to enforce small-index forklifts are preferred first.

$$\eta_1 \geq \eta_2 \geq \cdots \geq \eta_{|\mathcal{K}|} \tag{4.24}$$

It is assumed that the number of orders $|\mathcal{O}|$ is larger than the number of forklifts $|\mathcal{K}|$. We also introduce Equations (4.25) and (4.26) to break the symmetry of assigning orders to forklifts (Denton et al., 2010).

$$\begin{aligned} y_{1'1} &= 1 \\ y_{2'1} + y_{2'2} &= 1 \\ &\vdots \\ \sum_{k=1}^{|\mathcal{K}|} y_{|\mathcal{K}|'k} &= 1 \end{aligned} \tag{4.25}$$

For order $o = 1, \cdots, |\mathcal{K}|$, Equations (4.25) guarantee that forklifts with small indices are preferred by a single order. For example, order $2'$ can only be picked by forklift 1 or forklift 2. It eliminates the situation that forklift 3 is used while forklift 2 is idle. In more general cases, a forklift can pick multiple orders. If order 1 to order 4 are assigned to forklift 1 and 2, then Equations (4.26) enforces forklift 3 is used to pick order 5.

$$y_{ok} \leq \sum_{s=k-1}^{o-1} y_{s,k-1} \tag{4.26}$$

Table 4.2: Numerical experiments with and without SBC

Num. of fork.	Demand scen.	Num. of aisles	Num. of routes	Time in sec. (Opt. gap) With SBC	W.O. SBC
5	1	8	33	25.03	34.87
	2	8	33	24.10	112.05
	3	8	33	18.04	11.72
	1	10	88	180.54	403.62
	2	10	88	607.99	3600 (31.57%)
	3	10	88	551.95	1710.06
10	1	8	33	3600 (22.46%)	3600 (34.93%)
	2	8	33	3600 (21.78%)	3600 (35.75%)
	3	8	33	3600 (34.69%)	3600 (52.28%)
	1	8	88	3600 (50.28%)	3600 (84.93%)
	2	8	88	3600 (45.37%)	3600 (90.57%)
	3	8	88	3600 (51.33%)	3600 (92.04%)

Symmetry constraints (4.24) – (4.26) can be added together to the deterministic model. Note that the computation time can increase if we only add Equations (4.24) or other single symmetry breaking constraints. Without SBC, there are multiple optimal solutions making it easy to find the optimal solution via branch and bound method. Although SBC cuts off some feasible regions that do not influence the optimality, it can slow down finding the optimal solution while it is not strong enough to cut off most of the symmetric optimal solutions. It is recommended to add different types of SBC together to ensure that the computation saved from proving symmetric optimal solutions is larger than finding an optimal with SBC.

Table 4.2 shows the numerical experiments with and without SBC using CPLEX solver. SBC significantly reduces the computation time when the number of forklifts is 5. For large cases with 10 forklifts, the model with SBC can have smaller optimality gap than that without SBC in 1 hour.

4.5 The Two-Stage Stochastic Model

To consider the uncertainty of orders, a two-stage stochastic programming model is developed as follows.

$$\min_{\mathbf{z}} \quad W \sum_{a \in \mathcal{A}} c_a z_a + \rho \mathbb{E}\left[Q(\mathbf{z}; \mathbf{q}(\omega), \boldsymbol{\theta}(\omega))\right] \tag{4.27}$$

$$\text{s.t. } z_a \in \{0, 1\}, \forall a \in \mathcal{A} \tag{4.28}$$

The objective (4.27) of wireless charging location problem is to minimize the investment cost of wireless charging lanes and the expected operation cost. $\mathbb{E}\left[Q(\mathbf{z}; \mathbf{q}(\omega), \boldsymbol{\theta}(\omega))\right]$ is the expected travel time among all order demand scenarios of $\mathbf{q}(\omega)$ and order location scenarios of $\boldsymbol{\theta}(\omega)$. $Q(\mathbf{z}; \mathbf{q}(\omega), \boldsymbol{\theta}(\omega))$ is the recourse function of the first-stage variable $\mathbf{z}$ for a given scenario ω.

4.5.1 Monte Carlo Simulation for Scenario Generation

In the two-stage stochastic model, the objective function considers the expected operation cost for the uncertain amount of demand and demand location in warehouses. Assuming that orders arrive independently, we have 3 scenarios of demand amount which is 1, 2 and 3 for each order. A unit of order demand amount corresponds to an item stored in a single aisle. For example, a forklift needs to travel 2 random aisles to pick up an order if the demand of this order is 2. It is assumed that we have 20 orders in a 10-aisle warehouse and each order needs pick-up among random aisles. The number of demand location scenarios can reach $[\binom{10}{1}+\binom{10}{2}+\binom{10}{3}]^{20}$. Although we can enumerate all demand scenarios if the sources of uncertainty in a two-stage stochastic programming model are discrete, the model can be difficult to solve with these many scenarios. In addition, scenarios cannot be listed if the order demand is from a continuous distribution representing the physical volume of items.

Instead of considering all scenarios in this model, we use Monte Carlo simulation to sample a limited number of demand scenarios to feed the stochastic model which is known as sample average approximation (SAA) (Shapiro et al., 2009). Intuitively, the more scenarios we sample, the more likely that we obtain accurate solutions. With a sufficiently large number of scenarios, the objective value of SAA problem uniformly converges to the true objective value in (4.27) on the feasible set (Shapiro and Homem-de Mello, 1998).

4.5.2 Scenario Decomposition

Consider the two-stage stochastic programming problem as a MIP, the number of constraints increases significantly when the number of forklifts, the number of aisles and the number of orders increase. For the instance with 5 forklifts, 8 aisles and 10 scenarios of orders, the optimality gap of using CPLEX solver in 1 hour is 50%. In order to solve the problem efficiently, a scenario decomposition algorithm for 0-1 stochastic programs (Ahmed, 2013) is introduced.

With a finite number of scenarios generated in Section 4.5.1, we can rewrite Equation (4.27) and (4.28) as

$$\left\{ \min_{\mathbf{z}} W \sum_{a \in \mathcal{A}} c_a z_a + \rho \frac{1}{S} \sum_{s=1}^{S} Q(\mathbf{z}; \mathbf{q}(\omega_s), \boldsymbol{\theta}(\omega_s)) : z_a \in \{0,1\}, \forall a \in \mathcal{A} \right\}. \tag{4.29}$$

In order to implement scenario decomposition method, we need to make copies of the first-stage variables and reformulate Equation (4.29) as follows.

$$\left\{ \frac{1}{S} \min_{\mathbf{z}} \sum_{s=1}^{S} \left[W \sum_{a \in \mathcal{A}} c_a z_a^s + \rho Q(\mathbf{z}^s; \mathbf{q}(\omega_s), \boldsymbol{\theta}(\omega_s)) \right] : z_a^s \in \{0,1\}, z_a^s = z_a^{s-1}, \forall a \in \mathcal{A}, s \in \mathcal{S} \right\}. \tag{4.30}$$

Let μ^s represent the variables for $s \in \mathcal{S}$. The constraints at the second stages and binaries for the copies of the first stage variables are represented by $\mathcal{U}^s$ for all $s \in \mathcal{S}$. We use

$\sum_{s=1}^{S} \mathbf{A}_s \boldsymbol{\mu}^s = \mathbf{0}$ to represent the enforcement of $z_a^1 = z_a^2 = \cdots z_a^S$ for all $a \in \mathcal{A}$. Equation (4.30) is equivalent to abstract formulation (4.31).

$$Z = \left\{ \min \sum_{s=1}^{S} \mathbf{h}^\top \boldsymbol{\mu}^s : \boldsymbol{\mu}^s \in \mathcal{U}^s \ \ \forall s \in \mathcal{S}, \sum_{s=1}^{S} \mathbf{A}_s \boldsymbol{\mu}^s = \mathbf{0} \right\} \tag{4.31}$$

For the convenience of explaining the algorithm, we use Equation (4.31) in the following context.

The algorithm for solving the two-stage stochastic model can be summarized in Algorithm 8. The details for estimating lower bounds and upper bounds are discussed in Sections 4.5.2.1 and 4.5.2.2.

Algorithm 8 A Scenario Decomposition Method for Solving the Stochastic Wireless Charging Lane Deployment Problem

1: Let $UB = +\infty$, $LB = -\infty$, and $\mathcal{Z} = \emptyset$.
Initialize the Lagrangian multiplier λ, an extremely small positive step size φ and a termination tolerance ϵ.
2: If $UB - LB \geq \epsilon$, go to Step 3; otherwise, terminate.
3: Solve

$$D_s(\lambda) = \left\{ \min(\mathbf{h}^\top + \lambda^\top \mathbf{A}_s) \boldsymbol{\mu}^s : \boldsymbol{\mu}^s \in \mathcal{U}^s \right\}$$

for $s \in \mathcal{S}$.
Obtain the optimal solution $\hat{\boldsymbol{\mu}}^s$ for $s \in \mathcal{S}$ and compute $L(\lambda) = \sum_{s=1}^{S} D_s(\lambda)$ as LB. Go to Step 4.
4: Update $\lambda \to \lambda + \varphi \Delta(\hat{\lambda})$ where

$$\Delta(\hat{\lambda}) = \sum_{s=1}^{S} \mathbf{A}_s \hat{\boldsymbol{\mu}}^s.$$

Go to Step 5.
5: Extract new wireless charging lane solutions from $\hat{\boldsymbol{\mu}}^s$ for $s \in \mathcal{S}$ to $\mathcal{Z}$ and add cuts (4.34) in $\mathcal{U}^s$. Go to Step 6.
6: Solve (4.30) by fixing the wireless charging lane solution $\mathbf{z} \in \mathcal{Z}$ and update UB with the minimum objective value. Go to Step 2.

4.5.2.1 Lower Bounding

By dualizing the nonanticipativity constraints $\sum_{s=1}^{S} \mathbf{A}_s \boldsymbol{\mu}^s = \mathbf{0}$, we can obtain a lower bound for Equation (4.31). The Lagrangian dual is written as follows.

$$Z_{\text{LD}} = \max_{\lambda} L(\lambda) \tag{4.32}$$

where $L(\lambda) = \sum_{s=1}^{S} D_s(\lambda)$ and $D_s(\lambda)$ is defined as

$$D_s(\lambda) = \left\{ \min(\mathbf{h}^\top + \lambda^\top \mathbf{A}_s)\boldsymbol{\mu}^s : \boldsymbol{\mu}^s \in \mathcal{U}^s \right\} \tag{4.33}$$

Suppose $\tilde{\boldsymbol{\mu}}$ is an optimal solution for Problem (4.31), then $\tilde{\boldsymbol{\mu}}^s$ is a feasible solution for $D_s(\lambda), \forall s \in \mathcal{S}$ and $Z_{\text{LD}} \leq Z$. $L(\lambda)$ is a piecewise linear concave function. Let $\hat{\boldsymbol{\mu}}$ is an optimal solution for $L(\hat{\lambda})$ given $\hat{\lambda}$.Then, $\Delta(\hat{\lambda})$ is the subgradient of $L(\lambda)$ at $\hat{\lambda}$ where $\Delta(\hat{\lambda}) = \sum_{s=1}^{S} \mathbf{A}_s \hat{\boldsymbol{\mu}}^s$. Since the Lagrangian dual problem is concave and it is easy to find its subgradient, subgradient searches can be applied to solving the Lagrangian dual problem (4.32).

4.5.2.2 Upper Bounding

The lower bounding algorithm for (4.32) explores wireless charging lane solutions from subproblems $D_s(\lambda)$ given λ. The wireless charging lane solution $\mathbf{z}^s$ are extracted from subproblems as candidate primal feasible solutions to the original problem (4.29) when solving the Lagrangian dual for lower bounds. To improve the upper bounds, the explored solutions are then cut-off at later iterations of estimating Lagrangian dual (4.32). Since the constraints for the first-stage variables in this problem are only binaries, we can

add the integer cuts (4.34) to eliminate the explores first stage solutions

$$\sum_{a:\hat{z}_a=1} (1 - z_a^s) + \sum_{a:\hat{z}_a=0} z_a^s \geq 1, \hat{z} \in \mathcal{Z}, s \in \mathcal{S} \tag{4.34}$$

where $\mathcal{Z}$ is the set that contains all primal feasible solutions. Note that the cuts are applied to all scenario-based subproblems. The upper bounding in solving the two-stage stochastic model is summarized at Step 5 in Algorithm 8.

4.6 Case Studies

In this section, case studies for the proposed model are shown. Computational results and model analyses are discussed to obtain some useful guidance for installation of dynamic wireless charging infrastructure in parallel-aisle warehouses. Since the proposed model considers the short-term operation cost with a number of demand scenarios in a warehouse, the order set is not as large as the total number of items processed in a day. It is assumed that the number of orders assigned to a single trip is five times of the number of forklifts. If the demand data is available for warehouses, we can estimate the order set more precisely. Each order randomly includes one or two items with a discrete uniform distribution. We also use the discrete uniform distribution to sample the scenarios of demand locations. For example, if an order has one item, this order randomly passes an aisle in the warehouse. Given the historical order-aisle data, statistical analyses can be performed thus providing the distribution to sample demand locations. In this chapter, we consider the pick-then-sort picking strategy. Therefore, the demand q_o for order $o \in \mathcal{O}$ is the number of items in this order. All case studies in this section are based on single directional warehouses. To implement Algorithm 8 and solve the stochastic programming model, CPLEX solver of version 12.6 is used. The computational scheme is coded in the Julia Language with the JuMP.jl package (Dunning et al., 2017).

Table 4.3: Comparisons of computation time for 5-forklift 8-aisle instance with different number of scenarios

$\|\mathcal{S}\|$	CPLEX	Algorithm 8		
	Time (sec.)	Time (sec.)	Iterations	Subproblems
2	59	205	3	4
3	447	467	3	9
4	2707	799	2	16
5	3600	922	2	25
6	3600	1201	2	36
7	3600	1435	2	49
8	3600	1964	2	64
9	3600	2242	2	81
10	3600	2341	2	100

4.6.1 Computation Performances

To show the computation performance of Algorithm 8, computation time with different number of scenarios for a warehouse with 5 forklifts and 8 aisles is shown in Table 4.3 and Figure 4.3. Meanwhile, we directly use CPLEX to solve the stochastic programming model as comparisons. We use 1 hour as time limit for both CPLEX and Algorithm 8. CPLEX solver cannot solve the instances with more than 4 scenarios within 1 hour while Algorithm 8 shows an increasing computation time as the number of scenario increases. Table 4.3 shows the computation time of CPLEX and Algorithm 8 with the initial Lagrangian multiplier to be $\mathbf{0}$. Seen from Figure 4.3, the computation time of Algorithm 8 tends to increase linearly as the number of scenarios grows. Instead of solving the stochastic programming model with constraints for all scenarios, Algorithm 8 solves scenario-based subproblems. When the number of scenarios increases, the number of subproblems in Algorithm 8 increases but the problem size for each subproblem does not change. Therefore, Algorithm 8 can perform well in the proposed model even with a large number of scenarios.

In addition, the number of iterations for Algorithm 8 is sensitive to the value of Lagrangian multiplier λ. Figure 4.4 shows the lower bounds and upper bounds with ran-

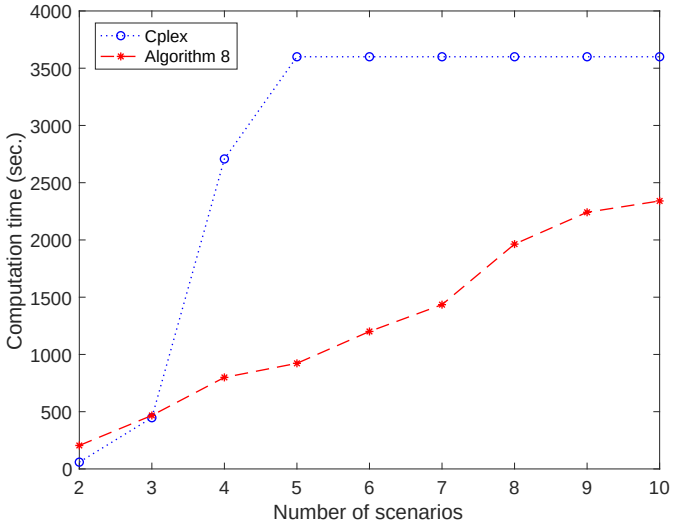

Figure 4.3: Computation time for 5-forklift 8-aisle instance with different number of scenarios with Cplex and Algorithm 8

dom generation of Lagrangian multiplier from $(-1, 1)$ Uniform distribution. More than 25 iterations are needed with a random Lagrangian multiplier while Table 4.3 shows 2 iterations with zero value of Lagrangian multiplier. Therefore, it is recommended to set the initial Lagrangian multiplier as zero.

For a fixed number of forklifts and scenarios, Table 4.4 shows the computation time with CPLEX and Algorithm 8 for different scale of warehouses. Without using Algorithm 7 to constructed a reduced route set, we solve the instances with all feasible routes. Both CPLEX and Algorithm 8 cannot solve the instance with $|\mathcal{A}| = 10$ with 1 hour time limit while Algorithm 8 with a reduced route set generated by Algorithm 7 can solve the instance within 3 minutes. If the size of warehouses increases, the number of routes grows dramatically. The deterministic model for a single scenario becomes challenging with a large number of routes. Algorithm 8 cannot be performed when scenario-based subproblems are hard. Hence, it is necessary to construct a reduced route set with Algorithm 7 for warehouses with more than 10 aisles.

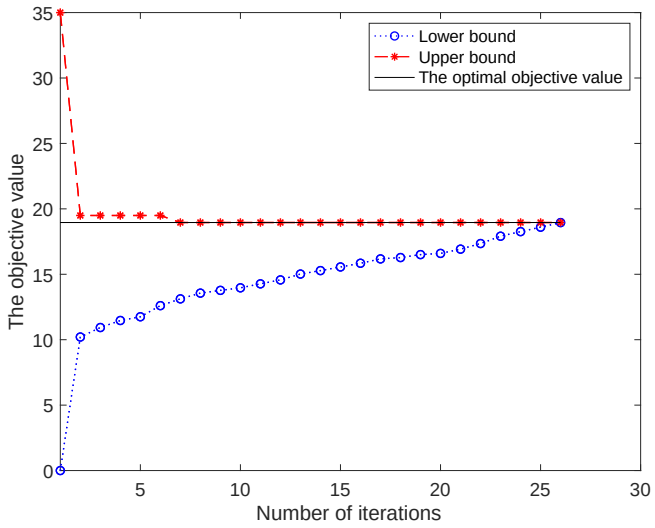

Figure 4.4: The value of upper bound and lower bound for 5-forklift 8-aisle and 5-scenario instance with Algorithm 8 with random λ

Table 4.4: Comparisons of computation time for 5-forklift 3-scenario instance with different number of aisles

$\lvert\mathcal{A}\rvert$	Computation time (sec.)		
	Cplex	Algorithm 8	Algorithm 7&8
2	3	7	7
4	8	47	49
6	129	201	41
8	447	467	81
10	3600	3600	156

4.6.2 The Value of Stochastic Solution

Given the size of a warehouse, the number of forklifts and the demand of orders for sampled scenarios, we can solve the stochastic programming model and obtain the optimal wireless charging lane solutions (ST) facing up to all demand scenarios.

The deterministic (DE) solution of wireless charging lane locations is estimated based the average demand. For continuous random parameters, it is straightforward to estimate the average scenario by weight averaging those parameters among all scenarios. The discrete random parameters, however, need some assumptions. Here, steps to analyze the average scenario data of demand are presented. First, we calculate the average demand $\bar{q}_o$ for each order $o \in \mathcal{O}$ among all scenario $s \in \mathcal{S}$. Since we sample the demand from (0,1) discrete uniform distribution, the demand for order $\hat{q}_o$ is 1 if $\bar{q}_o$ is less than 1.5 and $\hat{q}_o = 2$ otherwise. Then, we rank the number of times of passing aisle $a \in \mathcal{A}$ for order $o \in \mathcal{O}$ among all scenarios, we choose aisles for the order with top $\hat{q}_o$ visits. Feeding all scenarios with the DE solution, the operation cost of DE is computed.

We can also analyze the wait and see (WS) solution for wireless charging lanes. This can be obtained by the first lower bound of Algorithm 8 if we set $\mathbf{0}$ as initial Lagrangian multiplier.

We define the expected value of perfect information (EVPI) with Equation (4.35) and the value of stochastic solution with Equation (4.36).

$$\text{EVPI} = \frac{\text{Operation cost with ST} - \text{Average operation cost with WS}}{\text{Average operation cost with WS}} \tag{4.35}$$

$$\text{VSS} = \frac{\text{Operation cost with DE} - \text{Operation cost with ST}}{\text{Operation cost with ST}} \tag{4.36}$$

With different costs of wireless charging lanes, the value of stochastic solution for a warehouse with 5 forklifts and 8 aisles is Shown in Table 4.5. It is observed that the VSS decreases and EVPI increases as the costs of wireless charging lanes increases. In addition,

Table 4.5: The value of stochastic solution with different wireless charging lane cost for a 5-forklift 8-aisles and 5-scenario instance

wireless cost($/m.)	Operation cost			EVPI (%)	VSS (%)
	DE	WS	ST		
100	23.76	17.42	17.85	2.43	33.15
120	23.80	17.51	17.96	2.54	32.53
140	23.84	17.60	18.07	2.66	31.92
160	23.87	17.69	18.18	2.77	31.32
180	23.91	17.78	18.29	2.88	30.73
200	23.95	17.87	18.40	2.99	30.14
220	23.98	17.96	18.51	3.10	29.56
240	24.02	18.04	18.62	3.21	28.99
260	24.06	18.13	18.73	3.31	28.42
280	24.10	18.22	18.85	3.42	27.86
300	24.13	18.31	18.96	3.52	27.31

the ST and WS solution can be very close even though ST provides a unique solution for all scenarios and WS has wireless charging lanes in different aisles for different scenarios.

4.7 Concluding Remarks

To increase the operation efficiency of warehouse logistics, we propose a two-stage stochastic programming model for optimal deployment of dynamic wireless charging for electric forklifts. We consider the routing of forklifts to pick up orders arriving within a short-term in congested warehouses. In this problem, the uncertainties of order demand and order locations are addressed. A route set construction algorithm is introduced and a scenario decomposition algorithm is proposed to solve the two-stage stochastic programming model. The comparisons of computation time with CPLEX and the proposed algorithm are presented to show the performance of the proposed algorithm. We also demonstrate the value of stochastic solutions by comparing with deterministic solutions. In numerical experiments, the value of stochastic solutions is significant ranging from 27% to 33% for a warehouse with 5 forklifts and 8 aisles.

Although the proposed model captures essential components in warehouse logistics such as forklift routing, congestions and deployment of dynamic wireless charging, there exist limitations. First, the warehouse network and forklift routing in the proposed model is simplified with aisles. If a network is complicated, the forklift routing is challenging with the consideration of congestions. Second, we consider orders arriving within a short-term that can be picked up with a single trip. To pick up a large number of orders in a warehouse, forklifts need multiple trips. Despite that the computation can be very challenging, the deployment of dynamic wireless charging can be estimated more preciously via modeling forklifts routing with multiple trips.

5 Conclusion

In this dissertation, three optimization models are proposed for hazmat routing, hazmat transportation network design and dynamic wireless charging lane deployment in a congested warehouse.

We propose a few avenues for future research for hazmat routing. First, we can consider the uncertainty of data associated with risk in hazmat routing. Since there exist few accident statistics for hazmat transportation, we can incorporate data uncertainty into spectral risk measures to obtain safe paths. Second, a network design problem addressing spectral risks can be developed. In this design problem, decision makers can introduce a road banning policy or a road pricing policy to minimize the system-wide spectral risk measure value by considering routing behavior of hazmat carriers via bilevel optimization as in Stackelberg games. Third, we can apply SRM to other transportation problems. Since CVaR or related concepts, such as mean-excess measures, have been applied in other areas of transportation (Chen and Zhou, 2010; Chen et al., 2006; Soleimani and Govindan, 2014), it will be worth studying the shortcomings of CVaR in other applications and how SRM can be utilized.

For the hazmat network design model, the first limitation is that we did not consider any uncertainty from data sources and hazmat travel demand. Considering these additional sources of uncertainty will make the network design problem more challenging. Second, the RUM used in this paper is not the most advanced random route-choice model. More advanced RUM approaches are available, which may be incorporated within the network design problem suggested in this paper, at the cost of computational time increases. Third, we did not consider equity in the network design. Risk equity among

zones and cost equity among hazmat carriers should be considered for fair management of the road infrastructure. Addressing these limitations are promising future research directions. Another interesting extension of the proposed method will be the consideration of multiples modes of hazmat transportation as in multimodal or intermodal transportation. The discrete-choice model in RUM should be extended to consider mode choices in multi-modal transportation. This will create a nested logit model, for example, which adds significant computational and analytical complexity in the model.

In the dynamic wireless charging model, we consider a small number of orders that need to be batched for forklifts. In fact, there can be thousands of orders arriving in one hour. Therefore, developing an efficient algorithm for a large scale of orders is significant in the future. In addition, an interesting research direction to incorporate congestion is to construct a time-expanded network. Instead of capturing the congestion by the average workflows, a time-expanded network can cope with congestion more preciously. Also, developing an efficient algorithm for a time-expanded network aiming at large scale warehouses with a large number of orders can be a potential future research topic.

References

Abkowitz, M., Lepofsky, M., and Cheng, P. (1992a). Selecting criteria for designating hazardous materials highway routes. *Transportation Research Record*, 1333:30–35.

Abkowitz, M. D., Lepofsky, M., and Cheng, P. (1992b). Selecting criteria for designating hazardous materials highway routes. *Transportation Research Record*, (1333).

Acerbi, C. (2002). Spectral measures of risk: a coherent representation of subjective risk aversion. *Journal of Banking & Finance*, 26(7):1505–1518.

Acerbi, C. (2004). Coherent representations of subjective risk-aversion. In Szeö, G., editor, *Risk Measures for the 21st Century*, pages 147–207. New York: Wiley.

Acerbi, C. and Simonetti, P. (2008). Portfolio optimization with spectral measures of risk. http://arxiv.org/abs/cond-mat/0203607.

Acerbi, C. and Tasche, D. (2002). On the coherence of expected shortfall. *Journal of Banking & Finance*, 26(7):1487–1503.

Ahmed, S. (2013). A scenario decomposition algorithm for 0–1 stochastic programs. *Operations Research Letters*, 41(6):565–569.

Akgün, V., Erkut, E., and Batta, R. (2000). On finding dissimilar paths. *European Journal of Operational Research*, 121(2):232–246.

Alp, E. (1995). Risk-based transportation planning practice: overall methodology and a case example. *INFOR*, 33(1):4–19.

Artzner, P., Delbaen, F., Eber, J., and Heath, D. (1999a). Coherent measures of risk. *Mathematical Finance*, 9(3):203–228.

Artzner, P., Delbaen, F., Eber, J. M., and Heath, D. (1997). Thinking coherently: generalised scenarios rather than VaR should be used when calculating regulatory capital. *Risk-London-Risk Magazine Limited*, 10:68–71.

Artzner, P., Delbaen, F., Eber, J. M., and Heath, D. (1999b). Coherent measures of risk. *Mathematical Finance*, 9(3):203–228.

Battelle (2006). Hazardous materials routing survey analysis.

Ben-Akiva, M., Bergman, M., Daly, A. J., and Ramaswamy, R. (1984). Modeling inter-urban route choice behaviour. In *Proceedings of the 9th international symposium on transportation and traffic theory*, pages 299–330. VNU Science Press Utrecht, The Netherlands.

Ben-Akiva, M. and Bierlaire, M. (1999). Discrete choice methods and their applications to short term travel decisions. In *Handbook of Transportation Science*, pages 5–33. Springer.

Ben-Akiva, M. E., Lerman, S. R., and Lerman, S. R. (1985). *Discrete choice analysis: theory and application to travel demand*, volume 9. MIT press.

Benjaafar, S. (2002). Modeling and analysis of congestion in the design of facility layouts. *Management Science*, 48(5):679–704.

Birge, J. R. (1982). The value of the stochastic solution in stochastic linear programs with fixed recourse. *Mathematical Programming*, 24(1):314–325.

Bonvicini, S. and Spadoni, G. (2008). A hazmat multi-commodity routing model satisfying risk criteria: a case study. *Journal of Loss Prevention in the Process Industries*, 21(4):345–358.

Brandtner, M. (2016). Spectral risk measures: Properties and limitations: comment on Dowd, Cotter, and Sorwar. *Journal of Financial Services Research*, 49(1):121–131.

Brandtner, M. and Kürsten, W. (2017). Consistent modeling of risk averse behavior with spectral risk measures: Wächter/Mazzoni revisited. *European Journal of Operational Research*, 259(1):394–399.

Broadbent, A., Besant, C., Premi, S., and Walker, S. (1985). Free ranging agv systems: promises, problems and pathways. In *Proceeding of the 2nd international conference on automated materials handling*, pages 221–237.

Cao, Y., Tang, S., Li, C., Zhang, P., Tan, Y., Zhang, Z., and Li, J. (2012). An optimized ev charging model considering tou price and soc curve. *IEEE Transactions on Smart Grid*, 3(1):388–393.

Cascetta, E., Nuzzolo, A., Russo, F., and Vitetta, A. (1996). A modified logit route choice model overcoming path overlapping problems: specification and some calibration results for interurban networks. In *Proceedings of the 13th International Symposium on Transportation and Traffic Theory*, pages 697–711. Pergamon Oxford, NY, USA.

Chen, A. and Zhou, Z. (2010). The α-reliable mean-excess traffic equilibrium model with stochastic travel times. *Transportation Research Part B*, 44:493–513.

Chen, G., Daskin, M. S., Shen, Z. J. M., and Uryasev, S. (2006). The α-reliable mean-excess regret model for stochastic facility location modeling. *Wiley Periodicals, Inc. Naval Research Logistics*, 53:617–626.

Chen, T. D., Kockelman, K. M., Khan, M., et al. (2013). The electric vehicle charging station location problem: a parking-based assignment method for seattle. In *Transportation Research Board 92nd Annual Meeting*, volume 340, pages 13–1254.

Clarke, G. and Wright, J. W. (1964). Scheduling of vehicles from a central depot to a number of delivery points. *Operations research*, 12(4):568–581.

Coelho, L. C. and Laporte, G. (2013). The exact solution of several classes of inventory-routing problems. *Computers & Operations Research*, 40(2):558–565.

Daganzo, C. F. and Sheffi, Y. (1977). On stochastic models of traffic assignment. *Transportation Science*, 11(3):253–274.

Davis, G. A. (1994). Exact local solution of the continuous network design problem via stochastic user equilibrium assignment. *Transportation Research Part B: Methodological*, 28(1):61–75.

De Koster, M., Van der Poort, E. S., and Wolters, M. (1999). Efficient orderbatching methods in warehouses. *International Journal of Production Research*, 37(7):1479–1504.

Denton, B. T., Miller, A. J., Balasubramanian, H. J., and Huschka, T. R. (2010). Optimal allocation of surgery blocks to operating rooms under uncertainty. *Operations research*, 58(4-part-1):802–816.

Dial, R. B. (1971). A probabilistic multipath traffic assignment model which obviates path enumeration. *Transportation Research*, 5(2):83–111.

Dowd, K. and Blake, D. (2006). After VaR: the theory, estimation, and insurance applications of quantile-based risk measures. *Journal of Risk and Insurance*, 73(2):193–229.

Dowd, K., Cotter, J., and Sorwar, G. (2008). Spectral risk measures: properties and limitations. *Journal of Financial Services Research*, 34(1):61–75.

Duffie, D. and Pan, J. (1997). An overview of value at risk. *The Journal of Derivatives*, 4(3):7–49.

Dunning, I., Huchette, J., and Lubin, M. (2017). JuMP: a modeling language for mathematical optimization. *SIAM Review*, 59(2):295–320.

Egbelu, P. J. and Tanchoco, J. M. (1984). Characterization of automatic guided vehicle dispatching rules. *The International Journal of Production Research*, 22(3):359–374.

Emergency Response Guidebook (2012). Emergency response guidebook : A guidebook for first responders during the initial phase of a dangerous goods/hazardous materials transportation incident.

Erkut, E. and Gzara, F. (2008). Solving the hazmat transport network design problem. *Computers & Operations Research*, 35(7):2234–2247.

Erkut, E. and Ingolfsson, A. (2000a). Catastrophe avoidance models for hazardous materials route planning. *Transportation Science*, 34(2):165–179.

Erkut, E. and Ingolfsson, A. (2000b). Catastrophe avoidance models for hazardous materials route planning. *Transportation Science*, 34(2):165–179.

Erkut, E. and Ingolfsson, A. (2005). Transport risk models for hazardous materials: revisited. *Operations Research Letters*, 33(1):81–89.

Erkut, E., Tjandra, S. A., and Verter, V. (2007). Hazardous materials transportation. *Handbooks in Operations Research & Management Science*, 14:539–621.

Esfandeh, T., Batta, R., and Kwon, C. (2017). Time-dependent hazardous-materials network design problem. *Transportation Science*, 52(2):454–473.

Esfandeh, T., Kwon, C., and Batta, R. (2016). Regulating hazardous materials transportation by dual toll pricing. *Transportation Research Part B: Methodological*, 83:20–35.

Fan, T., Chiang, W.-C., and Russell, R. (2015). Modeling urban hazmat transportation with road closure consideration. *Transportation Research Part D: Transport and Environment*, 35:104–115.

Federal Motor Carrier Safety Administration (2001). Comparative risks of hazardous materials and nonhazardous materials truck shipment accidents/incidents.

Federal Motor Carrier Safety Administration (2018). National hazardous materials route registry.

Fontaine, P. and Minner, S. (2018). Benders decomposition for the hazmat transport network design problem. *European Journal of Operational Research*, 267(3):996–1002.

Frade, I., Ribeiro, A., Gonçalves, G., and Antunes, A. (2011). Optimal location of charging stations for electric vehicles in a neighborhood in lisbon, portugal. *Transportation research record: journal of the transportation research board*, (2252):91–98.

Gao, J. (2007). Traveling magnetic field for homogeneous wireless power transmission. *IEEE Transactions on Power Delivery*, 22(1):507–514.

Geoffrion, A. M. (1972). Generalized benders decomposition. *Journal of Optimization Theory and Applications*, 10(4):237–260.

Gong, Y. and De Koster, R. (2008). A polling-based dynamic order picking system for online retailers. *IIE Transactions*, 40(11):1070–1082.

Gzara, F. (2013). A cutting plane approach for bilevel hazardous material transport network design. *Operations Research Letters*, 41(1):40–46.

Heath, B. L., Ciarallo, F. W., and Hill, R. R. (2013). An agent-based modeling approach to analyze the impact of warehouse congestion on cost and performance. *The International Journal of Advanced Manufacturing Technology*, pages 1–12.

Hess, S., Quddus, M., Rieser-Schüssler, N., and Daly, A. (2015). Developing advanced route choice models for heavy goods vehicles using gps data. *Transportation Research Part E: Logistics and Transportation Review*, 77:29–44.

Hodgson, M. J. (1990). A flow-capturing location-allocation model. *Geographical Analysis*, 22(3):270–279.

Hong, S., Johnson, A. L., and Peters, B. A. (2012). Large-scale order batching in parallel-aisle picking systems. *IIE Transactions*, 44(2):88–106.

Hosseini, S. D. and Verma, M. (2018). Conditional value-at-risk (CVaR) methodology to optimal train configuration and routing of rail hazmat shipments. *Transportation Research Part B: Methodological*, 110:79–103.

II, C. G. P. (2000). An evaluation of order picking policies for mail order companies. *Production and operations management*, 9(4):319–335.

Jans, R. (2009). Solving lot-sizing problems on parallel identical machines using symmetry-breaking constraints. *INFORMS Journal on Computing*, 21(1):123–136.

Jeong, S., Jang, Y. J., and Kum, D. (2015). Economic analysis of the dynamic charging electric vehicle. *IEEE Transactions on Power Electronics*, 30(11):6368–6377.

Jin, H. and Batta, R. (1997). Objectives derived form viewing hazmat shipments as a sequence of independent bernoulli trials. *Transportation Science*, 31(3):252–261.

Jufer, M. (2008). Electric drive system for automatic guided vehicles using contact-free energy transmission. In *Power Electronics and Motion Control Conference, 2008. EPE-PEMC 2008. 13th*, pages 1–6. IEEE.

Kang, Y., Batta, R., and Kwon, C. (2014a). Generalized route planning model for hazardous material transportation with VaR and equity considerations. *Computers & Operations Research*, 43:237–247.

Kang, Y., Batta, R., and Kwon, C. (2014b). Value-at-risk model for hazardous material transportation. *Annals of Operations Research*, 222(1):361–387.

Kara, B. Y. and Verter, V. (2004). Designing a road network for hazardous materials transportation. *Transportation Science*, 38(2):188–196.

Kawamura, A., Ishioka, K., and Hirai, J. (1996). Wireless transmission of power and information through one high-frequency resonant ac link inverter for robot manipulator applications. *IEEE Transactions on Industry Applications*, 32(3):503–508.

Kim, J. H., Lee, B. S., Lee, J. H., Lee, S. H., Park, C. B., Jung, S. M., Lee, S. G., Yi, K. P., and Baek, J. (2015). Development of 1-mw inductive power transfer system for a high-speed train. *IEEE Transactions on Industrial Electronics*, 62(10):6242–6250.

Kim, K. H. and Tanchoco, J. (1993). Economical design of material flow paths. *International Journal of Production Research*, 31(6):1387–1407.

Kisacikoglu, M. C., Kesler, M., and Tolbert, L. M. (2015). Single-phase on-board bidirectional pev charger for v2g reactive power operation. *IEEE Transactions on Smart Grid*, 6(2):767–775.

Kurs, A., Karalis, A., Moffatt, R., Joannopoulos, J. D., Fisher, P., and Soljačić, M. (2007). Wireless power transfer via strongly coupled magnetic resonances. *science*, 317(5834):83–86.

Kwon, C. (2011). Conditional value-at-risk model for hazardous materials transportation. In Jain, S., Creasey, R. R., Himmelspach, J., White, K. P., and Fu, M., editors, *Proceedings of the 2011 Winter Simulation Conference*.

Kwon, C., Lee, T., and Berglund, P. (2013). Robust shortest path problems with two uncertain multiplicative cost coefficients. *Naval Research Logistics*, 60(5):375–394.

Lee, J., Choi, R. H.-G., and Khaksar, M. (1990). Evaluation of automated guided vehicle systems by simulation. *Computers & Industrial Engineering*, 19(1-4):318–321.

Lim, J. K., Lim, J. M., Yoshimoto, K., Kim, K. H., and Takahashi, T. (2002). A construction algorithm for designing guide paths of automated guided vehicle systems. *International Journal of Production Research*, 40(15):3981–3994.

List, G. F., Mirchandani, P. B., Turnquist, M. A., and Zografos, K. G. (1991). Modeling and analysis for hazardous materials transportation: Risk analysis, routing/scheduling and facility location. *Transportation Science*, 25(2):100–114.

Liu, H. and Wang, D. Z. (2015). Global optimization method for network design problem with stochastic user equilibrium. *Transportation Research Part B: Methodological*, 72:20–39.

Lukic, S. and Pantic, Z. (2013). Cutting the cord: Static and dynamic inductive wireless charging of electric vehicles. *IEEE Electrification Magazine*, 1(1):57–64.

Marcotte, P., Mercier, A., Savard, G., and Verter, V. (2009). Toll policies for mitigating hazardous materials transport risk. *Transportation Science*, 43(2):228–243.

Margot, F. (2003). Exploiting orbits in symmetric ilp. *Mathematical Programming*, 98(1-3):3–21.

Marhavilas, P. K., Koulouriotis, D., and Gemeni, V. (2011). Risk analysis and assessment methodologies in the work sites: on a review, classification and comparative study of the scientific literature of the period 2000–2009. *Journal of Loss Prevention in the Process Industries*, 24(5):477–523.

Maxwell, W. L. and Muckstadt, J. A. (1982). Design of automatic guided vehicle systems. *IIE Transactions*, 14(2):114–124.

Maybee, J., Randolph, P., and Uri, N. (1979). Optimal step function approximations to utility load duration curves. *Engineering Optimization*, 4(2):89–93.

Maza, S. and Castagna, P. (2005). A performance-based structural policy for conflict-free routing of bi-directional automated guided vehicles. *Computers in Industry*, 56(7):719–733.

McFadden, D. (1975). The revealed preferences of a government bureaucracy: theory. *The Bell Journal of Economics*, pages 401–416.

Occupational Safety and Health Administration (2017). Chemical hazards and toxic substances.

Oggero, A., Darbra, R., Munoz, M., Planas, E., and Casal, J. (2006). A survey of accidents occurring during the transport of hazardous substances by road and rail. *Journal of Hazardous Materials*, 133(1-3):1–7.

Ostrowski, J., Linderoth, J., Rossi, F., and Smriglio, S. (2011). Orbital branching. *Mathematical Programming*, 126(1):147–178.

Pflug, G. (2000). Some remarks on the value-at-risk and the conditional value-at-risk. In Uryasev, S. P., editor, *Probabilistic Constrained Optimization: Methodology and Applications*, volume 38 of *Nonconvex Optimization and Its Applications*, pages 272–281. Kluwer Academic Publishers, Dordrecht, The Netherlands.

Pipeline and Hazardous Materials Safety Administration (2017). Incident statistics.

Prashker, J. N. and Bekhor, S. (2004). Route choice models used in the stochastic user equilibrium problem: a review. *Transport Reviews*, 24(4):437–463.

Quattrone, A. and Vitetta, A. (2011). Random and fuzzy utility models for road route choice. *Transportation Research Part E: Logistics and Transportation Review*, 47(6):1126–1139.

Rajotia, S., Shanker, K., and Batra, J. (1998). A semi-dynamic time window constrained routeing strategy in an agv system. *International Journal of Production Research*, 36(1):35–50.

Ramming, M. S. (2001). *Network knowledge and route choice*. PhD thesis, Massachusetts Institute of Technology.

Rayas, V. M. and Serrato, M. A. (2017). A framework of the risk assessment for the supply chain of hazardous materials. *Netnomics: Economic Research and Electronic Networking*, 18(2-3):215–226.

ReVelle, C., Cohon, J., and Shobrys, D. (1991). Simultaneous siting and routing in the disposal of hazardous wastes. *Transportation Science*, 25(2):138–145.

Riemann, R., Wang, D. Z., and Busch, F. (2015). Optimal location of wireless charging facilities for electric vehicles: flow-capturing location model with stochastic user equilibrium. *Transportation Research Part C: Emerging Technologies*, 58:1–12.

Rockafellar, R. and Uryasev, S. (2002a). Conditional value-at-risk for general loss distributions. *Journal of Banking & Finance*, 26(7):1443–1471.

Rockafellar, R. T. and Uryasev, S. (2000). Optimization of conditional value-at-risk. *Journal of Risk*, 2:21–42.

Rockafellar, R. T. and Uryasev, S. (2002b). Conditional value-at-risk for general loss distributions. *Journal of Banking & Finance*, 26(7):1443–1471.

Ruben, R. A. and Jacobs, F. R. (1999). Batch construction heuristics and storage assignment strategies for walk/ride and pick systems. *Management Science*, 45(4):575–596.

Saccomanno, F. and Chan, A. (1985). Economic evaluation of routing strategies for hazardous road shipments. *Transportation Research Record*, 1020:12–18.

Santoso, T., Ahmed, S., Goetschalckx, M., and Shapiro, A. (2005). A stochastic programming approach for supply chain network design under uncertainty. *European Journal of Operational Research*, 167(1):96–115.

Severns, R., Yeow, E., Woody, G., Hall, J., and Hayes, J. (1996). An ultra-compact transformer for a 100 w to 120 kw inductive coupler for electric vehicle battery charging. In *Applied Power Electronics Conference and Exposition, 1996. APEC'96. Conference Proceedings 1996., Eleventh Annual*, volume 1, pages 32–38. IEEE.

Shapiro, A., Dentcheva, D., and Ruszczyński, A. (2009). *Lectures on stochastic programming: modeling and theory*. SIAM.

Shapiro, A. and Homem-de Mello, T. (1998). A simulation-based approach to two-stage stochastic programming with recourse. *Mathematical Programming*, 81(3):301–325.

Sherali, H. D., Bae, K. H., and Haouari, M. (2013). An integrated approach for airline flight selection and timing, fleet assignment, and aircraft routing. *Transportation Science*, 47(4):455–476.

Sherali, H. D. and Smith, J. C. (2001). Improving discrete model representations via symmetry considerations. *Management Science*, 47(10):1396–1407.

Sivakumar, R. A., Rajan, B., and Karwan, M. (1993). A network-based model for transporting extremely hazardous materials. *Operations Research Letters*, 13(2):85–93.

Smith, J. M. and Li, W. J. (2001). Quadratic assignment problems and m/g/c/c/state dependent network flows. *Journal of combinatorial optimization*, 5(4):421–443.

Soleimani, H. and Govindan, K. (2014). Reverse logistics network design and planning utilizing conditional value at risk. *European Journal of Operational Research*, 237(2):487–497.

Srinivasan, M. M. and Bozer, Y. A. (1992). Which one is responsible for wip: the workstations or the material handling system? *International journal of production research*, 30(6):1369–1399.

Su, L., Sun, L., Karwan, M., and Kwon, C. (2017). Spectral risk measure minimization in hazardous materials transportation. *IISE Transactions*. accepted.

Sun, L., Karwan, M. H., and Kwon, C. (2016). Robust hazmat network design problems considering risk uncertainty. *Transportation Science*, 50(4):1188–1203.

Sun, L., Karwan, M. H., and Kwon, C. (2018). Generalized bounded rationality and robust multi-commodity network design. *Operations Research*, 66(1):42–57.

Taslimi, M., Batta, R., and Kwon, C. (2017). A comprehensive modeling framework for hazmat network design, hazmat response team location, and equity of risk. *Computers & Operations Research*, 79:119–130.

Tomasoni, A. M., Garbolino, E., Rovatti, M., and Sacile, R. (2010). Risk evaluation of real-time accident scenarios in the transport of hazardous material on road. *Management of Environmental Quality: An International Journal*, 21(5):695–711.

Tompkins, J. A., White, J. A., Bozer, Y. A., and Tanchoco, J. M. A. (2010). *Facilities planning*. John Wiley & Sons.

Torretta, V., Rada, E. C., Schiavon, M., and Viotti, P. (2017). Decision support systems for assessing risks involved in transporting hazardous materials: a review. *Safety Science*, 92:1–9.

Toumazis, I. and Kwon, C. (2013). Routing hazardous materials on time-dependent networks using conditional value-at-risk. *Transportation Research Part C: Emerging Technologies*, 37:73–92.

Toumazis, I. and Kwon, C. (2016). Worst-case conditional value-at-risk minimization for hazardous materials transportation. *Transportation Science*, 50(4):1174–1187.

Toumazis, I., Kwon, C., and Batta, R. (2013). Value-at-risk and conditional value-at-risk minimization for hazardous materials routing. In Batta, R. and Kwon, C., editors, *Handbook of OR/MS Models in Hazardous Materials Transportation*. Springer.

Transportation Networks for Research Core Team (2018). Transportation networks for research. Last Accessed on February 22, 2018.

Van Raemdonck, K., Macharis, C., and Mairesse, O. (2013). Risk analysis system for the transport of hazardous materials. *Journal of Safety Research*, 45:55–63.

Verter, V. and Kara, B. Y. (2008). A path-based approach for hazmat transport network design. *Management Science*, 54(1):29–40.

Vosniakos, G. C. and Davies, B. (1989). On the path layout and operation of an agv system serving an fms. *The International Journal of Advanced Manufacturing Technology*, 4(3):243–262.

Wächter, H. P. and Mazzoni, T. (2013). Consistent modeling of risk averse behavior with spectral risk measures. *European Journal of Operational Research*, 229(2):487–495.

Williams, H. C. (1977). On the formation of travel demand models and economic evaluation measures of user benefit. *Environment and Planning A*, 9(3):285–344.

Woodruff, J. M. (2005). Consequence and likelihood in risk estimation: a matter of balance in UK health and safety risk assessment practice. *Safety Science*, 43(5-6):345–353.

Yang, J., Li, F., Zhou, J., Zhang, L., Huang, L., and Bi, J. (2010). A survey on hazardous materials accidents during road transport in China from 2000 to 2008. *Journal of Hazardous Materials*, 184(1-3):647–653.

Yen, J. Y. (1971). Finding the *K* shortest loopless paths in a network. *Management Science*, 17(11):712–716.

Zhang, M., Batta, R., and Nagi, R. (2008). Supplementary document for the paper "modeling of workflow congestion and optimization of flow routing in a manufacturing/warehouse facility".

Zhang, M., Batta, R., and Nagi, R. (2009). Modeling of workflow congestion and optimization of flow routing in a manufacturing/warehouse facility. *Management Science*, 55(2):267–280.

Appendix A Copyright Permissions

A.1 Reprint Permissions for Chapter 2

PUBLISHING AGREEMENT

In order to ensure both the widest dissemination and protection of material published in our Journal, we require Authors to execute an author agreement in writing with Institute of Industrial and Systems Engineers (IISE) (hereinafter 'the Society') for the rights of copyright for the Articles they contribute. This enables our Publisher, on behalf of IISE, to ensure protection against infringement.

This is an agreement under which you, the author, assign copyright in your article to the Society to allow us to publish your article, including abstract, tables, figures, data, and supplemental material hosted by us, as the Version of Record (VoR) in the Journal for the full period of copyright throughout the world, in all forms and all media, subject to the Terms & Conditions below.

Article (the "Article") entitled:	Spectral Risk Measure Minimization in Hazardous Materials Transportation
Article DOI:	10.1080/24725854.2018.1530488
Author(s):	Liu Su, Longsheng Sun, Mark Karwan, Changhyun Kwon
To publish in the Journal:	IISE Transactions
Journal ISSN:	2472-5862

STATEMENT OF ORIGINAL COPYRIGHT OWNERSHIP / CONDITIONS

In consideration of the publication of the Article, you hereby grant with full title guarantee all rights of copyright and related rights in the above specified Article as the Version of Scholarly Record which is intended for publication in all forms and all media (whether known at this time or developed at any time in the future) throughout the world, in all languages, for the full term of copyright, to take effect if and when the Article is accepted for publication in the Journal.

ASSIGNMENT OF PUBLISHING RIGHTS

I hereby assign the Society with full title guarantee all rights of copyright and related publishing rights in my article, in all forms and all media (whether known at this time or developed at any time in the future) throughout the world, in all languages, where our rights include but are not limited to the right to translate, create adaptations, extracts, or derivative works and to sub-license such rights, for the full term of copyright (including all renewals and extensions of that term), to take effect if and when the article is accepted for publication. If a statement of government or corporate ownership appears above, that statement modifies this assignment as described.

I confirm that I have read and accept the full Terms & Conditions below including my author warranties, and have read and agree to comply with the Journal's policies on peer review and publishing ethics.

Signed and dated: Changhyun Kwon, 30 September 2018

IISE, 30 September 2018

THIS FORM WILL BE RETAINED BY THE PUBLISHER.

RIGHTS RETAINED BY YOU AS AUTHOR

4. These rights are personal to you, and your co-authors, and cannot be transferred by you to anyone else. Without prejudice to your rights as author set out below, you undertake that the fully reference-linked Version of Record (VOR) will not be published elsewhere without our prior written consent. You assert and retain the following rights as author(s):
    i. The right to be identified as the author of your article, whenever and wherever the article is published, as defined in US Law 94-553 (Copyright Act) and, so far as is legally possible, any corresponding rights we may have in any territory of the world.
    ii. The right to retain patent rights, trademark rights, or rights to any process, product or procedure described in your article.
    iii. The right to post and maintain at any time the Author's Original Manuscript (AOM; your manuscript in its original and unrefereed form; a 'preprint').
    iv. The right to post at any time after publication of the VoR your AM (your manuscript in its revised after peer review and accepted for publication form; a 'postprint') as a digital file on your own personal or departmental website, provided that you do not use the VoR published by us, and that you include any amendments or deletions or warnings relating to the article issued or published by us; and with the acknowledgement: 'The Version of Record of this manuscript has been published and is available in <JOURNAL TITLE> <date of publication> http://www.tandfonline.com/<Article DOI>.'
        a. Please note that embargoes apply with respect to posting the AM to an institutional or subject repository. For further information, please see our list of journals with applicable embargo periods: PDF | Excel. For the avoidance of doubt, you are not permitted to post the final published paper, the VoR published by us, to any site, unless it has been published as Open Access on our website.
        b. If, following publication, you or your funder pay an Article Publishing Charge for retrospective Open Access publication, you may then opt for one of three licenses: CC BY, CC BY-NC, or CC BY-NC-ND; if you do not respond, we shall assign a CC BY licence. All rights in the article will revert to you as author.
    v. The right to share with colleagues copies of the article in its published form as supplied to you by Taylor & Francis as a digital eprint or printed reprint on a non-commercial basis.
    vi. The right to make printed copies of all or part of the article on a non-commercial basis for use by you for lecture or classroom purposes provided that such copies are not offered for sale or distributed in any systematic way, and provided that acknowledgement to prior publication in the Journal is given.
    vii. The right, if the article has been produced within the scope of your employment, for your employer to use all or part of the article internally within the institution or company on a non-commercial basis provided that acknowledgement to prior publication in the Journal is given.
    viii. The right to include the article in a thesis or dissertation that is not to be published commercially, provided that acknowledgement to prior publication in the Journal is given.
    ix. The right to present the article at a meeting or conference and to distribute printed copies of the article to the delegates attending the meeting provided that this is not for commercial purposes and provided that acknowledgement to prior publication in the Journal is given.
    x. The right to use the article in its published form in whole or in part without revision or modification in personal compilations, or other publications of your own work, provided that acknowledgement to prior publication in the Journal is given.
    xi. The right to expand your article into book-length form for publication provided that acknowledgement to prior publication in the Journal is made explicit (see below). Where permission is sought to re-use an article in a book chapter or edited collection on a commercial basis a fee will be due, payable by the publisher of the new work. Where you as the author of the article have had the lead role in the new work (i.e., you are the author of the new work or the editor of the edited collection), fees will be waived. Acknowledgement to prior publication in the Journal should be made explicit (see below):

        Acknowledgement: This <chapter or book> is derived in part from an article published in <JOURNAL TITLE> <date of publication> <copyright <the Society>, available online: http://www.tandfonline.com/<Article DOI>

If you wish to use your article in a way that is not permitted by this agreement, please contact permissionrequest@tandf.co.uk